Influence of Climatic Oscillations on Indian Ocean Tropical Cyclone Energy

by

Dicky Leroy Armstrong Jr

November, 2014

Director of Thesis: Scott Curtis

Major Department: Geography

Tropical Cyclones form in 4 independent regions of the Indian Ocean Basin ranging from the Arabian Sea, Bay of Bengal, Western South Indian, and Eastern South Indian Ocean. These cyclones lead to distinct patterns in their Accumulated Cyclone Energy for their particular region. The goal of this research article is to examine how the larger scale climate oscillations including ENSO, the Indian Ocean Dipole, and the Subtropical Indian Dipole of the Indian Ocean influence both the patterns in Tropical Cyclone Energy as well as the patterns in the large scale atmosphere of each of the aforementioned sub regions during high ACE events and lower ACE events. This analysis was done using linear regression techniques and appears to reveal the main influence on both ACE and the larger scale atmosphere of the basin is the phases, both warm (El Niño) and cold (La Niña), of the El Niño Southern Oscillation. This is especially true for the northern half of the basin with El Nino leading to higher shear, which is the main weather variable that has an impact on lowering ACE. The other Oscillations appear to have some impact through the placement of their warm pools in the southern portion of the region.

Influence of Climatic Oscillations on Indian Ocean Tropical Cyclone Energy

A Thesis

Presented To the Faculty of the Department of Geography

East Carolina University

In Partial Fulfillment of the Requirements for the Degree

Master of Arts

by

Dicky Leroy Armstrong Jr

December, 2014

Influence of Climatic Oscillations on Indian Ocean Tropical Cyclone Energy

by

Dicky Leroy Armstrong Jr.

APPROVED BY:

DIRECTOR OF
THESIS: _____
Scott Curtis, PhD

COMMITTEE MEMBER: _____
Rosana Nieto Ferreira, PhD

COMMITTEE MEMBER: _____
Tom Rickenbach, PhD

CHAIR OF THE DEPARTMENT
OF GEOGRAPHY, PLANNING
AND ENVIRONMENT: _____
Burell Montz, PhD

DEAN OF THE
GRADUATE SCHOOL: _____
Paul J. Gemperline, PhD

TABLE OF CONTENTS

LIST OF TABLES

LIST OF FIGURES

LIST OF EQUATIONS

1. Introduction

The meteorological phenomena of the Indian Ocean are some of the least studied of any of the major ocean basins. It has only been over the last several decades that researchers have begun to gain a better understanding of what occurs in this basin by applying knowledge about well-established large-scale circulations found in other oceans, in particular the Pacific. Further work is needed to assess the localized impacts of Indian Ocean climatic oscillations. These major climate oscillations, that will be discussed later in detail, control both the oceanography and to a large extent the meteorology of this basin. These oscillations and their effects on the surrounding atmosphere are slowly becoming clearer to us, especially through the use of reanalysis data. There are still knowledge gaps that haven't received significant attention by the scientific community, namely how the climate oscillations tie into tropical cyclone development within the Indian Ocean. By understanding how the tropical cyclones and oscillations interact, a better picture of tropical cyclone development can be made, which will aid in tropical cyclone forecasting and analysis.

Tropical cyclones form across the globe in a location where atmospheric-oceanic conditions are favorable for sustained tropical cyclogenesis. These locations are normally within the tropical and to some extent the subtropical oceans ranging in latitude from around 10 degrees north and south of the equator to around 40 degrees north and south of the equator. These are normally the prime locations to see tropical cyclogenesis with the peak development in a region between 10 and 20 degrees north and south of the equator. The six favorable factors for tropical cyclogenesis include

(i)	sufficient ocean thermal energy [SST > 26°C to a depth of 60 m],
(ii)	enhanced mid-troposphere (700 hPa) relative humidity,
(iii)	conditional instability,
(iv)	Enhanced lower troposphere relative vorticity.
(v)	weak vertical shear of the horizontal winds at the genesis site, and
(vi)	Displacement by at least 5° latitude away from the equator.

Table 1. The six main ingredients needed for tropical. They are commonly found within tropical and subtropical oceans worldwide. (https://www.meted.ucar.edu/)

These conditions are vital for the development of a tropical cyclone to form in every ocean basin including the Indian Ocean (Gray, 1968). For a disturbance to grow, it will need a warm water supply to give the system energy. The air has to be moist and unstable for tropical convection to grow. There also has to be vorticity in the atmosphere at the lower levels for a spin to develop and low shear to keep the top part of the cyclone from being displaced from the lower portion. Also a cyclone has to be on average at least 5 degrees from the equator so that planetary vorticity can aid in spinning up the cyclone. Any closer and the planetary vorticity is too low to aid in cyclogenesis. This planetary vorticity is needed because relative vorticity tends to be insufficient on its own to cause a significant cyclone to develop.

$$\eta = \zeta + f = \frac{\partial v}{\partial x} - \frac{\partial u}{\partial y} + f$$

.

Equation 1. The absolute vorticity equation for the atmosphere. It is found by summing relative vorticity of the parcel of air with planetary vorticity.

The above equation reveals how the absolute vorticity of a system is a combination of planetary vorticity and relative vorticity. This is why the equator is a dead zone for tropical cyclones, because it lacks the planetary vorticity that combines with the relative vorticity to get a cyclone spinning counterclockwise in the northern hemisphere and clockwise in the southern. This also explains why systems can't cross the equator, because the planetary vorticity goes to zero at the equator weakening the cyclone, and then the relative vorticity changes sign on the other side also weakening the cyclonic circulation. All of the conditions discussed above are found in a vast majority of the tropical and subtropical Indian Ocean.

The Indian Ocean is the smallest of the three main tropical ocean basins. This basin is bordered by Africa and Madagascar to the West, the Middle East and India to the North, and Australia and the maritime continent to the East. To the South you have the cold waters of the Southern Ocean and the Antarctic continent. This ocean basin spans from northern hemisphere midlatitudes southward through the tropics and into the southern hemisphere midlatitudes. This means that this basin occupies a large area of tropical and subtropical latitudes, which are favorable locations for tropical cyclogenesis.

Tropical cyclones in the Indian Ocean occur within two main regions, which can be subdivided into four smaller regions based on the geographic and atmospheric characteristics of the basin. The two major regions are the North Indian Ocean and the South Indian Ocean, which

are divided by the equator. The subdivided regions are the northwestern region associated with the Arabian Sea located between Pakistan and Iran to the North, Somalia to the South, India to the East, and the Arabian Peninsula to the West; northeastern region associated with the Bay of Bengal which is bordered by India and Sri Lanka to the West, Bangladesh to the North, Myanmar to the East; the southwestern region which is the waters near the island of Madagascar and Mozambique; and the southeastern region near the coast of northern Australia and Timor Sea. The longitude of the southern tip of India at approximately 75E can be used to divide the eastern and western sections. As seen in Figure 1, the northern regions are normally treated as one under the Tropical Prediction Center (TPC) New Delhi office. This is because of their small size, while the southern regions are split in half under control of La Reunion to the west and Darwin and Perth to the east. Each of these basins have seasons that can be considered year round but tend to have peaks when the Intertropical Convergence Zone or ITCZ is within their boundaries. This is unlike the Atlantic, which has a set season and can also have tropical cyclones develop from different sources such as decaying frontal boundaries or upper level troughs that become cutoff from the main jet stream flow (Bosart and Bartlo, 1991). This dependence on the ITCZ means that although the seasons do not have set boundaries they are limited by the amount of disturbances from the ITCZ. This explains why this basin tends to see fewer tropical cyclones than the other basins such as the Atlantic or Eastern Pacific which average around 10.1 and 14, respectively, tropical cyclones yearly. The Eastern Pacific sees extra development from convective complexes that exit the Central American continent whereas the Atlantic can see early and late season development potential from cold fronts that stall and weaken within the basin. On average the Indian Ocean sees around 8.6 cyclones per year. There is an extreme range, depending on location with the areas in the southwest seeing around 12.6

cyclones, areas near Australia 4.6, and both areas near the north combined for a total of 8.6 cyclones (Hall et al 2007).

Another one of the biggest differences between the Indian Ocean and the majority of the other ocean basins is that tropical cyclones can form North and South of the Equator simultaneously (Ferreria et al, 1996). This is common in the Indian Ocean basin as well as the very active Northwestern Pacific Ocean basin. The other basins are different with the North Atlantic having a distinct hurricane season while the South Atlantic isn't ever favorable for development, except for isolated instances, thanks to the small size of the basin and more importantly the high amount of vertical wind shear within the basin associated with the subtropical and polar branches of the jet stream. The Southeastern Pacific is similar to the South Atlantic but also tends to be affected by cooler sea surface temperatures commonly found on the eastern continental border associated with cool ocean currents that come from the South. These cool sea surface temperatures (SST) tend to be below the 26 degrees Celsius threshold needed for tropical cyclone formation. The tropical Eastern Pacific basin tends to have similar characteristics as the Atlantic Ocean Basin. All things said, the Indian Ocean has a different seasonal development of tropical cyclones than any of the other ocean basins although the global climate circulations that influence it are very similar.

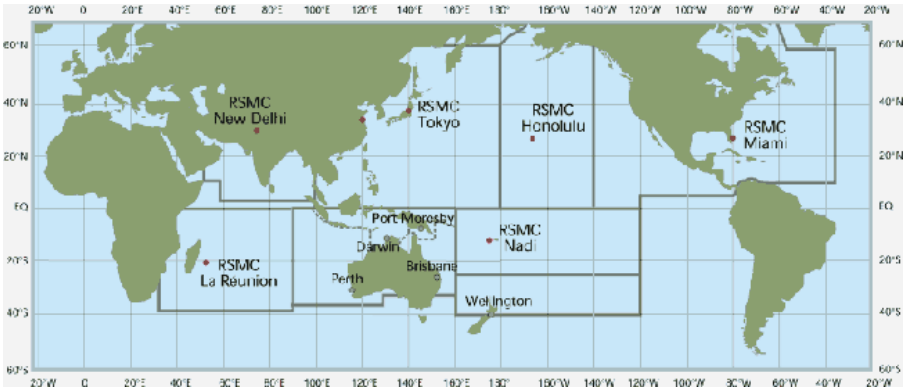

Figure 1. Tropical Cyclone Warning Areas. A map of the different tropical cyclone forecasting centers located across the Globe. As seen there are three main centers that handle the Indian ocean with the Australia theater being divided between Perth And Darwin (Australian Bureau of Meteorology).

Scientists have studied how the El Niño Southern Oscillation, commonly referred to as ENSO, has influenced the location of the monsoonal circulation in the Indian Ocean, and noticed large swings in precipitation and storm tracks in this basin (Webster and Yang 1992). As seen in Figure 2a ENSO is the warming (expansion) and cooling (contraction) of the equatorial waters off the coast of South America near Peru extending outwards as far as the central Pacific Ocean (Skowronska, 2012). During an El Niño warmer waters begin to pool in this region causing the area of strongest atmospheric lift to move into this region. This will then weaken the trade winds across the Pacific as the surrounding surface flow converges into the area (Figure 2b). During a La Niña episode the opposite occurs. Both events occur in a positive feedback until oceanic Rossby waves that have traveled towards Asia are reflected back bringing with them an area of warmer/cooler deep ocean waters canceling out the warming/cooling of the surface water temperatures (Pierce 1997). The ENSO cycle occurs on a 3-5 year time scale and leads to pressure perturbations that affect the average weather across the entire globe by changing the atmospheric flow. This can lead to regions of intense heat and drought or cooler regions and

flood. Researchers have also studied how ENSO influences tropical cyclone numbers in ocean basins across the world. This is done by understanding how the large-scale flow is changed during phases of ENSO. During an El Niño the Pacific Walker circulation shifts eastward and extends into the Atlantic increasing the vertical wind shear across the region. During a La Niña the Walker Circulation is confined to the Pacific, lowering Atlantic vertical wind shear (Henson and Trenberth 1998). As a community, researchers have a very good handle on the impacts of ENSO worldwide but there are still several regional climate oscillations discussed below that deserve further study as to how they influence the Indian Ocean basin's climatology.

A.

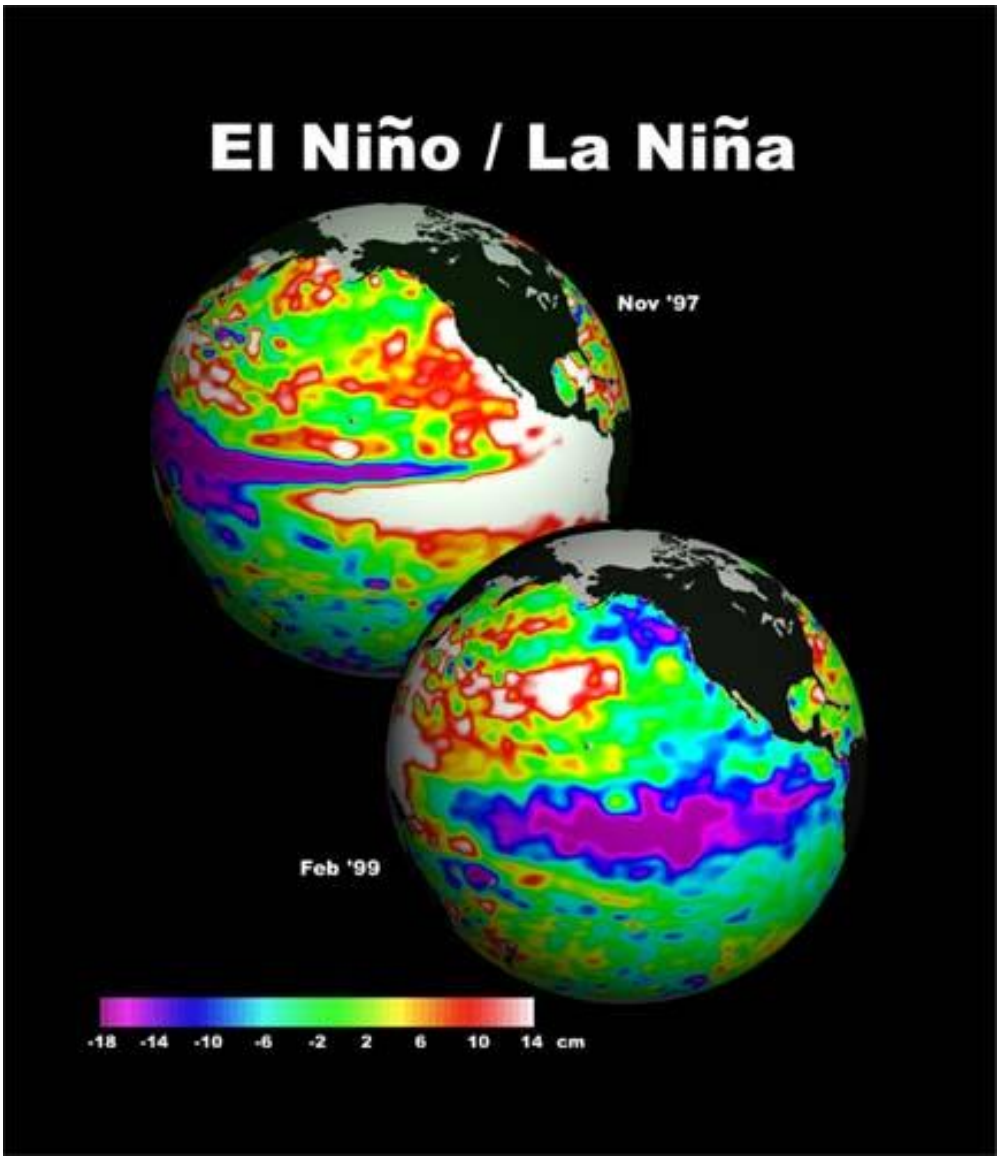

B.

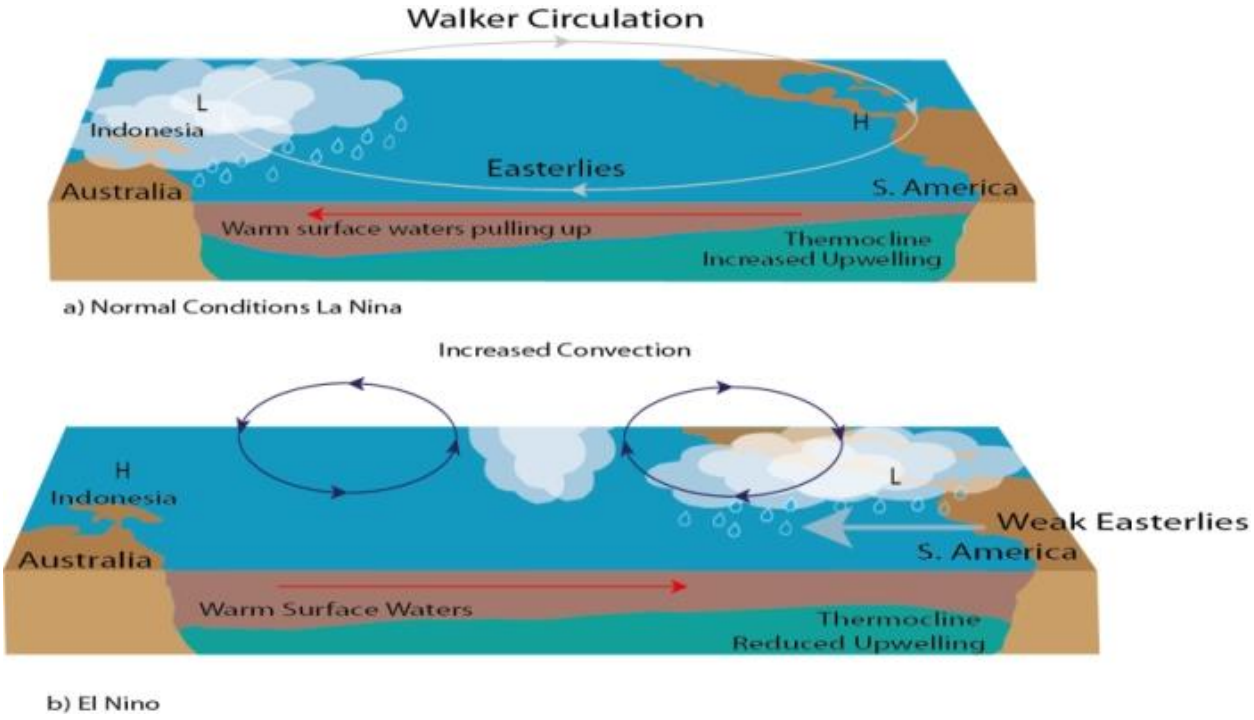

Figure 2A. An example of a strong El Niño in 1997 and a strong La Niña in 1999. The units being measured is the expansion and shrinkage of the water height from normal based of the thermal principles of water. Warm water expands while cooler water contracts (NASA).

Figure 2B. The movement of the Walker Circulation during a Normal Conditions/La Niña and b El Niño Condtions (Skowronska, 2011).

The Indian Ocean Dipole (IOD), The Southern Indian Ocean Dipole (SIOD), and ENSO are important responses to atmospheric-oceanic coupling in the Indian Ocean. The IOD and SIOD, which are both movements of warm and cold water anomalies across the Indian Ocean basin in a zonal (east-west) direction, influence the ocean currents such as the warm eddies, as well as the atmosphere such as the pressure over this basin. The IOD tends to be centered near or just south of the equator while the SIOD tends to be centered south of this region in the subtropics between 15-35 S (Li et al 2003). This can be seen in Figures 3 and 4. Also because

the pressure changes the wind directions and speeds will be influenced according to pressure gradient relationships. (BOM's IOD Page, Yamagata et al 2006) According to basic thermodynamic principles, locations that have warmer water anomalies will have on average lower pressures while cooler water anomalies tend to have the opposite effect on the atmosphere. This is because warmer water anomalies lead to rising air and lift which lowers surface pressures, with the opposite being true of colder water anomalies (Namias, 1973). Also large-scale winds on average will flow from areas of high pressure to areas of lower pressure. Early works show that they can influence the location of the monsoonal circulation as well, which in turn causes droughts and flooding in the southern portion of the Asian Continent (Webster and Yang, 1992).

A.

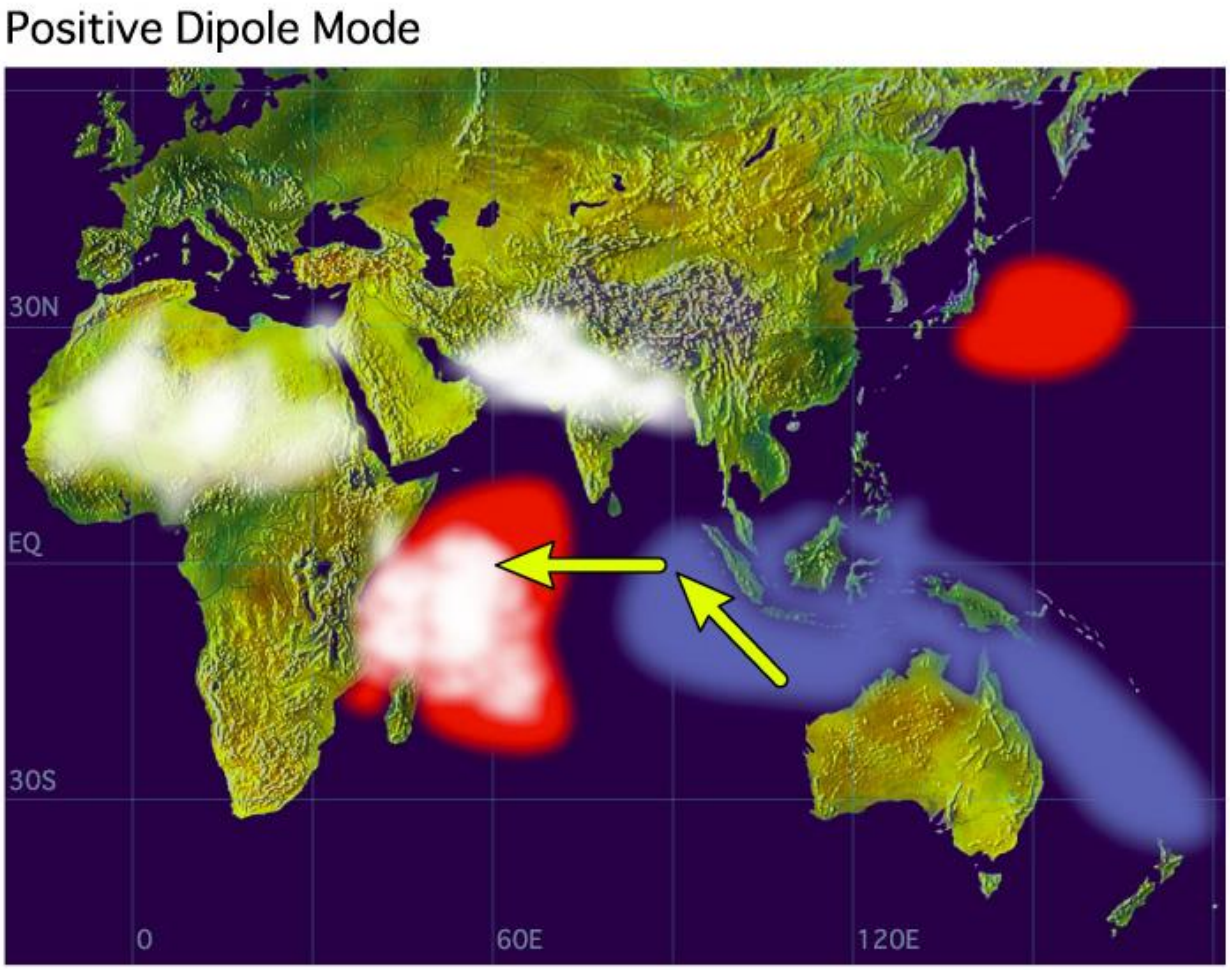

B.

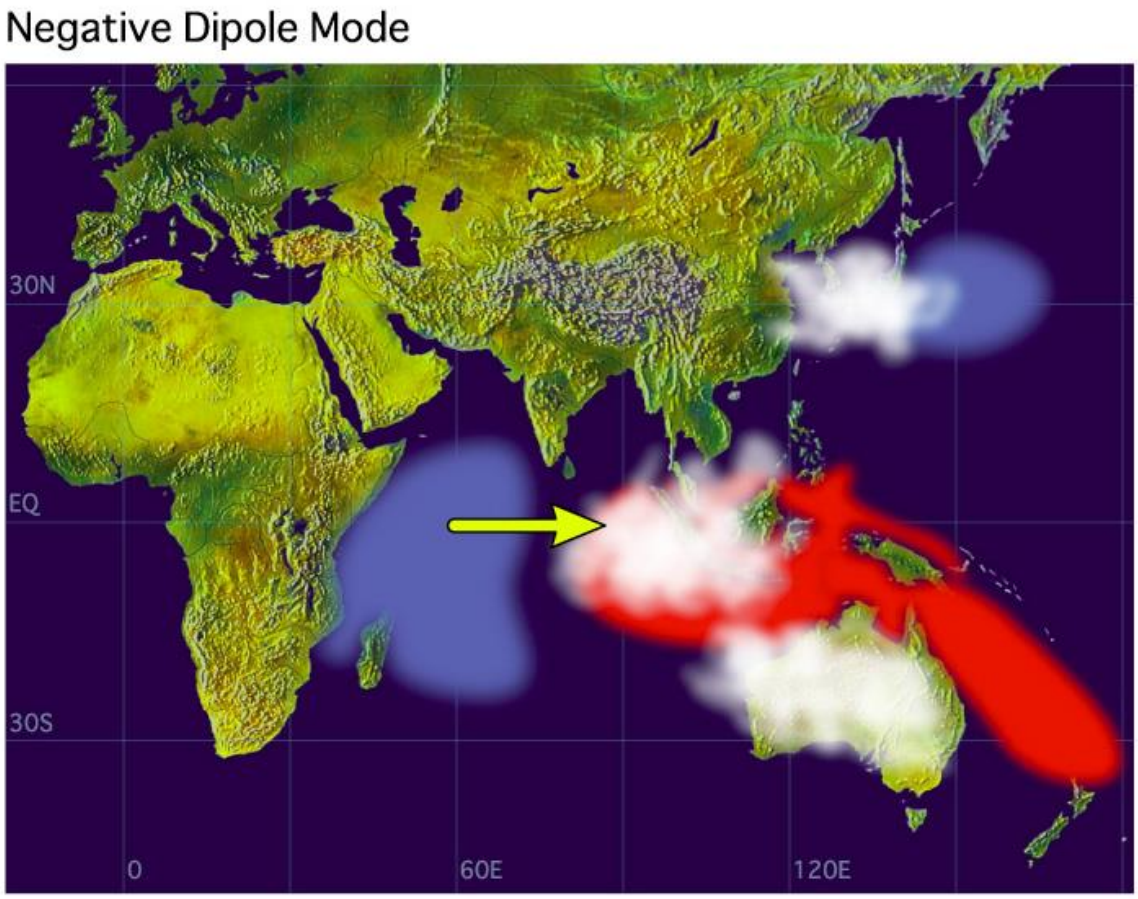

Figure 3.

A. An example of a positive Dipole event. The warmest waters are found near the Equator in the Western Portion of the basin. Where the warmer waters are located there is an increase in lift and moisture.

B. An example of a negative Dipole event which is the opposite of the positive event. The warmth and lift are located along the eastern side of the basin also extending into the Pacific Ocean (Jamstec).

A.

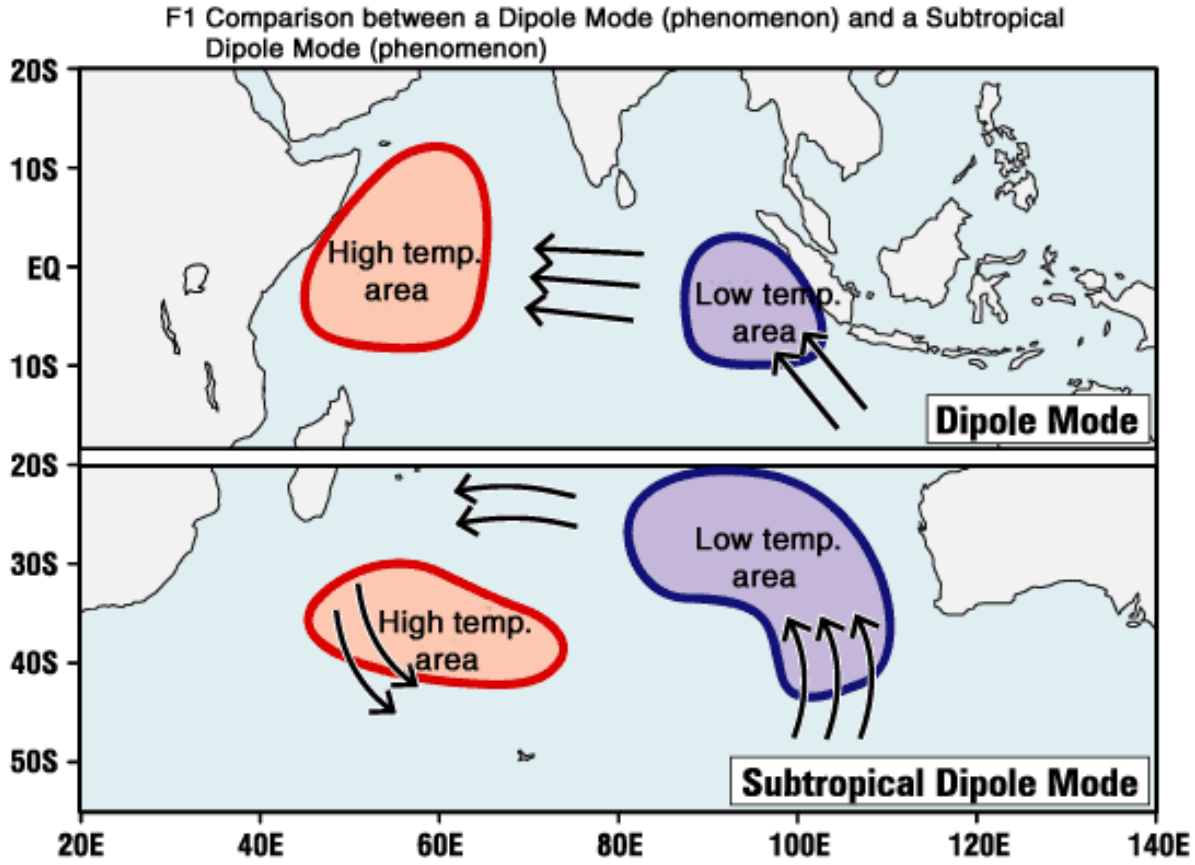
F1 Comparison between a Dipole Mode (phenomenon) and a Subtropical Dipole Mode (phenomenon)
20S
10S
EQ
10S
20S
30S
40S
50S
20E
40E
60E
80E
100E
120E
140E
High temp. area
Low temp. area
Dipole Mode
Low temp. area
High temp. area
Subtropical Dipole Mode

B.

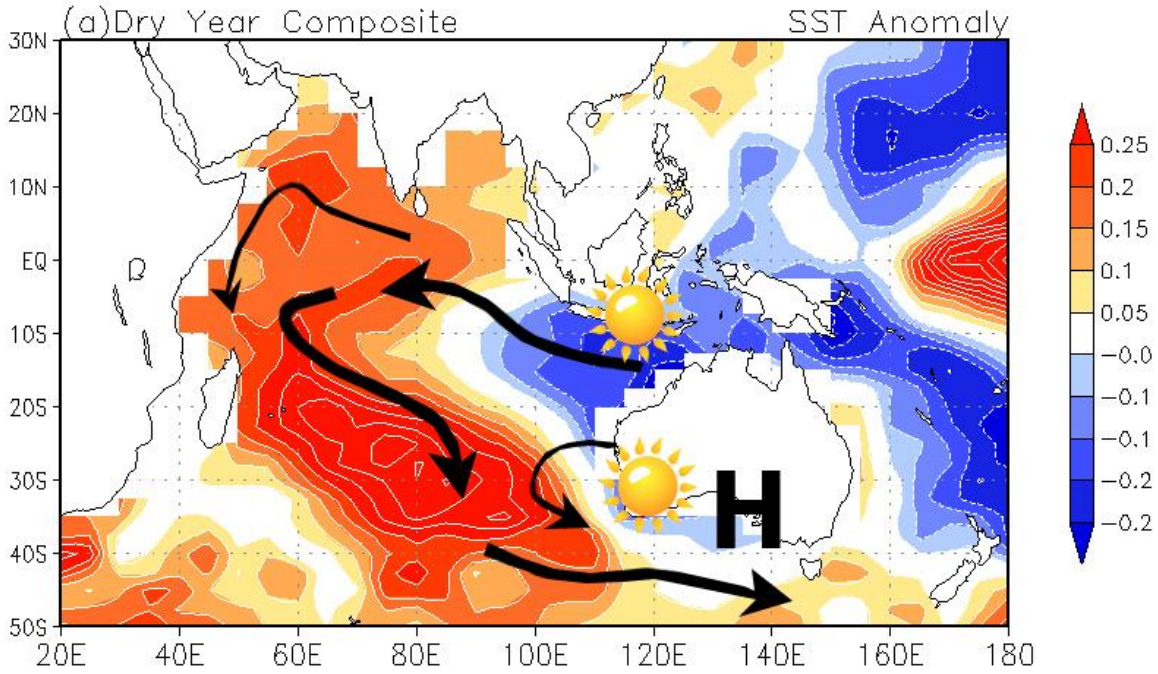
(a)Dry Year Composite
SST Anomaly
30N
20N
10N
EQ
10S
20S
30S
40S
50S
20E
40E
60E
80E
100E
120E
140E
160E
180
H
0.25
0.2
0.15
0.1
0.05
−0.0
−0.1
−0.1
−0.2
−0.2

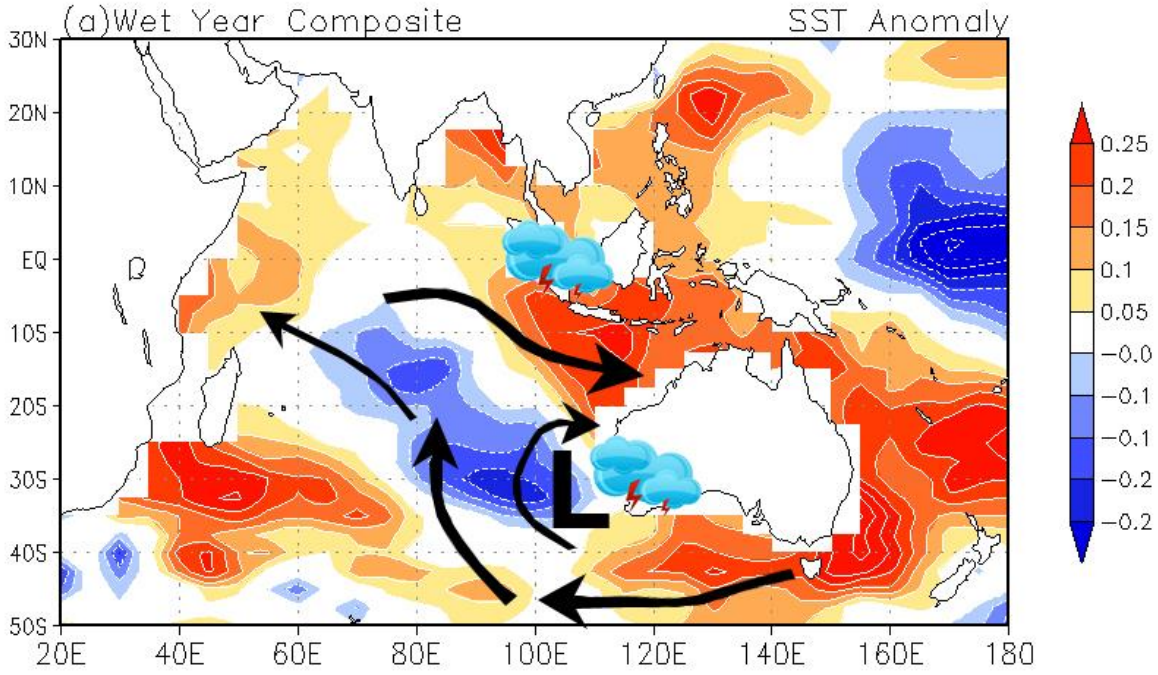
(a)Wet Year Composite
SST Anomaly
30N
20N
10N
EQ
10S
20S
30S
40S
50S
20E
40E
60E
80E
100E
120E
140E
160E
180
L
0.25
0.2
0.15
0.1
0.05
−0.0
−0.1
−0.1
−0.2
−0.2

Figure 4a. The key differences between the Indian Ocean Dipole (top) and the Subtropical Indian Ocean Dipole (bottom). The arrows indicate the motion of travel of the water anomalies. From this diagram you can see that the Subtropical Indian Ocean Dipole could favor tropical Cyclogenesis in its warm eddy during its negative phase as warmer waters would develop near the coast of Australia. This is because it is located away from the equator and increases lift - both key ingredients in trpical cyclogenesis (Jamstec).

Figure 4b. The atomospheric flow changes between phases of the Subtropical Indian Ocean Dipole. Air flows on average from cooler locations to warmer locations. Eventually creating a cyclonic anomaly.

The biggest gap in our knowledge is the exact impacts of these oceanographic circulations on the atmospheric circulation over this basin. There is a lack of knowledge on how these warm and cold eddies that are produced by these circulations play a role in the atmosphere and how, in turn, this changed atmosphere influences the genesis and track of tropical cyclones in this basin. So while researchers have noticed trends in precipitation and water temperature, no one has developed an exact theory on how climate oscillations influence the track and intensity of Indian Ocean tropical cyclones.

2. Research Objectives:

1. **Examine the major climatic oscillations within the Indian Ocean basin.**
2. **Develop a complete climatology of Indian Ocean Tropical Cyclones using their Accumulated Cyclone Energy (ACE). This will include the differences in energy that occur between different phases of the aforementioned oscillations.**
3. **Also show how the large-scale atmosphere over the Indian Ocean changes during each of the oscillations and how that might influence tropical cyclone ACE**
4. **Note any extreme differences between tropical cyclones in the different regions.**
5. **Analyze the effects of ENSO on the basin through its known influence on shear associated with the Walker Circulation.**
6. **Analyze the effects of the IOD on the basin through its known influence of water anomalies within the equatorial region of the basin.**
7. **Analyze the effects of the SIOD on the basin through its known influence of water anomalies within the subtropical region of the basin.**

This will aid in determining the location of possible extreme events in all of the countries that border the Indian Ocean Basin, as we will know which areas will be more or less likely to see a tropical cyclone than other areas in a particular year. It will also aid in seasonal forecasting and preparing for tropical cyclones within this otherwise lesser-studied basin.

3. Brief Description of the Climate of the Indian Ocean

The Indian Ocean basin (Figure 5) is controlled by large-scale climate cycles similar to the other ocean basins of the world. There are a few differences that lead to complications in tropical cyclone prediction in this basin. Furthermore, the Indian Ocean does not have a long record of reliable surface observations. Most of the affected countries cannot afford to fund and maintain necessary in situ observing platforms (World Bank GDP- World Development Indicators 2009-2013). The data voids are just now being filled with the process of setting up a basin wide buoy system sponsored mainly by NOAA as well as the availability of satellites that can be used for climatic studies in recent decades (NOAA, 2009). It still has only been in the past 10 years that this location has become an object of increased study by scientific organizations worldwide.

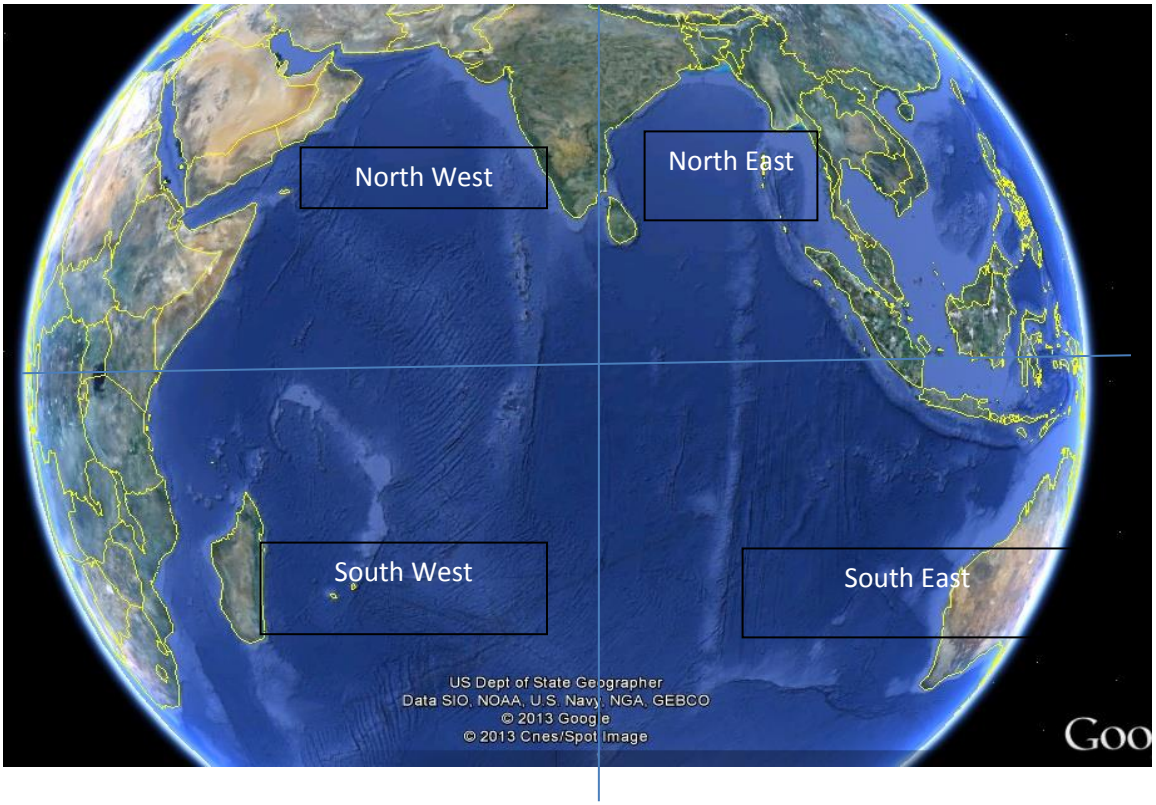

Figure 5. Map of the Indian Ocean showing the sub regions of the Indian Ocean that will be used in this study. Note that the northern portion of the basin is smaller and defined while the southern portion is larger (Google Earth).

The fact that the Indian Ocean's weather has different developmental characteristics is caused at least partially by the monsoonal circulation which plays a larger role in the large scale flow patterns in this basin than any of the other tropical basins. Importantly for this study, the monsoonal circulation influences the main precipitation producer in the area: The Intertropical Convergence Zone. The ITCZ is a band of convection and precipitation caused by the meeting of the easterly trade winds near the equator (Sikka and Gadgil, 1980). The Intertropical Convergence Zone (ITCZ) migrates from as far south as 20 degrees south to as far north as 20 degrees north throughout the year (Figure 6). The monsoonal circulation is caused by the differences in temperature between the air mass over the land and the ocean. When the land

becomes warmer the air blows in from the ocean bringing in moisture and eventually the ITCZ. When the ocean is warmer the air blows seaward. The monsoonal circulation basically functions as a large-scale sea breeze circulation (Waliser 2002).

Figure 6. The Movement of the ITCZ. The migration of the ITCZ and its influence on tropical cyclone development can be seen here. Yellow is the Northern Hemisphere winter while Purple is the Northern Hemisphere summer. Storm development (green dots) tends to follow the ITCZ (Hall et al 2007).

The differences in position of the ITCZ influence when and where tropical cyclones can form in this basin. This comes from knowing that cyclones can't form from the ITCZ while it is over land and while it is near the Equator as seen in Figure 6. During those times the disturbances are missing some of the key ingredients needed for tropical cyclogenesis. Cyclones can form either in the North Indian Ocean including the Arabian Sea and the Bay of Bengal and cyclones can also form in the South, which includes areas like Mozambique Channel near Africa and the Timor Sea near Australia or anywhere in between because there is more open water in this portion of the basin (Figure 5, Schott and McCreay 2001).

4. Tropical Cyclones and Precipitation

For at least the northern half of the Indian Ocean basin we know that there tends to be two peaks in the tropical cyclone season during the time that the monsoonal circulation places the ITCZ over water and north of the equator. This typically occurs during the months of April and May when the monsoon is becoming active and again in October and November when the monsoon is ending. This double peak tends to occur less in years that the monsoonal circulation is less active because the ITCZ remains in the basin longer (Li et al, 2013). Those years also tend to have an active southern hemisphere season basin wide, albeit with no clear effect on the southwestern portion of the region near Madagascar. However, storms from the eastern region do move into this area (Behera 2005).

As far as precipitation is concerned, the areas in the northern portion of the basin receive more during an active monsoonal season and less during a less active season. The area near Australia receives more rain from tropical cyclones when the monsoonal circulation has moved South allowing for more ITCZ convection as well as large and precipitation heavy monsoonal tropical cyclones. This tends to occur more frequently during a La Niña event (Wang and Hendon, 2007). Similarly, the area near Mozambique tends to receive less precipitation during El Niño because again it appears there are less tropical cyclones and less ITCZ convection in the region. Interestingly the two areas tend to be opposites during their rainy seasons when one is having large amounts of precipitation the other area tends to be dry but the exact mechanism that causes this is still not completely known (Matyas 2011, Pui 2012).

One interesting result, shown in Figure 7, is that there are a large number of tropical cyclone days near the area that is between La Reunion and Madagascar. Tropical Cyclone days

are number of days per year on average that a tropical cyclone is within a location. Genesis, which is the probability that a cyclone will form in this region, is strong in this region as well. This was found by Dowdy and Kuleshov (2012) by analyzing past satellite data indicating tropical cyclone development and occurrences to create a rough climatology of tropical cyclones in the southern hemisphere. This means that storms are frequent in this area and that they both develop in this region and move into this region from other areas in the Indian Ocean (Dowdy and Kuleshov 2012).

Also of note is the fact that as seen from Figure 7 the genesis probability remains strong all around the island of Madagascar right up to the coast of Africa. This means that cyclones can form in the small area that is the Mozambique Channel. This is possibly aided by the shape of the coastline. The curved nature of the coastline may both induce spin on the circulation as well as tighten the circulation. This may explain why the storms that do begin to develop in this region tend to become stronger and smaller than storms in other regions of this basin (Dowdy and Kuleshov 2012).

A.

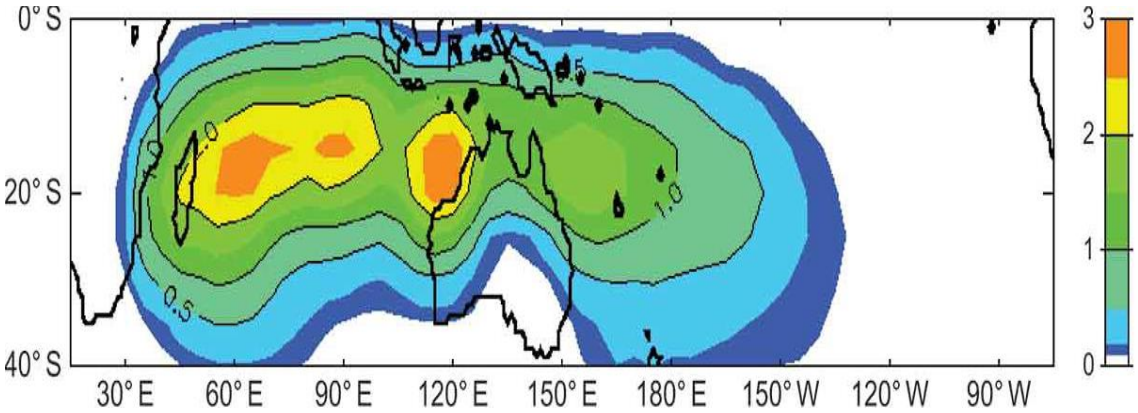

B.

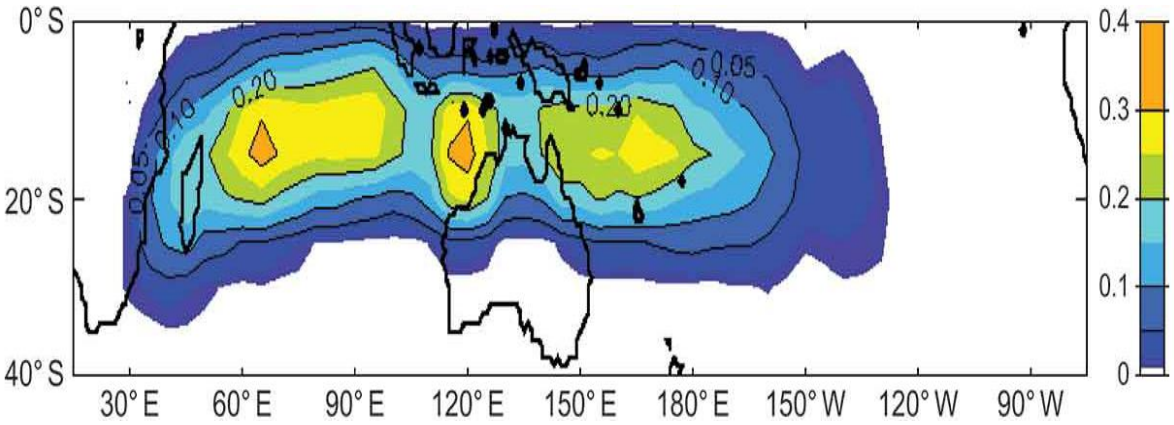

Figure 7 A. Average Days of Tropical Cyclones. This is the average number of days that a location will have a tropical cyclone impacting it each year.

7 B. Average Genesis Locations of Tropical Cyclones This is the probability that a cyclone will form in this region based off of the long term averages of tropical cyclone development in this area (reproduced from Dowdy and Kuleshov 2012)

Also noteworthy, the basin wide oscillations can lead to precipitation deficits and surpluses in southern Africa and Eastern Australia. It appears that these precipitation episodes are influenced by the SIOD, the IOD, and the ENSO circulations to differing degrees. From the past research (Pui 2012) it appears that when the eastern side of the basin is facing excess precipitation the western side is facing reduced precipitation coinciding with the evolution of the oscillations. Excess precipitation in some cases can result from enhanced convective activity, which may be the result of tropical cyclone activity. As of yet, researchers do not understand what has the greatest influence on the precipitation, but more research is being done (Pui 2012).

5. Global Scale Circulations Impacts

El Niño and La Niña play a huge role in the movement of the ITCZ with El Niño weakening the monsoonal cycle and positioning the ITCZ more southerly and less overland in India and parts of Eurasia (Wu and Kirtman, 2003). Thus, this increases the landmass's likelihood of drought but increases the chances that a tropical cyclone can form. The increase in tropical cyclone numbers occurs for much of the basin, but interestingly not in the Southwestern portion of the basin near the island of Madagascar and the African country of Mozambique. It is at this location that the number of tropical cyclones decreases, which conversely increases the amount of drought that this region suffers (Schott and McCreay 2001).

Another thing of interest relating to ENSO is that when it is in its positive phases the Indian Monsoonal circulation is weaker leading to less rain for the region around India. This also means less in the way of precipitation and tropical cyclones in the area around Africa. When the ENSO is negative it leads to much more precipitation in western Africa and India as well as leaving behind a huge warm pool in the Western Indian Ocean that the tropical cyclones can tap for energy. This is caused by a weakening of the zonal circulation across the basin reducing the movement of water allowing it to become warmer (Hastenrath 2007).

Finally, tropical cyclone development is related to the Madden Julian Oscillation - a pulse of energy and lift that travels across the world in the subtropics originating in the waters near the eastern Indian Ocean and Western Pacific Ocean. The pulse begins in the Indian Ocean and travels across the Pacific weakening until it ends near the coast of South America. Increased lift and energy can also make it into the Atlantic while missing a portion of its convective element. Associated with this is on average lower surface pressures, which aids in tropical

cyclone development. Positive phases lead to increased lift and energy while a negative phase leads to decreased lift and an increase in surface pressures across the region. In Figure 8 positive phases are marked in green, representing areas of increased velocity potential, which coincide with increased upper level divergence. Those marked in brown are areas of decreased upper level divergence or even convergence (Liebman et al, 1994 and Gottschalck etal, 2005).

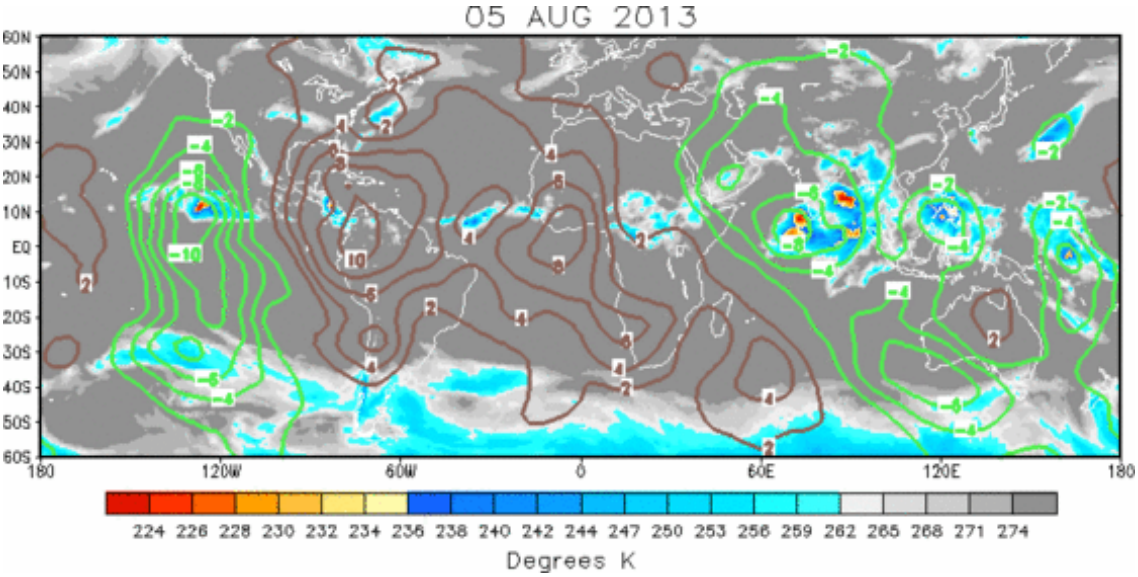

Figure 8. A figure using velocity potential anomalies to show areas if increased lift (green) and decreased lift (brown) associated with the MJO. These pulses generally move from west to east across the ocean basins but occasionally will stall or retrograde.

Because of the smaller time scale ranging from 30-90 days and because of the complicated nature of this oscillation it will not be analyzed in this study. This study focuses on larger scale oscillations that tend to be more consistent in location and strength over a seasonal time period,

6. Indian Ocean Oscillation Impacts

The Southern Indian Ocean Dipole is a sea surface temperature anomaly that is found in the southern portion of the Indian Ocean from just south of the equator to around 35 degrees south. The location can be seen clearly in Figure 4b. During the positive phase the waters west of 50-70 East are warmer than average while the waters east of 90-110 East are colder. During the negative phase the water temperature anomaly reverses with the warmer waters pooling in the eastern portion of the basin. These water anomalies tend to occur as a result of the large scale wind patterns across the basin. Researchers have found that the positive and negative phases of this oscillation can influence significantly the track of tropical cyclones in the southwestern Indian Ocean. Another finding about the Southern Indian Ocean Dipole was that it can interact with ENSO phases to produce differences in the track of cyclones in the southern Indian Ocean. For example El Niño and negative SIOD leads to storms that recurve quickly south and eastward into the main flow while a La Niña and a positive or warm SIOD leads to storms that remain on a more westward course and travel more into the western portion of the basin (Ash and Matyas 2012).

Another oscillation that acts as a mitigating factor is the Indian Ocean Dipole (see Fig. 4a). It is like the SIOD because it is an anomaly of water temperatures that moves between the western portion of the basin and the eastern portion of the basin, but the major difference from the other oscillation is that it occurs along the equatorial regions. Therefore when warm water anomalies are near Africa, there is actually a lack of lift in the region of the southern Indian Ocean south of the equator near the coast of southern Africa because of sinking air moving into this region from the north. And when the cold waters are in the West there tends to be more lift

within this region because the sinking air is occurring near the equator allowing lift to occur in the subtropical region. The basic convective process can be stated as follows: the warm pool causes lift of the overlying air mass, allowing for low-level convergence and upper-level divergence. Air parcels then sink and diverge at the surface in regions of cooler air associated with cooler water pools. This cuts off the convective process in those remote locations helping to shut down system development. This dipole has peak amplitude in the September to November months (Singh 2008, Matya and Silva 2011, Shi 2012).

The Indian Ocean Dipole can be modeled using the water temperature anomalies located near the equator along with the anomaly associated with the equatorial zonal component of the wind. This wind vector will change direction relating to the phase of the dipole that is occurring. According to recent work by Saji and Yamagata in 2003**,**

> "a canonical IOD is thus defined as having the following properties: 1) Strongly anomalous zonal SST gradient or DMI (Dipole Mode Index) develops around boreal spring to early summer but vanishes after fall; peak DMI occurs in late summer or fall with anomalous activity prevailing for two to three seasons. 2) Anomalous Western Indian Ocean (WIN) temperature anomaly develops in boreal summer and lasts for two to three seasons before vanishing around late fall to winter; peak WIN anomaly occurs around fall. 3) Anomalous Eastern Indian Ocean (EIN) temperature anomaly develops around spring to early summer, lasts for two to three seasons, and vanishes around fall to winter with a peak around fall. 4) Anomalous U_{eq} (zonal wind) develops around spring to early summer, and lasts for two to three seasons before vanishing around late fall to winter; anomalous U_{eq} peaks in the boreal fall."

SIOD events behave in a similar cross-basin manner as their equatorial counterpart (Saji and Yamagata 2003).

7. Literature Summary

Past literature has shown that the aforementioned oscillations including ENSO, IOD, and the SIOD do have an impact on the tropical cyclones of the basin. The amount of impact is what is called into question, especially when you consider all of them together.

For example Camargo et al. (2007) concluded that relative humidity, vertical wind shear, and to a lesser extent vorticity were the main variables that changed during ENSO events, which subsequently influence tropical cyclones in the middle and southern portion of the Indian Ocean Basin. This was done by analyzing their genesis potential index or the potential for a storm to develop based off past events with similar conditions during El Niño events and La Niña events. They also broke it down by the 3 month January February March average and the August September October average. Their analysis found that El Niño was more favorable for tropical cyclogenesis especially near the area around Australia while La Niña was more favorable near the Bay of Bengal during the JFM timeframe. During the ASO timeframe the Northern portion is favorable during La Niña and only the coastal Bay of Bengal during El Niño. The southwestern portion is favorable for cyclogenesis during El Niño while it is unfavorable on the southeastern portion. This reverses during La Niña. Their results also show that El Niño leads to favorable wind shear while also leading to more unfavorable relative humidity during both seasons (Camargo et al, 2007).

It appears that the Indian Ocean tropical cyclone climatology over the entire basin is controlled by what happens with the Monsoonal Circulation and its location. The monsoonal circulation is controlled by ENSO and its phases: positive El Niño and negative La Niña. They

seem to control the development in the northern portion of the basin more than other factors while the southern portion gets its climatic influence from another source.

The development of tropical cyclones in the southern portion of the basin is influenced by the SIOD index and associated sea surface temperatures in the region. It, in combination with ENSO, influences the track and possibly some of the development of tropical cyclones in the southern and central portions of the basin. The IOD can act to influence cyclogenesis off the equator in the eastern and western portions of the basin due to changes in convective potential.

The literature has left a lot of gaps as to which oscillations are the most influential to the development of tropical cyclones. A definitive answer as to the relationship between remote and local climate oscillations and tropical cyclones via changes to the atmosphere and ocean is needed so that we will have an understanding of this basin, similar to the other ocean basins. This will be done by computing multivariate statistical analyses, and examining composite maps of key variables based on the aforementioned climate oscillations.

My hypotheses are as follows:

1. As Camargo et al. (2007) suggest, the ENSO will have the largest influence on tropical cyclogenesis, and thus ACE, in the basin. During El Nino, the weakened Walker Circulation will cause less shear in the vicinity of the Maritime Continent causing greater ACE in the southeastern basin. The opposite will occur during La Nina.

2. The negative phase of the SIOD (when the waters are warm to the west of Australia, Fig. 4a) will likely lead to an increase in ACE in both of the southern sub-basins. The positive phase of the SIOD will have little affect on ACE as the warm waters are too far south for cyclogenesis.

3. The IOD will have remote effects due to changes in meridional circulations. During the positive phase the warm waters in the western equatorial Indian Ocean will lead to reduced ACE in the southwest and northwest and enhanced ACE in the northeast and southeast. The opposite will hold true for the negative phase of the IOD.

8. Methods

The following section will discuss the methodology of the research project by first examining the data sets that were used during this analysis followed by the steps needed to calculate the results. In this way, the factors and assumptions involved in performing this research project as well as any of the limitations in the process will be clearly defined. Any transformations of the data set will also be clearly stated in this section.

Accurate tropical cyclone data was available as early as 1958 for select regions of the basin, while on average only ranging back to the mid-1970s. Data previous to this was spotty and suspect. Further, IOD and SIOD from JAMSTEC both stopped becoming available during the year 2010. On average there was around 30 years' worth of data per sector of the Indian Ocean basin for analysis. This is of sufficient size to give an accurate view of the influence of the oscillations on the Accumulated Cyclone Energy.

The range in timeframe of the data used in this analysis is seen in Table 2. The region with the largest amount of data is the southeastern region near Australia and the region with the least amount of continuous high quality data is the southwestern region near Africa and the island of Madagascar.

Basin	Beginning Year	Ending Year	Border Latitude	Border Longitude
Northwest	1975	2010	0 to 30N	50 to78E
Northeast	1972	2010	0 to 30N	78 to 100E
Southwest	1979	2010	0 to 30 S	35 to 78E
Southeast	1958	2010	0 to 30S	78 to 130E

Table 2. The temporal and spatial ranges of the data sets used in this analysis. The southwestern region had the shortest amount of data available ranging from 1979 to 2010 while the southeastern region had the longest amount of data ranging from as early as 1958 to 2010.

Tropical cyclone data was taken from the United States Navy's Joint Typhoon Warning Center's collection that is a part of the reanalysis project for tropical cyclone data worldwide. This is an ongoing project to collect a complete list of tropical cyclones from around the globe. The northern hemisphere data ranged in time from 1971 until present while the southern hemisphere data ranged in time from 1958 until present. The northern hemisphere data was split using the 78 degree longitude or roughly the central part of India into its northwestern region and its northeastern region. This was to account for any of the rare monsoonal tropical cyclones that may form while along the edge of the Indian Subcontinent. The southern region data had to be reviewed thoroughly because data in the original format also included tropical cyclone points from the southern Pacific Ocean, which, if included, would skew the results by significantly increasing the activity of the southeastern region. The eastern edge of the domain was set at 130 East because this allows the Sea of Timor, which is a branch of the Indian Ocean to remain in the

analysis. This area is a hotspot of southern Indian Ocean activity. Points east of that longitude were considered Pacific while west of that longitude they were considered primarily Indian. Again the 78 East longitude was used to split this southern basin into its southwestern and southeastern portions.

Storms that were below the 35 knot (40 mph) cut off point for tropical storms were then removed from the dataset. Below this threshold systems were considered tropical disturbances and weak tropical depressions. The storms that are included are tropical storms (cyclones), Intense Cyclones (hurricanes), and very Intense Cyclones (major hurricanes). After this series of filters were used, the data was then ready to convert to Accumulated Cyclone Energy or ACE.

The conversion to ACE from wind speed was performed using the standard formula as stated by the governing body the World Meteorological Organization. The formula is:

$$\mathrm{ACE} = 10^{-4} \Sigma\, v^2 \max$$

Equation 2. The equation to calculate the Accumulated Energy of a Cyclone as stated by the World Meteorological Organization. This equation is used to summarized the severity of tropical cyclones over a certain period of time by summing up their energy based off their maximum wind speeds.

Equation 2 is used to calculate Accumulated Cyclone Energy and it is equal to 10^{-4} times the sum of the maximum storm velocity squared. ACE is typically measured using the English units of kts^2. The max velocity is normally taken at 6 hours increments throughout the day at 00, 06, 12, 18 UTC. This is then summed up first per storm and then per month. ACE was then accumulated over the months that tropical cyclones occurred. The scaling factor 10^{-4} was included so that the result will have manageable numbers. ACE can show how active a season, or in this particular case a month was, with tropical cyclones. More intense storms will add to ACE

because of the wind speeds, the longer a storm lasts the greater ACE will be because of the summation time, and ACE will rise when there are more cyclones to be summed into the analysis. This is different than the standard of counting the number of tropical cyclones, which is normally used, and will give a better representation of the severity of the season.

The ACE was divided by the month that it occurred so that inactive periods (months) of tropical cyclones during the year could be eliminated to give a more accurate representation of the tropical cyclone seasons when analyzing the results. Inactivity marked with a 0 in the results column will skew the data leading to false results making it harder to come to a conclusion of the influence the oscillations actually have on the ACE values. Table 3 below shows a period of mixed activity with a few isolated very active years in the Northeast Region.

Year	October	November	December
2000	0.98	4.0425	3.815
2001	0	0	0
2002	0	1.97	0.98
2003	0	0	3.0575
2004	0	0	0
2005	1.215	2.185	11.9475
2006	1.675	0	0
2007	0	63.5625	0
2008	0.6925	3.4775	0.735
2009	0	0	1.7
2010	18.505	4.565	0

Table 3. A sample of the ACE data set showing ACE with units of kts^2. This is by month and year for the Northeastern Region

ENSO data can be found easily in the form of an index from the United States Climate Prediction Center also known as the CPC located at http://www.cpc.ncep.noaa.gov/. Index data represents ENSO as positive, negative or neutral as well as how strong or weak the event is. This is in the form of water temperature anomalies in the Nino 3.4 region of the Pacific Ocean basin. This region, located in the eastern and central Pacific gives off the largest signal during an ENSO event. A larger negative number means a stronger La Niña while a larger positive number means that it is a stronger El Niño. The values near zero also mean that ENSO is near neutral with average trade winds and no substantial water temperature anomalies to be found in the Pacific Ocean. An El Niño event starts after a 3-month average time period of Nino 3.4 is above 0.5 and likewise a La Niña below negative 0.5 degrees. This data is available from the year 1950 until the present (Table 4).

Year	DJF	JFM	FMA	MAM	AMJ	MJJ	JJA	JAS	ASO	SON	OND	NDJ
1958	**1.8**	**1.6**	**1.2**	**0.9**	**0.7**	**0.6**	**0.5**	0.3	0.3	0.4	**0.5**	**0.6**
1959	**0.6**	**0.6**	**0.5**	0.3	0.2	-0.1	-0.2	-0.3	-0.1	0	0.1	0
1960	-0.1	-0.2	-0.2	-0.1	-0.1	0	0.1	0.2	0.2	0.1	0.1	0.1
1961	0	0	0	0.1	0.3	0.4	0.2	-0.1	-0.3	-0.3	-0.2	-0.1
1962	-0.2	-0.3	-0.3	-0.3	-0.2	-0.2	0	-0.1	-0.2	-0.3	-0.4	-0.5
1963	-0.4	-0.2	0.1	0.3	0.3	**0.5**	**0.8**	**1.1**	**1.2**	**1.3**	**1.4**	**1.3**
1964	**1.1**	**0.6**	0.1	-0.4	**-0.6**	**-0.6**	**-0.6**	**-0.7**	**-0.8**	**-0.8**	**-0.8**	**-0.8**
1965	**-0.60.6**	-0.3	0	0.2	**0.5**	**0.8**	**1.2**	**1.5**	**1.7**	**1.9**	**1.9**	**1.7**

Table 4. A sample of the monthly ENSO anomaly data from the CPC in units of degrees Celsius. Values represent the anomaly from the mean water temperature in the Nino 3.4 region. Values marked in red have reached the threshold of being considered El Niño while values marked in blue are considered La Niña.

The data for the IOD and SIOD both come from JAMSTEC found at (http://www.jamstec.go.jp/e/). JAMSTEC stands for Japan Agency for Marine-Earth Science and Technology and is the Japanese equivalent of NOAA and the American Satellite Service Division. This agency, like NOAA, is tasked with the monitoring of both weather and climate

data as well as aiding in the continued research of Marine Earth and Atmospheric Sciences. The IOD and SIOD data is available in index format similar to ENSO. A positive phase is when the positive temperature anomalies are in the western Indian Ocean. Similar to ENSO the base state is zero meaning that the conditions fit the long-term average. The data for these two variables was subdivided by month per year so that the analysis could be done on the months with tropical cyclone activity according to ACE. The difference between these measurements and the ENSO is that for the IOD it is a gradient measurement between the western equatorial Indian Ocean 50-70 E, 10S-10N and the southeastern equatorial Indian Ocean 90-110 Eand 10S-0N SST. The Subtropical dipole is the SST gradient found between the western 55-65E, 37-27S and eastern 90-100E, 28-18S Indian Ocean.

Atmospheric-oceanic data collected included Outgoing Longwave Radiation (OLR), shear between the 850 to 200mb level, sea surface temperatures (SSTs), and relative humidity at the 700mb level. These variables, as mentioned in Table 1, are those that are necessary for tropical cyclogenesis and the survival of the tropical cyclone outside of being displaced from the equator. OLR reveals if there is a disturbance in the area by showing areas of low radiation (or temperatures) emitted by cloud tops. This reveals where there is convection, which will lead to the growth of any relative vorticity that may be present. Shear shows if the system will be torn apart as it tries to grow in the vertical, SSTs show if there is an energy supply for the system, as tropical cyclones are warm core systems, and relative humidity shows if there is enough moisture in the region for the storm to develop or alternatively be chocked off from a lack of moisture and instability. Vector wind speed, which was used to compute shear, and relative humidity data came from the NCEP reanalysis dataset which has a timeframe of 1948 to the present. OLR data was taken from the NOAA interpolated OLR dataset with a timeframe of 1974 to the present and

SSTs were taken from NOAAs extended reconstructed SST dataset with a timeframe of 1854 to present. SST data had 2.0 degree latitude x 2.0 degree longitude grid spacing and while the remaining variables had a spacing of 2.5 degrees latitude x 2.5 degrees longitude. All the above weather variables had missing data filled in with reanalysis data.

These variables match each of the conditions needed for cyclogenesis except distance from the equator but that is standard across the world with only rare cases of systems developing closer to the equator.

Data was averaged over each sub-basin (Table 2) and entered into a linear multiple regression model using SPSS. The peak month ACE for each sub-basin was used as the dependent variable while the independent variables were ENSO, IOD, and SIOD and the reanalysis variables. This was to analyze whether the atmospheric patterns affected ACE directly or indirectly through changes in the climate oscillations. Also, the weather variable averages were input as the dependent variables and the oscillations were the independent variables. This was to determine if the oscillations impacted the climate of the Indian Ocean basin, without affecting tropical cyclone activity.

Two methods of linear regression were used: The first method is called the enter method and is the most basic form of linear regression and also the least accurate form. It is used as a first step in the analysis in developing a statistical model. To create this model you use all independent variables to see the result on the dependent variable. A second method that was used is the backwards method. It is created in the same way as the enter method but this method removes independent variables until it creates the liner regression with the most significance. This method is used to find the best statistical model using the data that has been given. This

method removes variables that lead to a lower significance in the model. If none of the independent variables lead to a significant result in the tropical cyclone ACE then the only term that will remain is a constant and it can be inferred that an outside source is the greatest influence on ACE (Landau and Everitt, 2004).

Another tweak to the model came in the form of using the 3-month or seasonal average of the peak season and also using a delayed or lagged relationship between the ACE and oscillations. A delayed average involved taking the 3-month average of the oscillations for the 3 months skewed 1 month before the 3-month average of the ACE. This means, for example, the average for the oscillations would be months ABC while the average for the Accumulated Cyclone Energy would be months BCD. The delayed average had merit because of the fact that the changes in the atmosphere can lag behind remote changes in the ocean temperature, which would be the case for ENSO.

The averaged months for the different areas are seen in Table 5. The northwestern area peaks in the 3 months of May-June-July, which is when the Intertropical Convergence Zone moves into the region, while the northeastern region peaks in the months of October-November-December when the ITCZ is moving out of the region. The Southwestern region peaks during the months of January-February-March, which is the southern hemisphere summer and would be expected. The Southeastern region is similar but slightly delayed with its 3-month average peak occurring in February-March-April.

Location	**Average/Delayed Average (ACE Value)**
Nw Arabian Sea	May-June-July (61.2)
Ne	October-November-December

Bay of Bengal	(108.5)
Sw Near Africa	January-February-March (667.4)
Se Near Australia	February-March-April (576.1)
Nw	May-June
Ne	October-November
Sw	December-January
Se	January-February

Table 5. The region and the months used to calculate the 3-month average in maximum ACE with the average ACE value. Also included is the centroid month for the time period used in the delayed average methodology in the format oscillation average month-ACE average month.

Finally, composite maps were made for each of the meteorological variables that had significance with an oscillation for each of the aforementioned regions. This was done using NOAA's Earth Systems Research Laboratories. For example OLR was a significant variable with ENSO in the Northwest region. Maps of OLR were made using composites of the strongest La Niñas and the strongest El Niños to show how each oscillation changed the weather pattern. This was done by taking a composite of the 10 strongest negative/ low event years as well as a composite of the 10 strongest positive/high years. The top 10 events are used because of data limitations. If more years were included Neutral years would skew the results. This 10-year composite method was also used because of the fact that there were many years with no storms in the basin and zero ACE. If more years had been used inactive seasons may have been factored into the composite that represents the active years. This was especially true in the Arabian Sea, which had few active years but the ones that did occur had high values of ACE.

Ten years is also sufficient to average out any outliers and discrepancies that could occur in an individual year.

9. Results

In the following section a brief description of the results of the analysis will be presented. First there will be broad overview of the results followed by individual sections for each of the study regions. In this way a complete understanding of the results of the analysis can be found from the smaller scale sub-basins to the entire Indian Ocean basin as an oceanographic and meteorological unit.

9.1 General

An initial analysis as seen in Table 6 revealed that the oscillations appear to have some correlation between them. IOD and SIOD have a significant correlation with ENSO. IOD has a positive correlation with a value of .371 while the SIOD has a negative correlation with a value of -.201. This means that positive (negative) phases of ENSO tend to associate with positive (negative) phases of IOD and negative (positive) phases of SIOD.

Correlations				
		ENSO	IOD	SIOD
ENSO	Pearson Correlation	1	.371**	-.201**
	Sig. (2-tailed)		.000	.000
	N	600	600	600
IOD	Pearson Correlation	.371**	1	.056
	Sig. (2-tailed)	.000		.170
	N	600	600	600
SIOD	Pearson Correlation	-.201**	.056	1
	Sig. (2-tailed)	.000	.170	
	N	600	600	600

Table 6. A correlation table of the climate oscillations. This analysis was done to reveal if any of the variables were correlated with one another. Results with strong correlation are marked with **

In most of the regions it was found that only ENSO was correlated favorably with the ACE. The significance of the IOD and SIOD were low enough such that they fell out of the models using the backwards method. As noted above the backwards method creates a model with the minimum amount of variables and the most significance. This occurred for both the average and delayed average methods. The only exception appeared to be in the Southeastern region near Australia where the IOD, and to a slightly lesser extent the SIOD, became significant as will be discussed in more detail below. This also relates to the SIOD having a connection with the OLR in the southwestern and southeastern regions and ACE having a strong connection with IOD. This was further studied below using the maps created by NOAAS ESRL website.

The southern region also had the highest ACE values as seen in Table 5. This is because there is a larger surface area of ocean for the tropical cyclones to develop and in general a more favorable environment for development as compared to regions in the northern half of the basin. The annual cycle of ACE for the different regions is seen below. This reveals clearly the double peak in ACE that is found in the Northern Hemisphere with the hemisphere summer peak being stronger in the Arabian Sea and the hemisphere winter peak being larger in the Bay of Bengal. Also of note is the fact that the Southern Hemisphere has a significantly higher percentage of ACE than the northern counterpart.

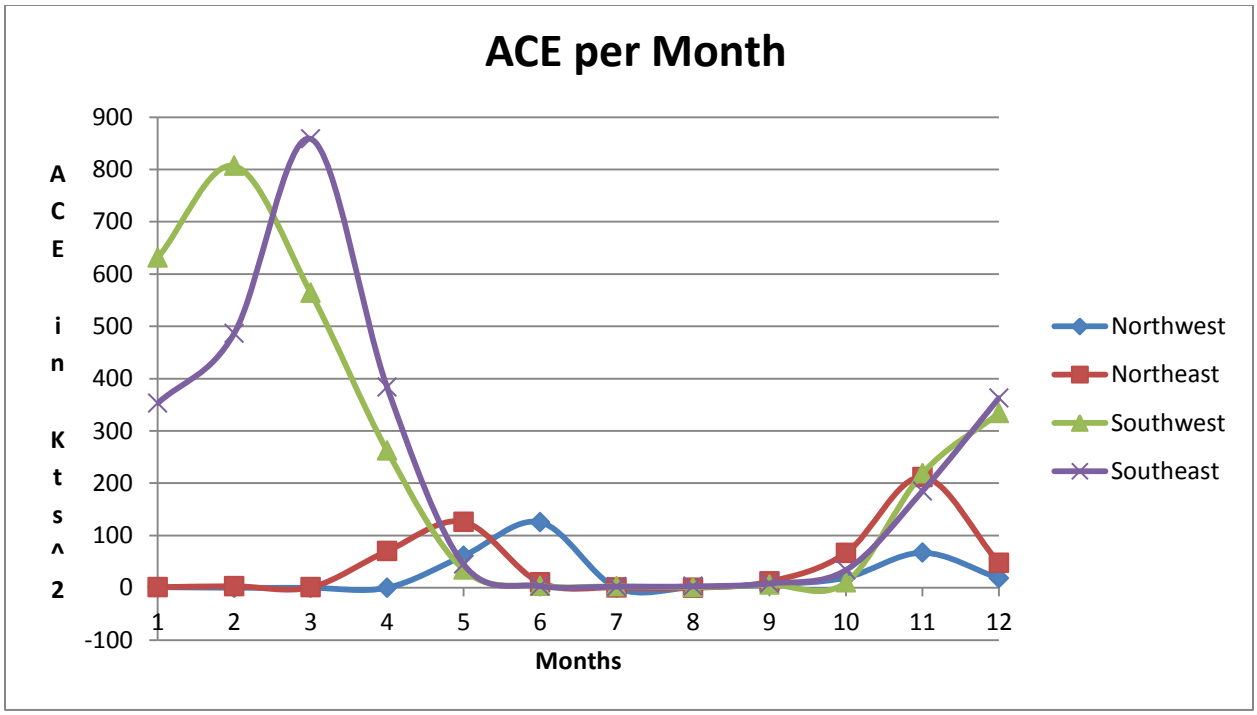

Figure 9. Timescale for ACE. This reveals ACE per month of the year. Southern Hemisphere ACE is significantly higher than Northern Hemisphere which is broken into double peaks.

9.2 Northwest

The northwest region's ACE had a significant connection with Outgoing Longwave Radiation when using the backwards methods. This was the only meteorological variable to relate to the ACE in this region with the others falling out when performing a backwards linear regression technique. The ACE also had a connection with ENSO in this region using both the average and delayed average methods. There was also a relationship found between ENSO and the weather variables specifically OLR in this region using the backwards method.

A.

Method 1	Method2	Dependent	Enso	te	Sige	IOD	ti	Sigi	SIOD	ts	Sigs	constant	tc	Sigc
Enter	Avg (MJJ)	ACE	-0.387	-2.006	0.054	0.154	0.825	0.416	0.051	0.283	0.779	1.513	2.518	0.018
Back	Avg (MJJ)	ACE	-0.317	-1.862	0.072							1.535	2.612	0.014
Enter	M-J Delay	ACE	-0.257	-1.419	0.167	0.067	0.366	0.717	0.09	0.498	0.622	1.499	2.43	0.022
Enter	Avg (MJJ)	OLR	0.409	2.225	0.034	0.01	0.056	0.956	0.107	0.623	0.538	264.4	328.431	0
Back	Avg (MJJ)	OLR	0.439	2.718	0.011							264.391	337.841	0

B.

Method1	Method2	f	fsig	R	R^2	AdjustedR^2
Enter	Avg (MJJ)	1.358	0.275	0.351	0.123	0.033
Back	Avg (MJJ)	3.466	0.072	0.317	0.101	0.072
Enter	M-J Delay	0.744	0.535	0.267	0.071	-0.025
Enter	Avg (MJJ)	2.465	0.082	0.451	0.203	0.121
Back	Avg (MJJ)	7.39	0.011	0.439	0.192	0.166

Table 7A. The above images reveal the Method that was used, the values for the variables, and the significance of the variables. Enso, IOD, and SIOD columns give the individual regression values; te, ti, and ts are the t-test values, and Sige, Sigi, and Sigs are the p-values. The t- values represent the quality of the model while the p-values represent the quality of the particular variable to the model. This is for the northwestern region analysis comparing the oscillations with ACE and weather Variables.

Table 7B. This data table shows the F values and their significances for the Methods seen in A as well as the R, R square, and Adjusted R square values for the models.

From Table 7 it can be seen that backwards method for both the ACE and the OLR retains the ENSO influence. Only the ENSO-OLR relationship is significant at the 5% level, which calls for a closer analysis of ENSO's influence on OLR in the region. This analysis is seen below.

A.

Method1	Method2	Dependent	olr	tolr	sigolr	constant	tc	sigc
Enter	Avg (MJJ)	ACE	-0.535	-2.285	0.029	91.844	0.96	0.345
Backwards	Avg (MJJ)	ACE	-0.441	-2.867	0.007	96.517	2.918	0.006

B.

Method1	Method2	f	f sig	R	R^2	adjusted R^2
Enter	Avg (MJJ)	2.345	0.076	0.482	0.232	0.133
Backwards	Avg (MJJ)	8.218	0.007	0.441	0.195	0.171

Table 8A. The above is the comparison of the significant meteorological variables with the ACE. olr gives the individual regression values; tolr the t-test values, and sigolr the p-values.

Table 8B. F values and their significances for the Methods seen in A as well as the R, R square, and Adjusted R square values for the models.

From Table 8, it can be seen that using the backwards method to compare the meteorological variables and ACE only keeps OLR as a significant variable explaining the ACE found within the region. The significance of the variable is around 0.007, significance of the model f is 0.007 and the adjusted R square is 0.171.

This analysis reveals that ACE has a negative correlation with ENSO supporting the theory that La Niña would have a favorable impact on the tropical cyclone energy. OLR is positively correlated with ENSO meaning that El Niño supports higher levels of radiation, or less convection, within this basin. Consistent, OLR is negatively correlated with ACE, which means convection is related to greater tropical cyclone energy. These results mean that favorable conditions for development are possible with a La Niña producing lower levels, on average, of OLR within the basin. These results also support the theory that ENSO is the most important player within the basin.

A.

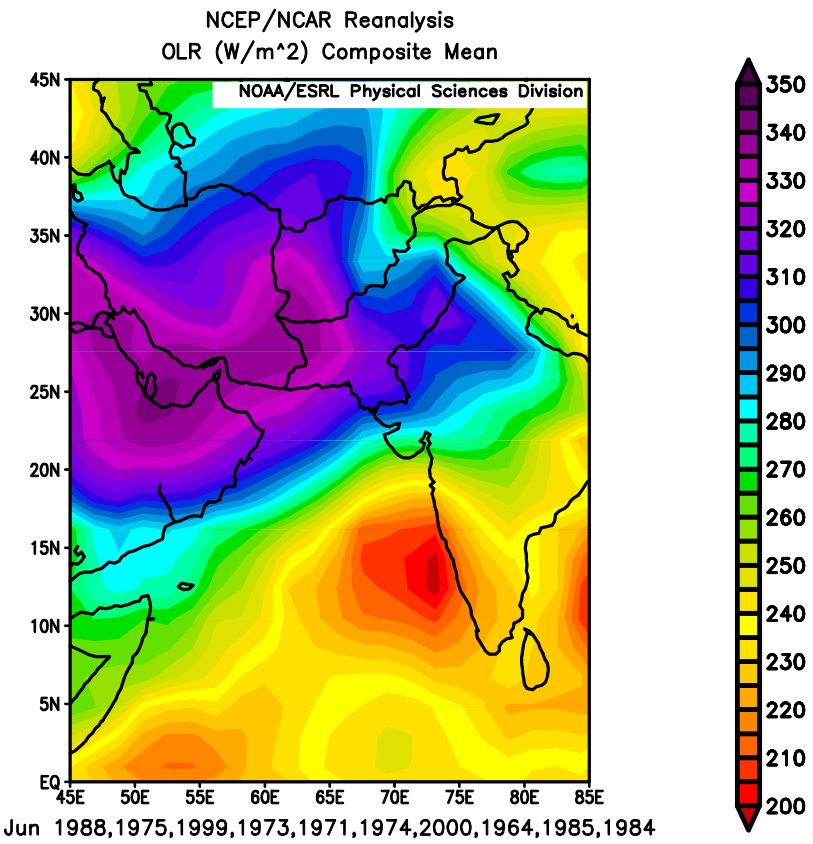
NCEP/NCAR Reanalysis
OLR (W/m^2) Composite Mean
NOAA/ESRL Physical Sciences Division
45N
40N
35N
30N
25N
20N
15N
10N
5N
EQ
45E
50E
55E
60E
65E
70E
75E
80E
85E
350
340
330
320
310
300
290
280
270
260
250
240
230
220
210
200
Jun 1988,1975,1999,1973,1971,1974,2000,1964,1985,1984

B.

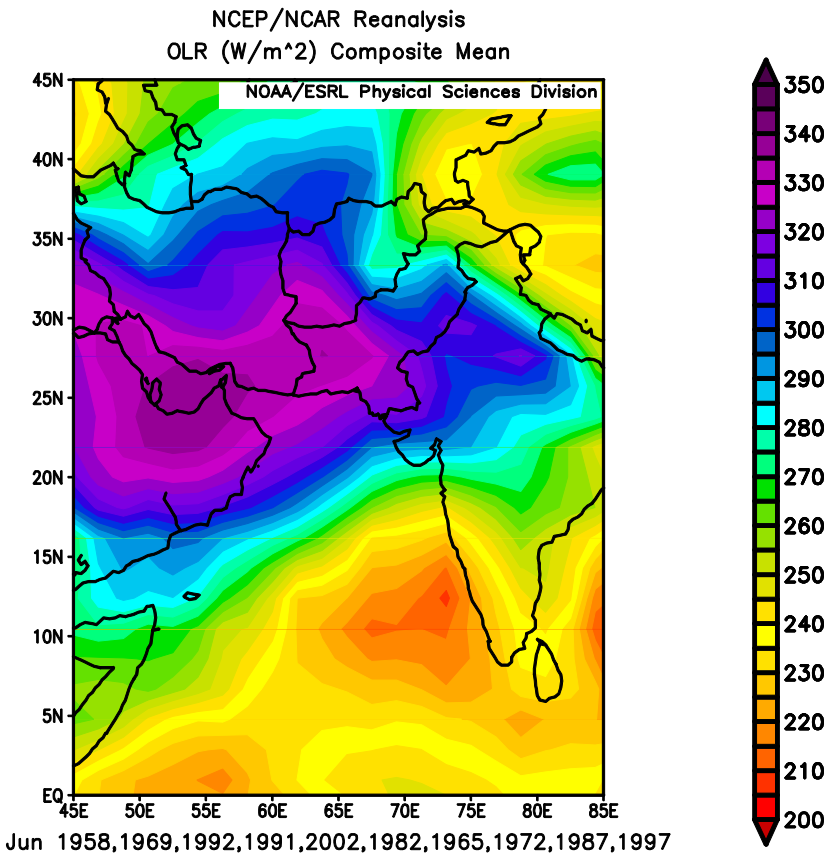
NCEP/NCAR Reanalysis
OLR (W/m^2) Composite Mean
NOAA/ESRL Physical Sciences Division
45N
40N
35N
30N
25N
20N
15N
10N
5N
EQ
45E
50E
55E
60E
65E
70E
75E
80E
85E
Jun 1958,1969,1992,1991,2002,1982,1965,1972,1987,1997
350
340
330
320
310
300
290
280
270
260
250
240
230
220
210
200

C.

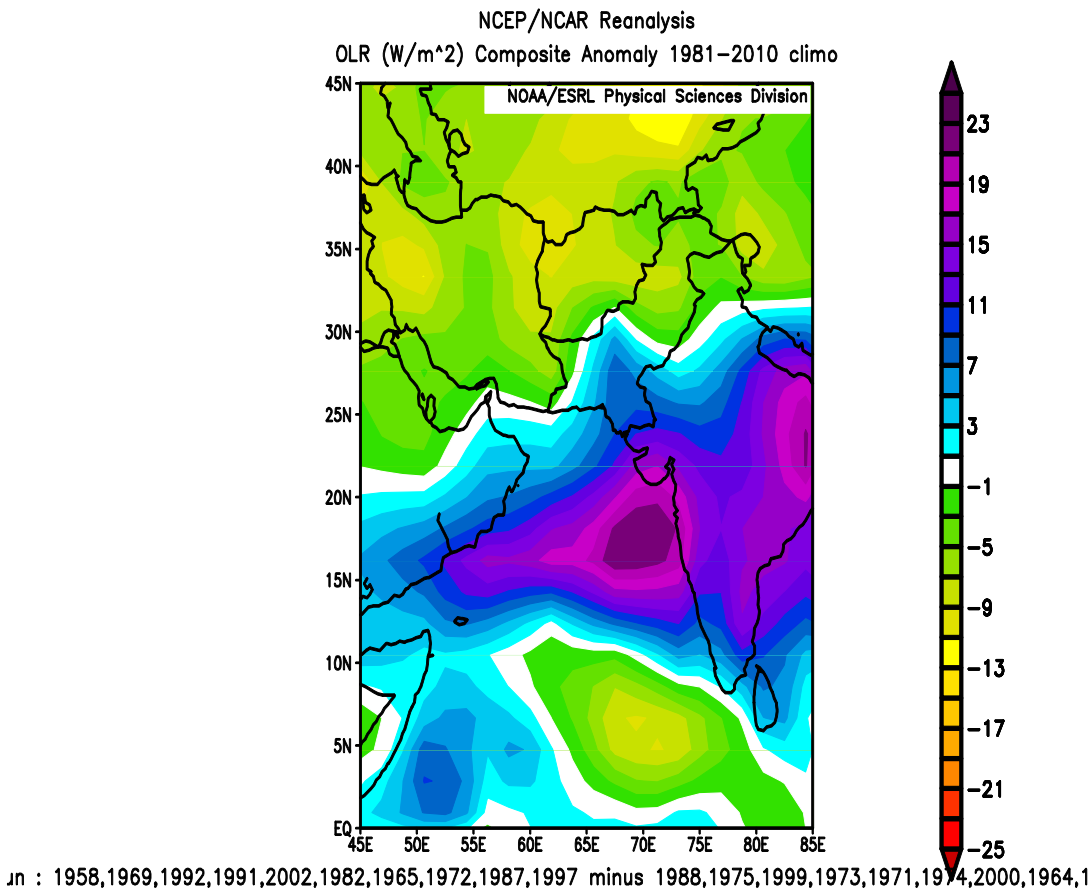

Figure 10A. Plotted is the composite of the OLR for the top 10 La Niña events for the region during the month of June. The years include are 1988, 1999, 1975, 1973, 1974, 2000, 1971, 1985, 1964, 1984

Figure 10B. Plotted is the composite of the OLR for the top 10 El Niño events for the region during the month of June. The years included are 1958, 1983, 2002, 1982, 1991, 1992, 1965, 1972, 1997, 1987.

Figure 10C. Plotted is the Difference Anomaly Composite of the OLR for the top 10 El Niño and La Niña events for the region during the month of June

Figure 10 shows composites of OLR for the 10 strongest La Niña events and 10 strongest El Niño events during the month of June to compare the differences that arise in the Northwestern Indian Ocean basin. Looking at the difference map it can be seen that OLR is

much lower over the waters during La Niña than during El Niño with values falling to or below the 200 W m^{-2} mark.

A.

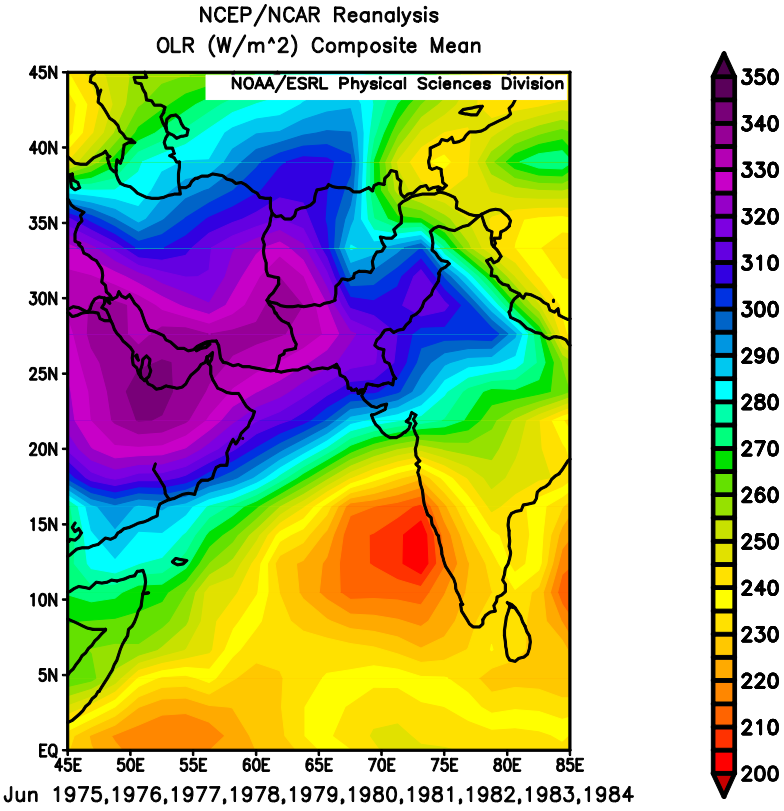

.

B.

.

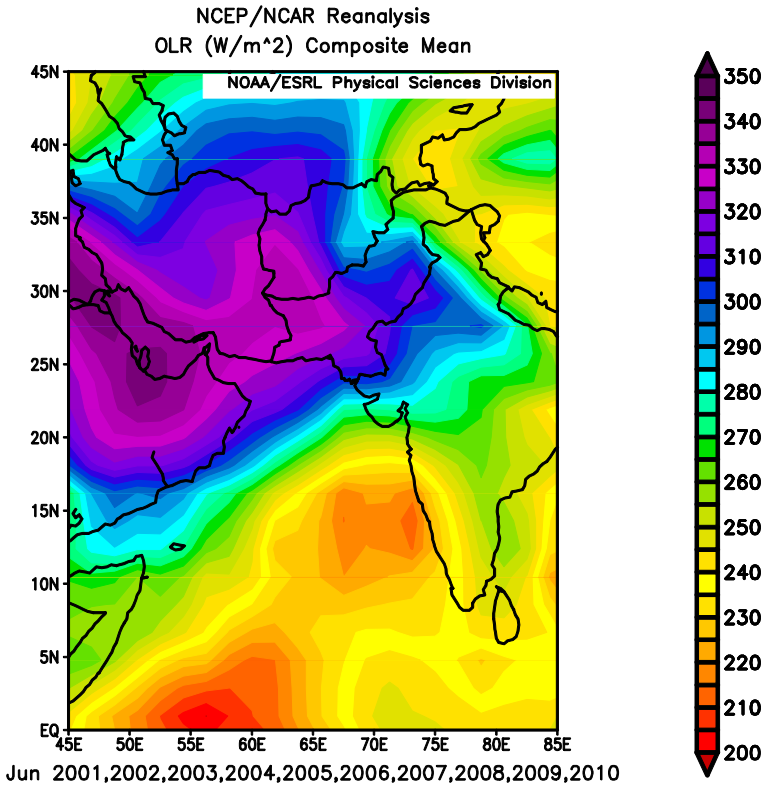
NCEP/NCAR Reanalysis
OLR (W/m^2) Composite Mean
NOAA/ESRL Physical Sciences Division
45N
40N
35N
30N
25N
20N
15N
10N
5N
EQ
45E
50E
55E
60E
65E
70E
75E
80E
85E
Jun 2001,2002,2003,2004,2005,2006,2007,2008,2009,2010
350
340
330
320
310
300
290
280
270
260
250
240
230
220
210
200

C.

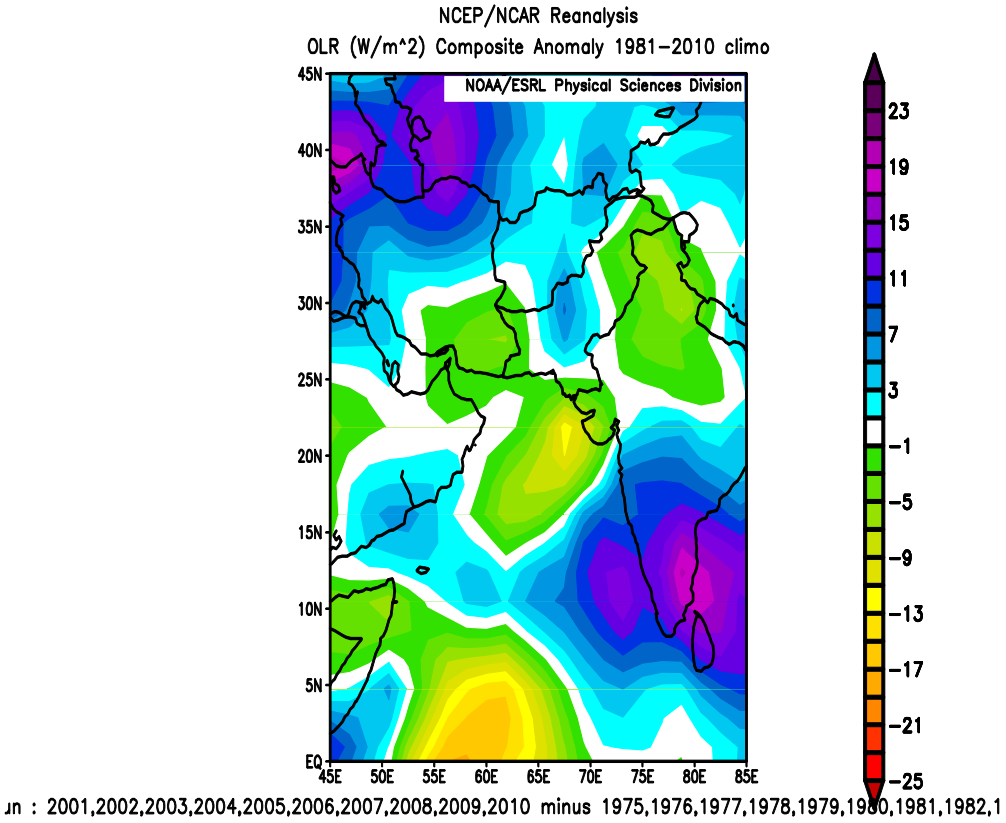

Figure 11A. Plotted is the OLR for the top 10 lowest ACE years over the region for the month of June. The years included are1975, 1976, 1977, 1978, 1979, 1980, 1981, 1982, 1983, 1984.

Figure 11B. Plotted is the OLR for the top 10 highest ACE years over the region for the month of June. The years included are, 2001, 2002, 2003, 2004, 2005, 2006, 2007, 2008, 2009, 2010

Figure 11C. Plotted is the OLR difference maps for the top 10 highest ACE years vs the lowest 10 ACE years over the region for the month of June.

Figure 11 compares the difference in OLR between years that had high ACE and low ACE. This was computed because of the correlation between tropical cyclone ACE and OLR that was found in the analysis. Interestingly, OLR during the lowest ACE years indicates greater convection off the west coast of India (a main development region, Fig. 6), which seems counterintuitive. This suggests that there are increases in disturbances that simply do not become significant tropical cyclones. However, convection is

enhanced in high ACE years in the southwest region off the coast of Somalia extending from the equator to around 10 N, suggesting a favored area of development near the southern extent of the basin (At least 5 degrees from equator). Also, convection is enhanced in the north Arabian Sea.

9.3 Northeast Region

The northeast region ACE had a significant negative correlation with ENSO using the backwards method. One noteworthy result is that the northeast region oddly had no significant connection between ACE and any of the significant meteorological variables using the backwards method. There was however a strong connection between ENSO and Shear, OLR, and SST in this region but surprisingly none of these variables had any influence on ACE in this region.

A.

Method1	Method2	Dependent	Enso	te	Sige	IOD	ti	Sigi	SIOD	Ts	Sigs	constant	tc
Enter	Avg (OND)	ACE	-0.582	-2.619	0.013	0.007	0.031	0.976	-0.309	-1.681	0.102	2.765	4.814
Back	AVG (OND)	ACE	-0.578	-3.452	0.002				-0.311	-1.859	0.072	2.765	4.89
Enter	O-N Delay	ACE	-0.49	-2.029	0.051	0.064	0.244	0.809	-0.206	-1.152	0.258	2.729	4.591
Back	O-N Delay	ACE	-0.412	-2.636	0.013							2.8	4.722
Enter	Avg (OND)	Shear	-0.396	-1.647	0.109	-0.044	-0.168	0.867	-0.204	-1.027	0.312	4.808	20.535
Back	Avg (OND)	Shear	-0.335	-2.073	0.046							4.814	20.851
Enter	Avg (OND)	OLR	0.433	1.897	0.067	0.05	0.204	0.839	-0.017	-0.091	0.928	243.635	459.425
Back	Avg (OND)	OLR	0.477	3.165	0.003							243.633	473.39
Enter	Avg (OND)	SST	0.269	1.123	0.27	0.101	0.39	0.699	-0.056	-0.282	0.779	28.561	430.102
Back	Avg (OND)	SST	0.369	2.313	0.027							28.561	441.16
Enter	Avg (OND)	RH	0.079	0.309	0.759	0.118	0.431	0.67	-0.005	-0.024	0.981	29.746	35.955

B.

Method1	Method2	Sigc	f	fsig	R	R^2	AdjustedR^2
Enter	Avg (OND)	0	3.885	0.018	0.517	0.267	0.198
Back	AVG (OND)	0	6.009	0.006	0.517	0.267	0.198
Enter	O-N Delay	0	3.029	0.044	0.47	0.221	0.148
Back	O-N Delay	0	6.947	0.013	0.412	0.17	0.145
Enter	Avg (OND)	0	1.766	0.173	0.377	0.142	0.062
Back	Avg (OND)	0	4.297	0.046	0.335	0.112	0.086
Enter	Avg (OND)	0	3.176	0.037	0.479	0.229	0.157
Back	Avg (OND)	0	10.019	0.003	0.477	0.228	0.205
Enter	Avg (OND)	0	1.82	0.163	0.382	0.146	0.066
Back	Avg (OND)	0	5.349	0.027	0.369	0.136	0.111
Enter	Avg (OND)	0	0.386	0.764	0.187	0.035	-0.056

Table 9A. Enso, IOD, and SIOD columns give the individual regression values; te, ti, and ts are the t-test values, and Sige, Sigi, and Sigs are the p-values. This is for the northeastern region analysis comparing the oscillations with ACE and weather Variables.

Table 9B. F values and their significances for the Methods seen in A as well as the R, R square, and Adjusted R square values for the models.

Table 9 shows that ENSO is favorable as a forcing for all the variables, including ACE. It also shows that the SIOD contributes to ACE as well (although the p-value is above 0.05). The model's adjusted R squares range from a low of -0.056 to a high of 0.198 (which is between ENSO and ACE)

As with the Northwest region, in this region ACE and ENSO are negatively correlated. Shear also has a negative correlation with ENSO while OLR and SST have a positive correlation. This reveals that La Niña leads to lower shear and lower OLR suggesting more disturbances, and higher ACE. However SSTs are higher during an El Niño. This is consistent with Camargo et al.

(2007) that OLR and especially shear are more important factors than SSTs for this particular basin.

A.

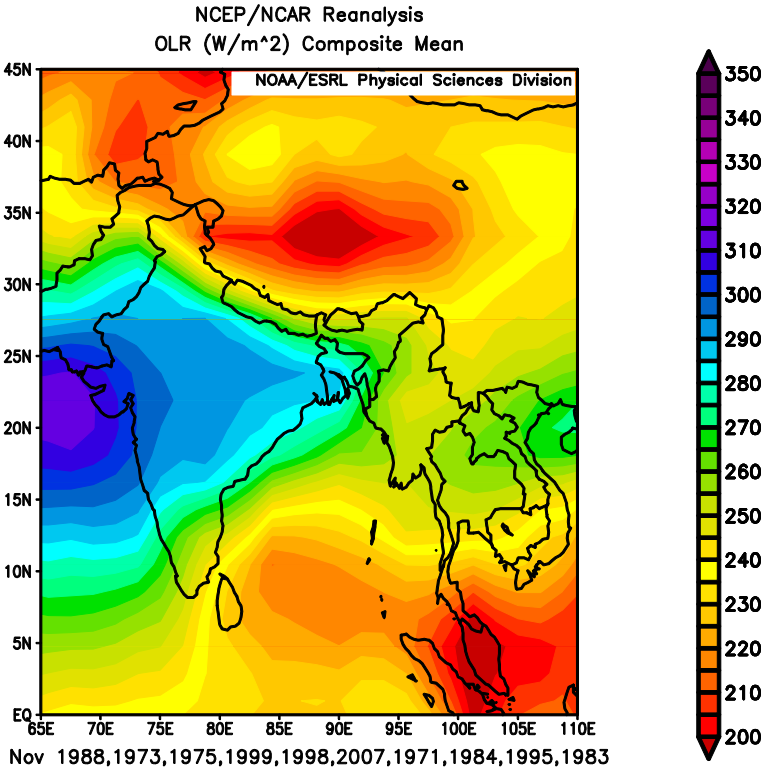

B.

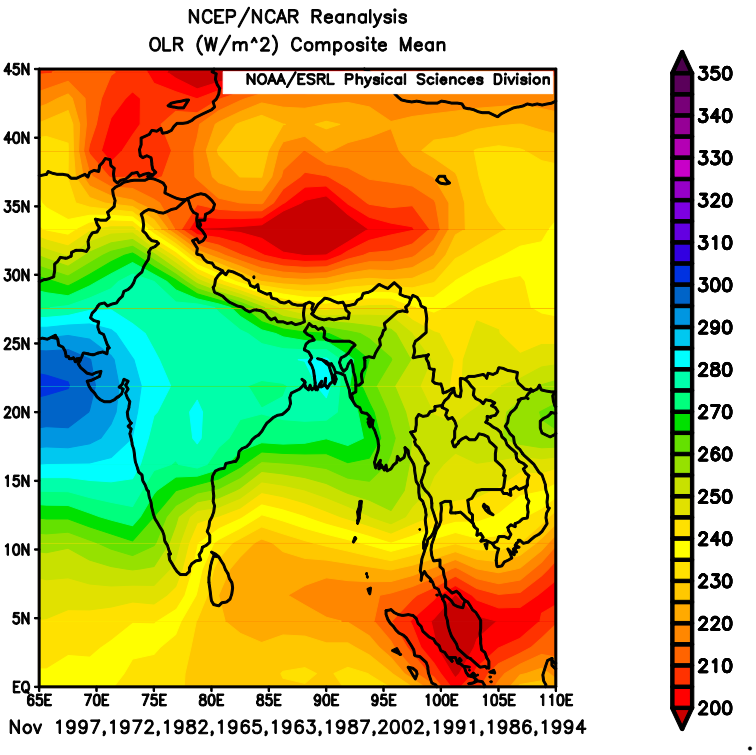
NCEP/NCAR Reanalysis
OLR (W/m^2) Composite Mean
NOAA/ESRL Physical Sciences Division
45N
40N
35N
30N
25N
20N
15N
10N
5N
EQ
65E
70E
75E
80E
85E
90E
95E
100E
105E
110E
Nov 1997,1972,1982,1965,1963,1987,2002,1991,1986,1994
350
340
330
320
310
300
290
280
270
260
250
240
230
220
210
200

C.

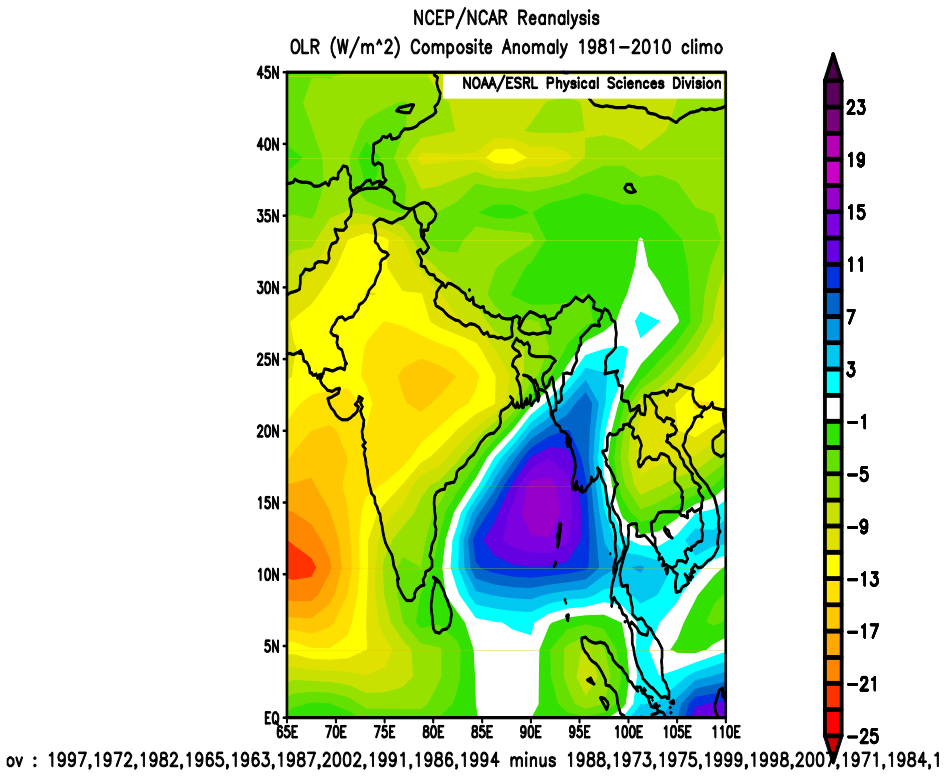
NCEP/NCAR Reanalysis
OLR (W/m^2) Composite Anomaly 1981-2010 climo
NOAA/ESRL Physical Sciences Division
45N
40N
35N
30N
25N
20N
15N
10N
5N
EQ
65E
70E
75E
80E
85E
90E
95E
100E
105E
110E
23
19
15
11
7
3
-1
-5
-9
-13
-17
-21
-25
ov : 1997,1972,1982,1965,1963,1987,2002,1991,1986,1994 minus 1988,1973,1975,1999,1998,2007,1971,1984,1

D.

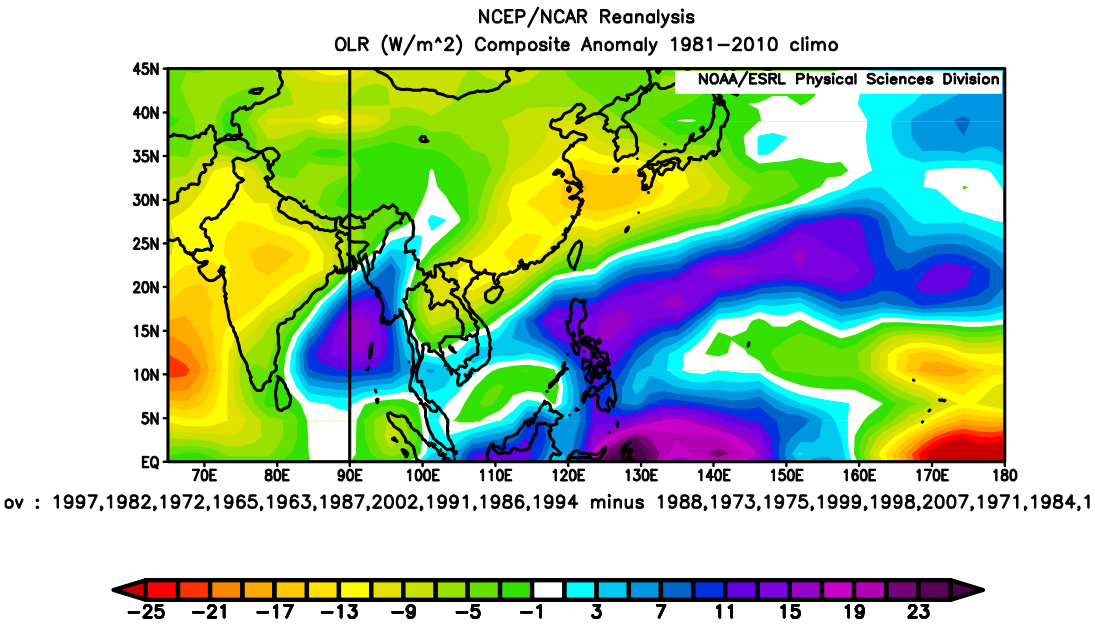

Figure 12A. Plotted is the composite of the OLR for the top 10 La Niña events for the region during the month of November. The years included are 1988, 1973, 1975, 1999, 1998, 2007, 1971, 1984, 1995, 1983.

Figure 12B. Plotted is the composite of the OLR for the top 10 El Niño events for the region during the month of November. The years included are 1994, 1986, 1991, 2002, 1987, 1963, 1965, 1982, 1972, 1997.

Figure 12C. Plotted is the composite anomaly of the OLR for the top 10 El Niño events vs the top 10 La Niña even for the region during the month of November.

Figure 12D. Plotted is an extended difference composite into the Western Pacific.

As earlier in the analysis, Figure 12 compares OLR between ENSO phases. The composite years were for the month of November and reveal a similar result. During El Niño the OLR is higher than during the La Niña years. The lower values of OLR also extend greater into the subtropical regions during La Niña. This is clearly seen in the difference maps. The map is expanded (Fig. 12d) to show the differences between El Niño and La Niña in the Western Pacific. These differences show the expected result with OLR being higher over the Maritime

Continent and lower over the central Pacific, which is typical during an El Niño event. This is further proof that the method is working correctly.

A.

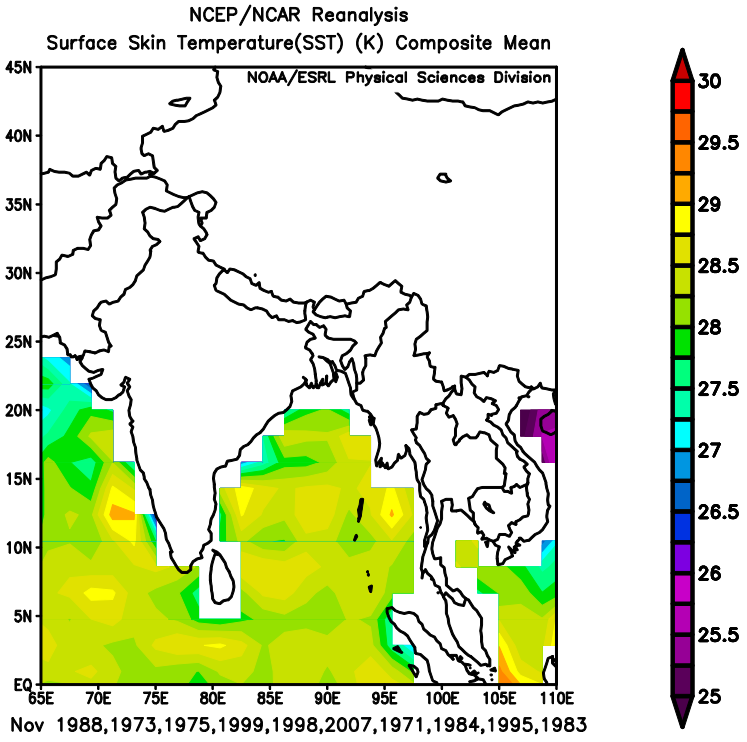

B.

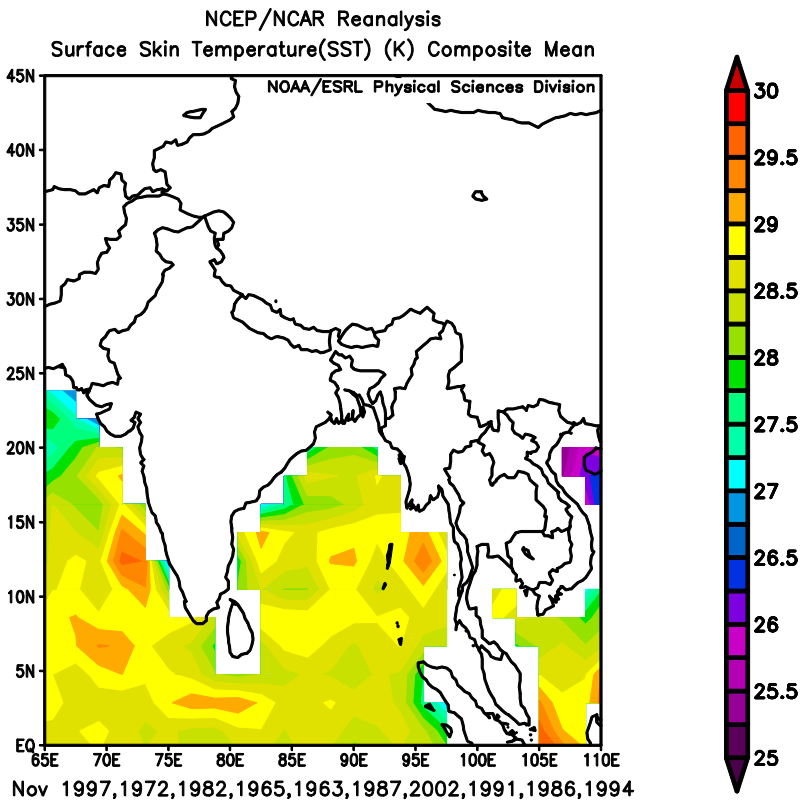
NCEP/NCAR Reanalysis
Surface Skin Temperature(SST) (K) Composite Mean
NOAA/ESRL Physical Sciences Division
45N
40N
35N
30N
25N
20N
15N
10N
5N
EQ
65E
70E
75E
80E
85E
90E
95E
100E
105E
110E
Nov 1997,1972,1982,1965,1963,1987,2002,1991,1986,1994
30
29.5
29
28.5
28
27.5
27
26.5
26
25.5
25

C.

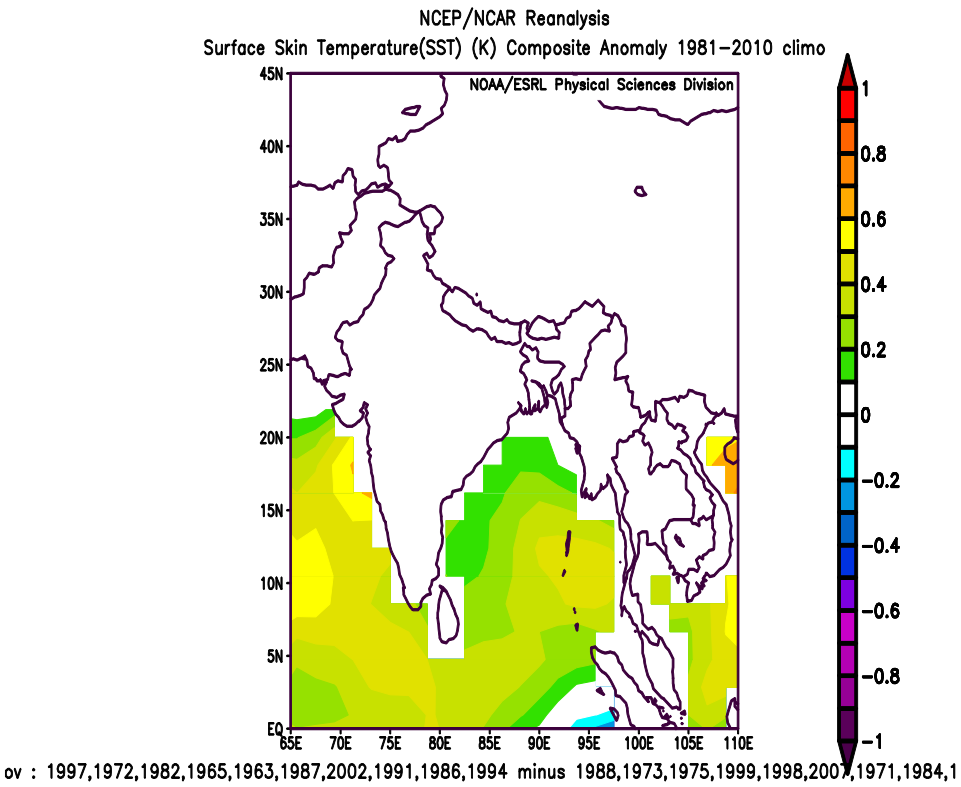

Figure 13A. Plotted are the SST's composite from the top 10 strongest November La Niña events in Northeastern region of the Indian Ocean Basin. The years included are 1988, 1973, 1975, 1999, 1998, 2007, 1971, 1984, 1995, 1983.

Figure 13B. Plotted are the SST's composite for the top 10 strongest November El Niño events in the Northeastern region of the Indian Ocean Basin. The years included are 1994, 1986, 1991, 2002, 1987, 1963, 1965, 1982, 1972, 1997.

Figure 13C. Plotted are the SST's composite anomalies for the top 10 strongest November El Niño events vs the top 10 strongest La Niña events in the Northeastern region of the Indian Ocean Basin

During the month of November it can be seen from Figure 13 that El Niño has a positive relationship with SSTs within this region. The spatial coverage of 28.5 degrees Celsius and above is increased. There is also an increase in the pockets of warmer water approaching 29.5 degrees Celsius.

A.

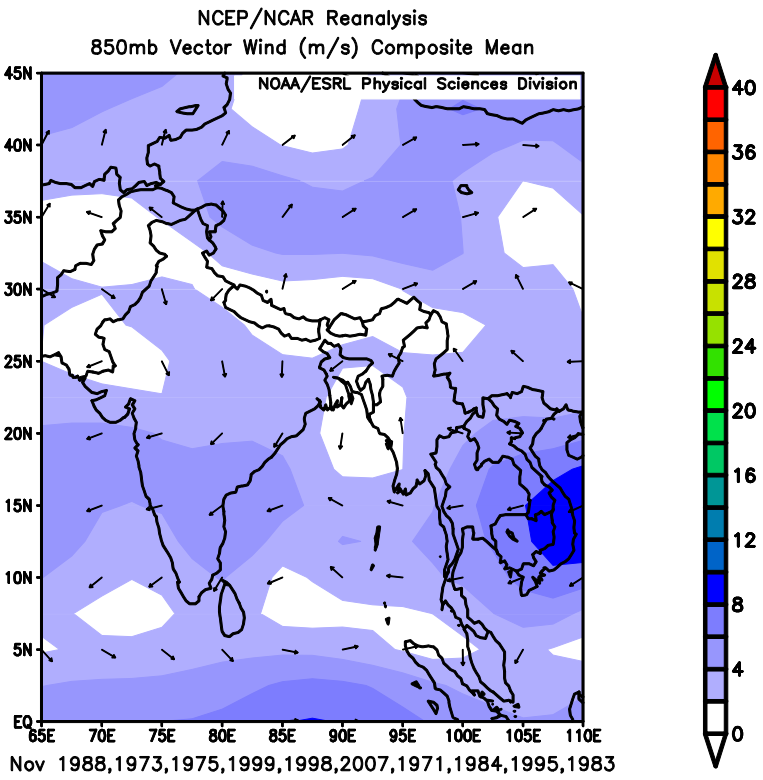
NCEP/NCAR Reanalysis
850mb Vector Wind (m/s) Composite Mean
NOAA/ESRL Physical Sciences Division
45N
40N
35N
30N
25N
20N
15N
10N
5N
EQ
65E
70E
75E
80E
85E
90E
95E
100E
105E
110E
Nov 1988,1973,1975,1999,1998,2007,1971,1984,1995,1983
40
36
32
28
24
20
16
12
8
4
0

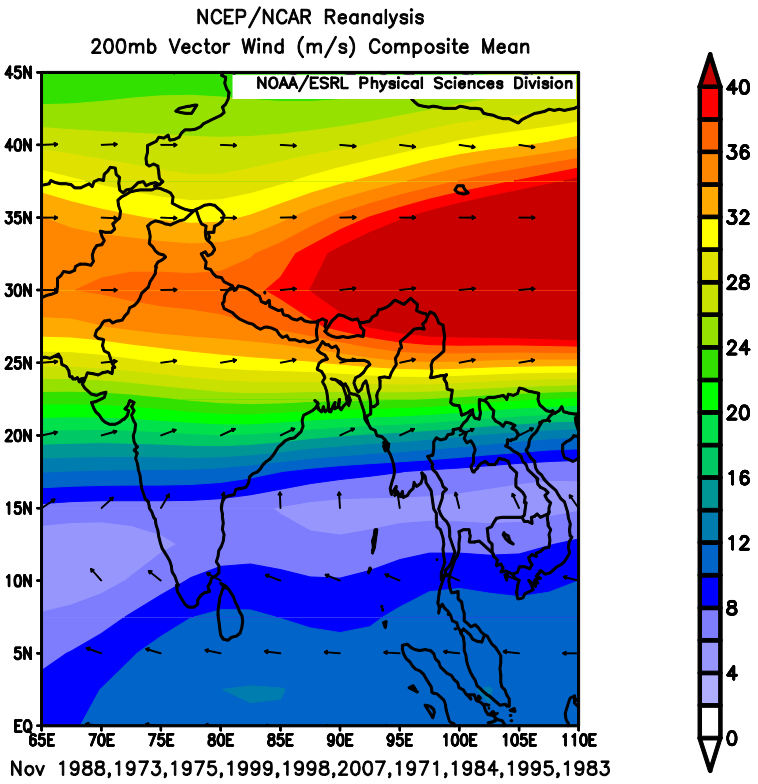
NCEP/NCAR Reanalysis
200mb Vector Wind (m/s) Composite Mean
NOAA/ESRL Physical Sciences Division
45N
40N
35N
30N
25N
20N
15N
10N
5N
EQ
65E
70E
75E
80E
85E
90E
95E
100E
105E
110E
40
36
32
28
24
20
16
12
8
4
0
Nov 1988,1973,1975,1999,1998,2007,1971,1984,1995,1983

B.

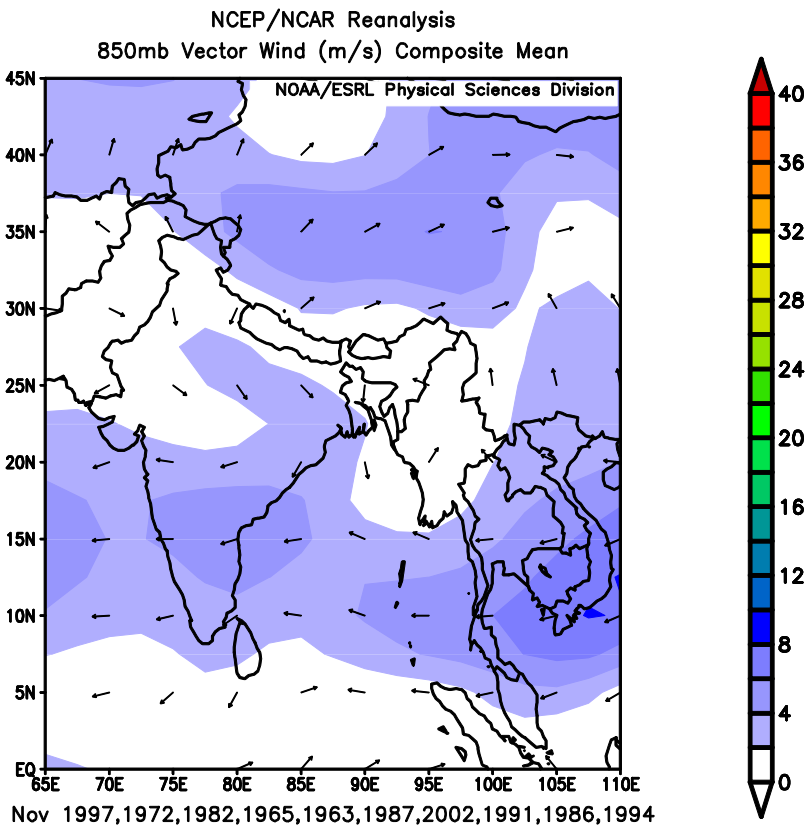
NCEP/NCAR Reanalysis
850mb Vector Wind (m/s) Composite Mean
NOAA/ESRL Physical Sciences Division
45N
40N
35N
30N
25N
20N
15N
10N
5N
EQ
65E
70E
75E
80E
85E
90E
95E
100E
105E
110E
Nov 1997,1972,1982,1965,1963,1987,2002,1991,1986,1994
40
36
32
28
24
20
16
12
8
4
0

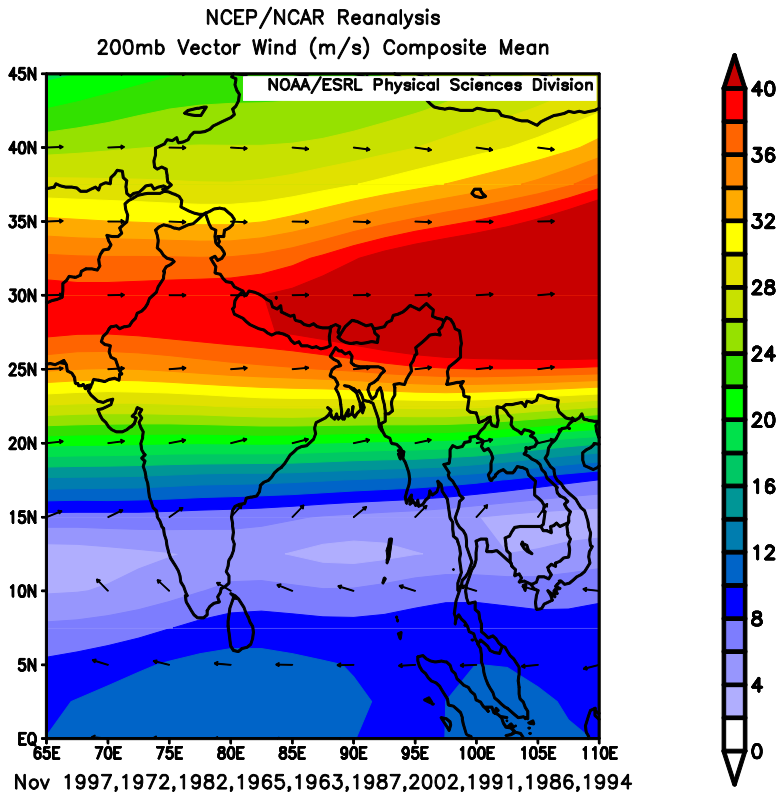
NCEP/NCAR Reanalysis
200mb Vector Wind (m/s) Composite Mean
NOAA/ESRL Physical Sciences Division
45N
40N
35N
30N
25N
20N
15N
10N
5N
EQ
65E
70E
75E
80E
85E
90E
95E
100E
105E
110E
40
36
32
28
24
20
16
12
8
4
0
Nov 1997,1972,1982,1965,1963,1987,2002,1991,1986,1994

C.

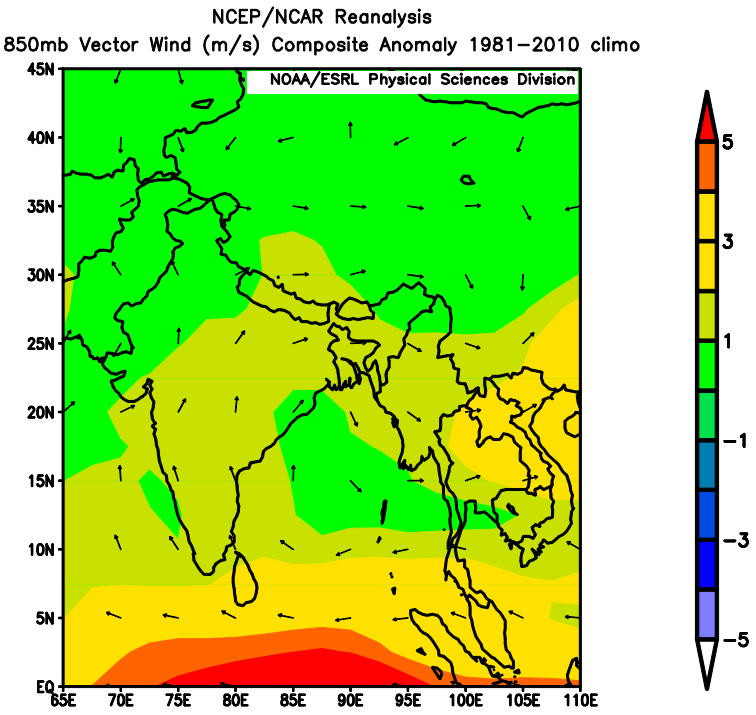

ov : 1997,1972,1982,1965,1963,1987,2002,1991,1986,1994 minus 1988,1973,1975,1999,1998,2007,1971,1984,1

.

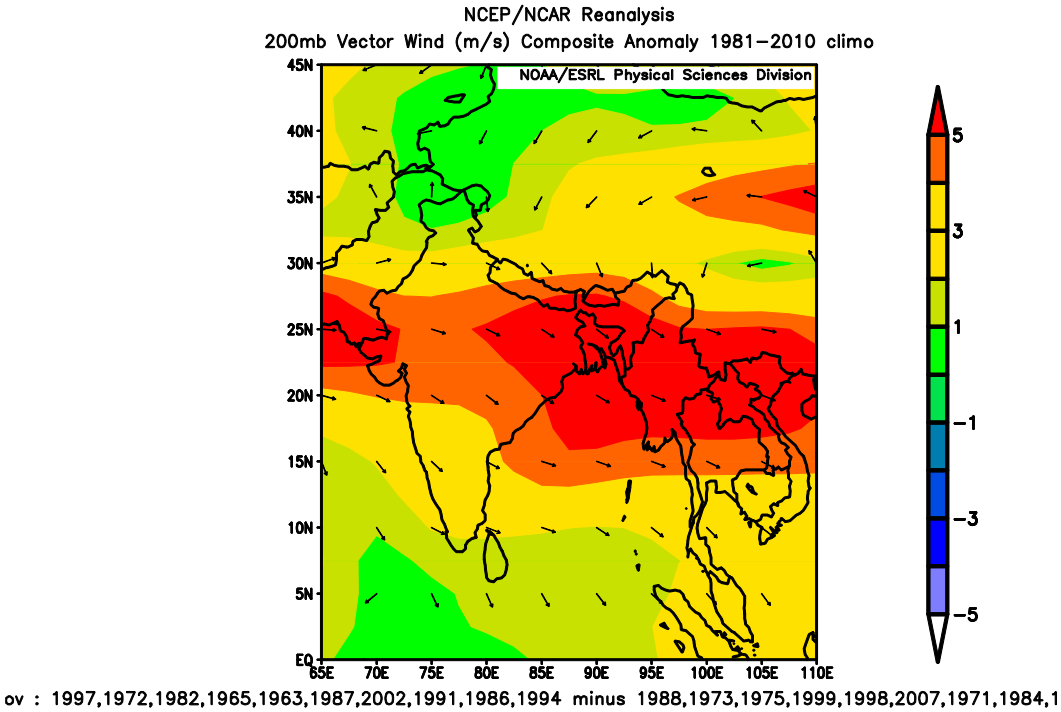

Figure 14A. Plotted are the 850mb winds and 200 mb winds for this region during the peak La Niña months (ten Novembers). . The years included are 1988, 1973, 1975, 1999, 1998, 2007, 1971, 1984, 1995, 1983.

Figure 14B. Plotted are the 850mb winds and 200 mb winds for this region during the peak El Niño months (ten Novembers). The years included are 1994, 1986, 1991, 2002, 1987, 1963, 1965, 1982, 1972, 1997.

Figure 14C. Plotted are the difference maps for the 850mb winds and 200 mb winds for this region during the peak El Niño/La Niña months (ten Novembers a piece).

The influence on wind shear can be seen by breaking down the wind shear into its component forms. The standard wind shear levels are around 850mb for the lower level and around 200mb for the upper level. In this case, even though ENSO has a negative correlation with wind shear it doesn't appear to have a significant result on the apparent weather pattern. The band of high shear associated with the midlatitudes westerlies remains to the north of the basin at all times.

9.4 Southwest

The southwest region is the location with no significant results. There was no significant relationship between any of the oscillations and the ACE using the preferred backwards method. There was also no connection between the ACE and any of the main meteorological variables used in this study. However OLR in this region had a positive relationship with the SIOD and SSTs had a positive relationship with ENSO. This means that the oscillations are influencing the variables but there appears to be no significant impact on the ACE by an oscillation or a weather variable in this region.

A.

Method1	Method2	Dependent	Enso	te	Sige	IOD	ti	Sigi	SIOD	Ts	Sigs	constant	tc	Sigc
Enter	AVG (JFM)	ACE	-0.062	-0.309	0.76	0.084	0.427	0.673	0.026	0.123	0.903	17.403	5.501	0
Enter	D-J Delay	ACE	-0.133	-0.616	0.544	0.289	1.312	0.201	0.019	0.093	0.927	20.101	6.289	0
Enter	Avg (JFM)	Shear	0.244	1.152	0.261	0.119	0.586	0.563	0.32	1.426	0.167	4.913	8.147	0
Enter	AVG (JFM)	OLR	0.091	0.444	0.661	-0.027	-0.135	0.893	0.482	2.229	0.035	235.06	376.828	0
Backwards	AVG (JFM)	OLR							0.435	2.465	0.021	235.127	411.471	0
Enter	AVG (JFM)	SST	0.641	3.479	0.002	-0.002	-0.013	0.99	0.174	0.893	0.381	27.484	561.873	0
Backwards	AVG (JFM)	SST	0.568	3.522	0.002							27.496	614.813	0
Enter	AVG (JFM)	RH	-0.02	-0.098	0.922	0.311	1.565	0.131	-0.405	-1.849	0.077	46.975	64.976	0

B.

Method1	Method2	f	fsig	R	R^2	AdjustedR^2
Enter	AVG (JFM)	0.137	0.937	0.12	0.014	-0.091
Enter	D-J Delay	0.655	0.587	0.27	0.073	-0.038
Enter	Avg (JFM)	1.258	0.311	0.369	0.136	0.028
Enter	AVG (JFM)	1.952	0.148	0.443	0.196	0.096
Backwards	AVG (JFM)	6.077	0.021	0.435	0.189	0.158
Enter	AVG (JFM)	4.265	0.015	0.59	0.348	0.266
Backwards	AVG (JFM)	12.407	0.002	0.568	0.323	0.297
Enter	AVG (JFM)	1.677	0.199	0.416	0.173	0.07

Table 10A. Enso, IOD, and SIOD columns give the individual regression values; te, ti, and ts are the t-test values, and Sige, Sigi, and Sigs are the p-values. This is for the northeastern region analysis comparing the oscillations with ACE and weather Variables.

Table 10B. F values and their significances for the Methods seen in A as well as the R, R square, and Adjusted R square values for the models.

Table 10 shows that for this region SIOD has an influence on OLR and ENSO has influence on SSTs but that none of the major oscillations have a significant influence using the backwards method on the ACE. The meteorological variables also do not tend to have a strong influence on ACE.

This region's anomalies show OLR being positively correlated with the SIOD and SST being positively correlated with ENSO. This reveals that favorable conditions for development in this region would tend to occur with a negative phase of the SIOD and an El Niño event. This would bring lower levels of OLR into the region as well as higher ocean temperatures within the main developmental areas. This is at odds with the phase of the SIOD, which would bring warmer water anomalies into the southern portion of this region.

A.

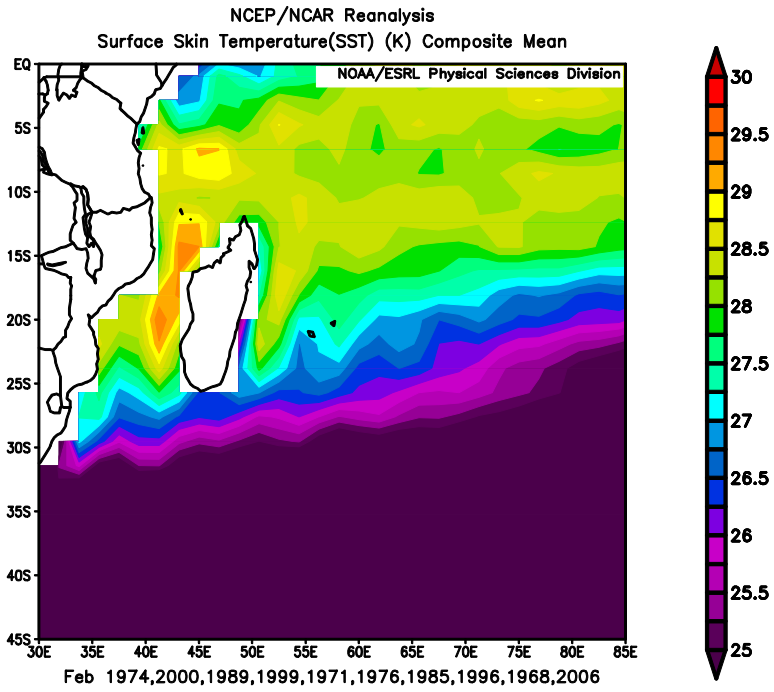
NCEP/NCAR Reanalysis
Surface Skin Temperature(SST) (K) Composite Mean
NOAA/ESRL Physical Sciences Division
EQ
5S
10S
15S
20S
25S
30S
35S
40S
45S
30E
35E
40E
45E
50E
55E
60E
65E
70E
75E
80E
85E
Feb 1974,2000,1989,1999,1971,1976,1985,1996,1968,2006
30
29.5
29
28.5
28
27.5
27
26.5
26
25.5
25

B.

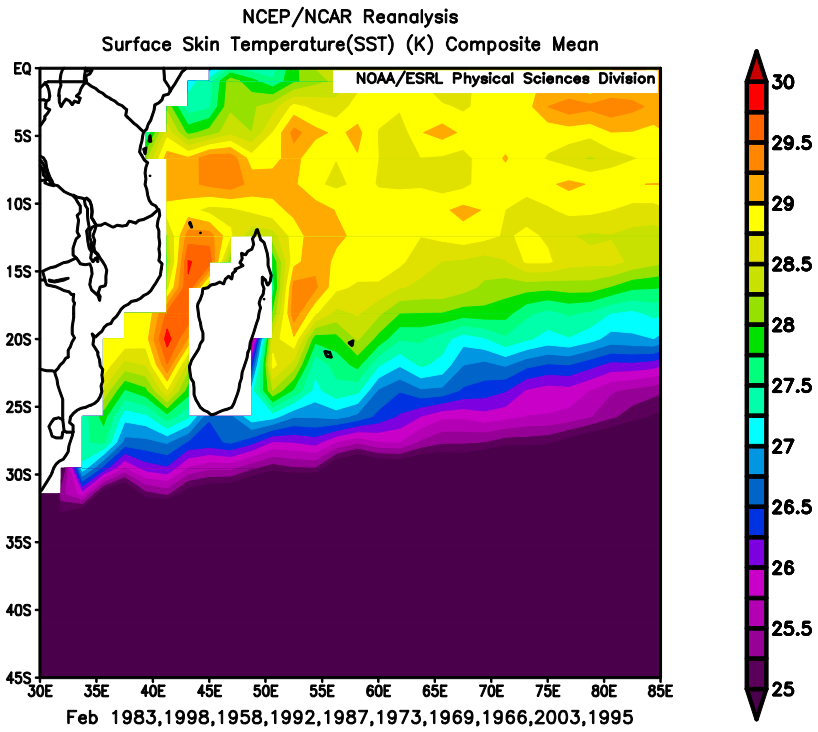
NCEP/NCAR Reanalysis
Surface Skin Temperature(SST) (K) Composite Mean
NOAA/ESRL Physical Sciences Division
EQ
5S
10S
15S
20S
25S
30S
35S
40S
45S
30E
35E
40E
45E
50E
55E
60E
65E
70E
75E
80E
85E
Feb 1983,1998,1958,1992,1987,1973,1969,1966,2003,1995
30
29.5
29
28.5
28
27.5
27
26.5
26
25.5
25

C.

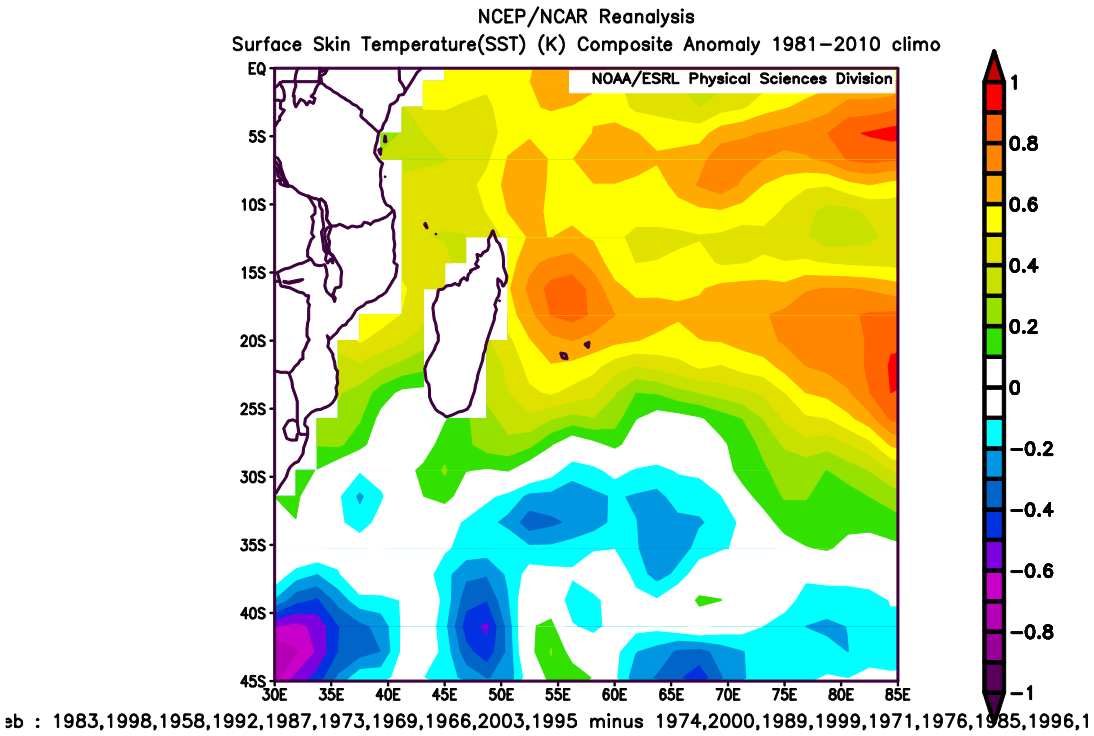

Figure 15A. The sea surface temperatures for southwestern region for the top 10 strongest February La Niñas. The years included are 1974, 2000, 1989, 1999, 1971, 1976, 1985, 1996, 1968, 2006.

Figure 15B. The sea surface temperatures for the southeastern region for the top 10 strongest February El Niños. 1995, 2003, 1966, 1969, 1973, 1987, 1992, 1958, 1998, 1983.

Figure 15C. The sea surface temperature anomalies for the southeastern region for the top 10 strongest February El Niños vs La Niñas.

Figure 15 shows the correlation of Sea Surface Temperatures with ENSO in this region. The El Niño years have an expansive area of warm waters with the warmest waters approaching 30 degrees Celsius centered near the island of Madagascar. The La Niña years on the other hand are cooler with temperatures peaking around 29 degrees Celsius, with again the warmest waters being centered on the island. The difference maps reveal that the water temperatures are about one degree warmer near the island.

A.

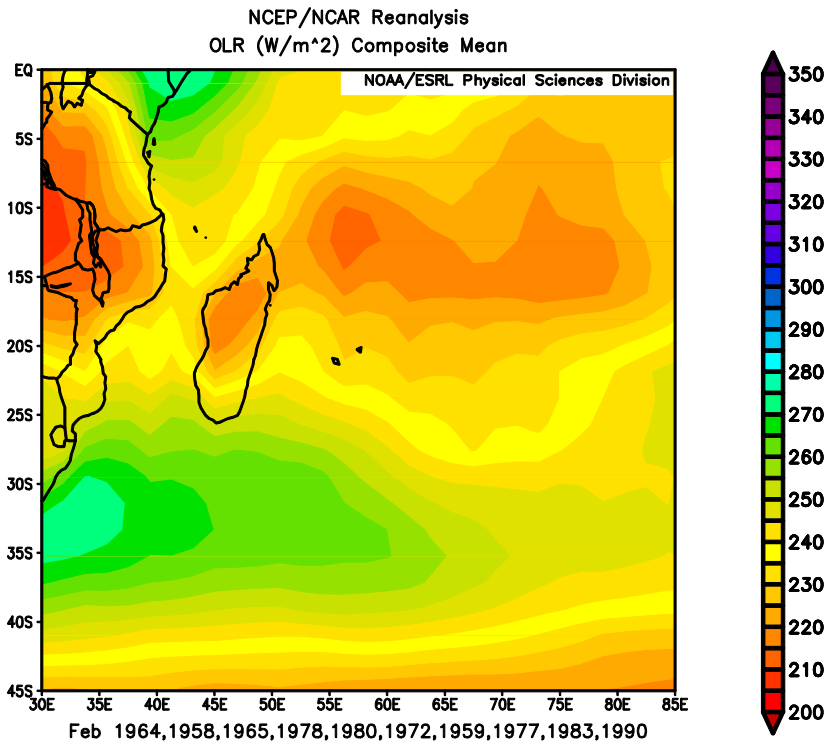
NCEP/NCAR Reanalysis
OLR (W/m^2) Composite Mean
NOAA/ESRL Physical Sciences Division
EQ
5S
10S
15S
20S
25S
30S
35S
40S
45S
30E
35E
40E
45E
50E
55E
60E
65E
70E
75E
80E
85E
Feb 1964,1958,1965,1978,1980,1972,1959,1977,1983,1990
350
340
330
320
310
300
290
280
270
260
250
240
230
220
210
200

B.

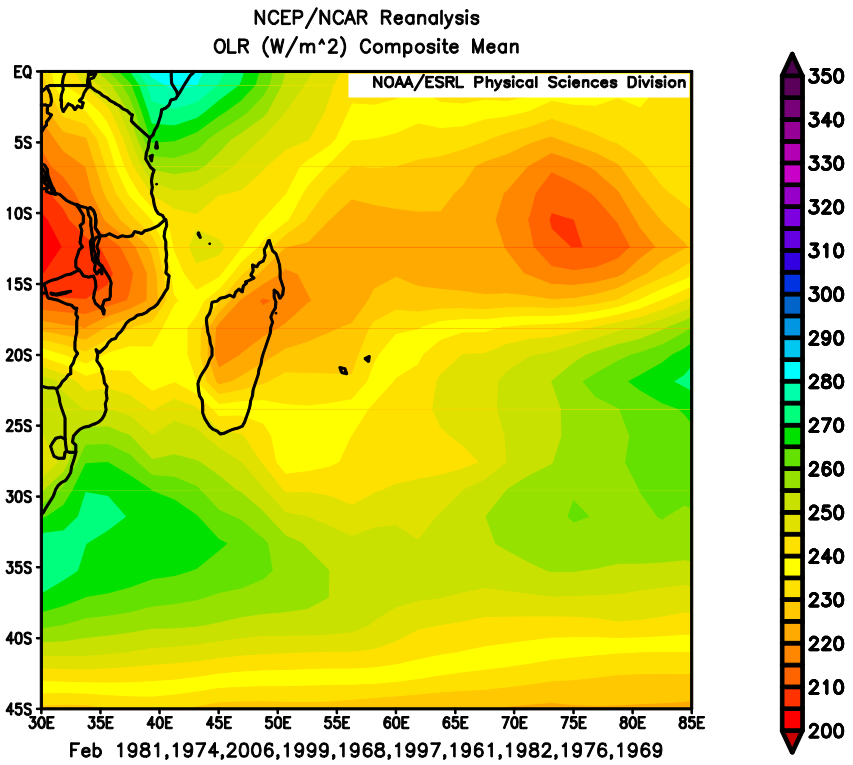
NCEP/NCAR Reanalysis
OLR (W/m^2) Composite Mean
NOAA/ESRL Physical Sciences Division
EQ
5S
10S
15S
20S
25S
30S
35S
40S
45S
30E
35E
40E
45E
50E
55E
60E
65E
70E
75E
80E
85E
Feb 1981,1974,2006,1999,1968,1997,1961,1982,1976,1969
350
340
330
320
310
300
290
280
270
260
250
240
230
220
210
200

C.

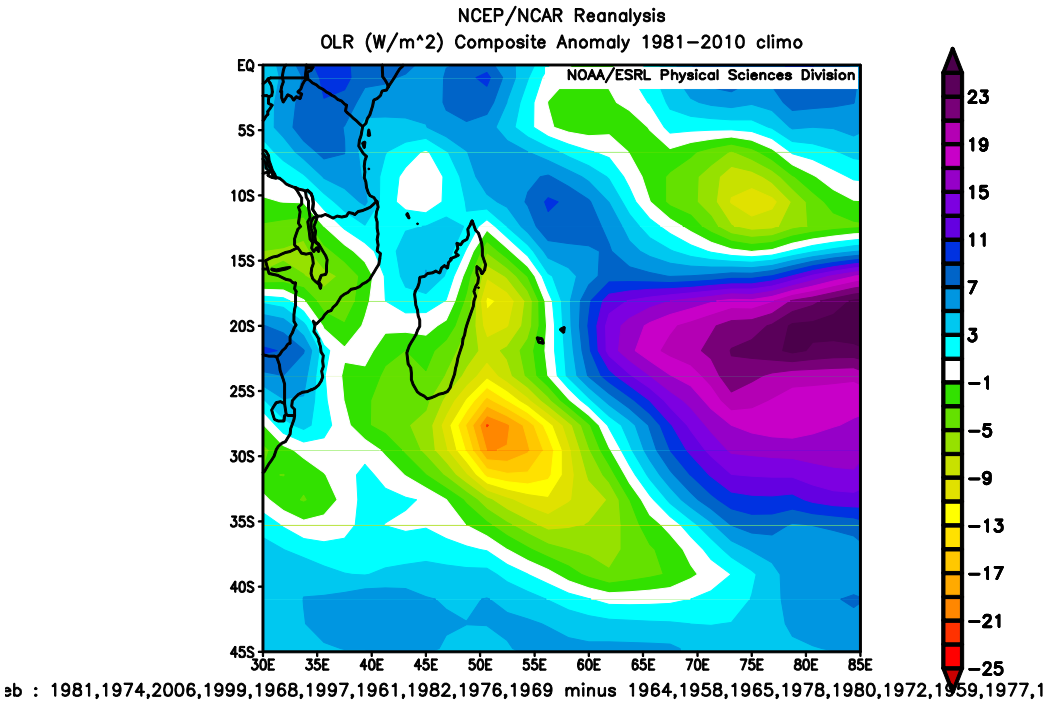

Figure 16A. February OLR averaged over the top 10 strongest negative SIOD events in the southwestern portion of the basin. The years included are 1964, 1958, 1965, 1978, 1980, 1972, 1959, 1977, 1983, 1990.

Figure 16B. February OLR averaged over the top 10 strongest positive SIOD events in the southwestern portion of the basin. The years included are 1969, 1976, 1982, 1961, 1997, 1968, 1999, 2006, 1974, 1981.

Figure 16C. February OLR anomalies averaged over the top 10 strongest positive vs top 10 strongest negative SIOD events in the southwestern portion of the basin.

Comparing the SIOD's influences on OLR for the peak month of February, there are slightly higher levels of OLR in the main development region during positive events as compared to negative events. The bullseye of lower OLR moves from between 55 and 60 East and between 10 and 15 South to near or just slightly outside this region between 75 and 80 East and 10 and 15 South. The OLR over the subtropics actually becomes lower during the positive SIOD event rather than a negative event. This is centered near 35 degrees south. These patterns represent typical characteristics of the SIOD.

9.5 Southeast

This region was the most complex among all of the regions in this study. The ACE has a strong connection with the SIOD and IOD using the backwards method. There was no connection with ENSO. This is the only region to have a strong connection between the IOD and the ACE. There is also a connection between SSTs and shear with the ACE. The relation between the atmospheric variables and the oscillations shows a connection between shear and ENSO as well as OLR and ENSO in this region but no connection with the other oscillations.

A.

Method1	Method2	Dependent	Enso	te	Sige	IOD	ti	Sigi	SIOD	ts	Sigs	constant	tc	Sigc
Enter	AVG (FMA)	ACE	-0.035	-0.244	0.808	-0.417	-2.935	0.005	0.279	1.833	0.073	9.769	5.892	0
Backwards	AVG (FMA)	ACE				-0.417	-2.965	0.005	0.292	2.071	0.044	9.742	5.948	0
Enter	J-F Delay	ACE	0.216	1.274	0.209	-0.392	-2.439	0.019	0.286	1.994	0.052	9.686	5.793	0
Backwards	J-F Delay	ACE				-0.296	-2.147	0.037				9.974	5.849	0
Enter	AVG (FMA)	Shear	0.537	4.193	0	-0.053	-0.421	0.676	-0.096	-0.713	0.48	9.629	33.998	0
Backwards	AVG (FMA)	Shear	0.579	4.924	0							9.627	34.388	0
Enter	AVG (FMA)	OLR	-0.28	-1.926	0.06	0.069	0.479	0.634	0.168	1.097	0.278	250.022	316.063	0
Backwards	AVG (FMA)	OLR	-0.351	-2.601	0.012							250.036	316.457	0
Enter	AVG (FMA)	SST	0.419	3.477	0.001	-0.224	-1.879	0.067	-0.246	-1.931	0.06	27.119	678.376	0
Enter	AVG (FMA)	RH	-0.205	-1.328	0.191	-0.06	-0.393	0.696	0.075	0.458	0.649	46.25	74.173	0

B.

Method1	Method2	f	Fsig	R	R^2	AdjustedR^2
Enter	AVG (FMA)	3.309	0.028	0.421	0.177	0.124
Backwards	AVG (FMA)	5.034	0.01	0.42	0.176	0.141
Enter	J-F Delay	3.071	0.037	0.408	0.167	0.113
Backwards	J-F Delay	4.611	0.037	0.296	0.088	0.069
Enter	AVG (FMA)	8.237	0	0.591	0.349	0.307
Backwards	AVG (FMA)	24.251	0	0.579	0.336	0.322
Enter	AVG (FMA)	2.909	0.044	0.399	0.159	0.105
Backwards	AVG (FMA)	6.763	0.012	0.351	0.123	0.105
Enter	AVG (FMA)	11.259	0	0.651	0.423	0.386
Enter	AVG (FMA)	0.915	0.441	0.237	0.056	-0.005

Table 11A. Enso, IOD, and SIOD columns give the individual regression values; te, ti, and ts are the t-test values, and Sige, Sigi, and Sigs are the p-values. This is for the northeastern region analysis comparing the oscillations with ACE and weather Variables.

Table 11B. F values and their significances for the Methods seen in A as well as the R, R square, and Adjusted R square values for the models.

In Table 11 it is seen that for this region IOD and SIOD have the strongest influence on the ACE with an R squared value of .141 using the season average. ENSO loses its significance using the backwards method. When relating to the atmospheric variables ENSO has the strongest connection.

A.

Method1	Method2	Dependent	sst	tsst	sigsst	shear	tshear	sigshear	constant	tc	sigc
Enter	Average	ACE	0.482	3.25	0.002	-0.236	-1.623	0.112	-517.779	-2.741	0.009
Backwards	Average	ACE	0.423	3.096	0.003	-0.296	-2.167	0.035	-374.074	-2.945	0.005

B.

Method1	Method2	f	f sig	R	R^2	adjusted R^2
Enter	Average	3.231	0.021	0.472	0.223	0.154
Backwards	Average	5.675	0.006	0.441	0.195	0.16

Table 12A. The above is the comparison of the significant meteorological variables with the ACE. Sst and shear give the individual regression values; tsst and tshear the t-test values, and sigsst and sigshear the p-values.

Table 12B. F values and their significances for the Methods seen in A as well as the R, R square, and Adjusted R square values for the models.

Table 12 reveals that using the backwards method SST and shear both have strong connections with ACE. The adjusted R squared values are 0.16 Meaning 16 percent of the ACE is explained by these variables.

The IOD is negatively correlated with ACE while the SIOD has a positive correlation. ENSO is positively correlated with shear but negatively correlated with OLR. SSTs are positively correlated with ACE whereas shear has a negative correlation. This means that for favorable conditions this basin would have a negative phase of the IOD (Warm water anomaly north of the region) and positive phase of the SIOD (warm water anomaly within the southwestern region). ENSO is less clear. Higher wind shear, but lower OLR appear to occur with El Niño. It appears from the northern portion of the basin that wind shear is more effective for development supporting previous research. It also seems that when both sides of the southern Indian Ocean are warm (negative IOD and positive SIOD) there is more tropical cyclone energy in the southeast.

A.

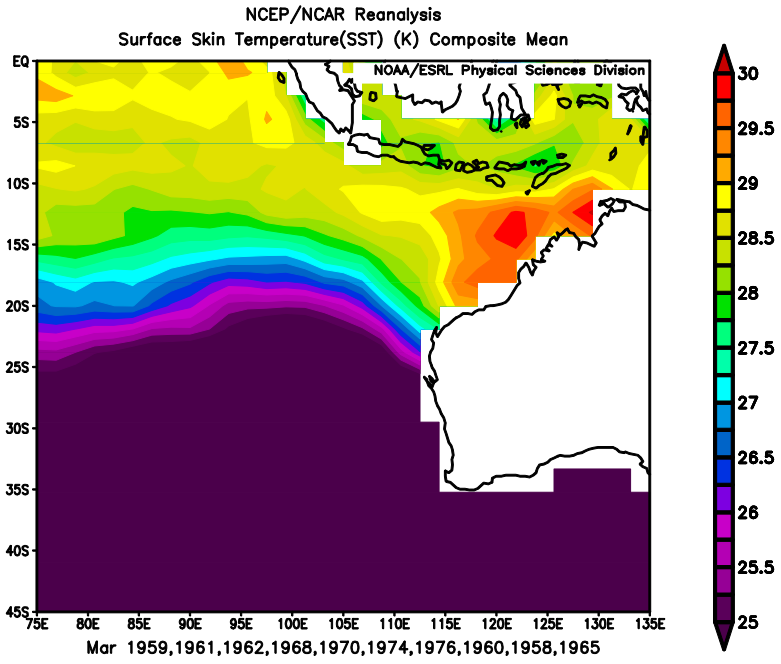
NCEP/NCAR Reanalysis
Surface Skin Temperature(SST) (K) Composite Mean
NOAA/ESRL Physical Sciences Division
EQ
5S
10S
15S
20S
25S
30S
35S
40S
45S
75E
80E
85E
90E
95E
100E
105E
110E
115E
120E
125E
130E
135E
30
29.5
29
28.5
28
27.5
27
26.5
26
25.5
25
Mar 1959,1961,1962,1968,1970,1974,1976,1960,1958,1965

B.

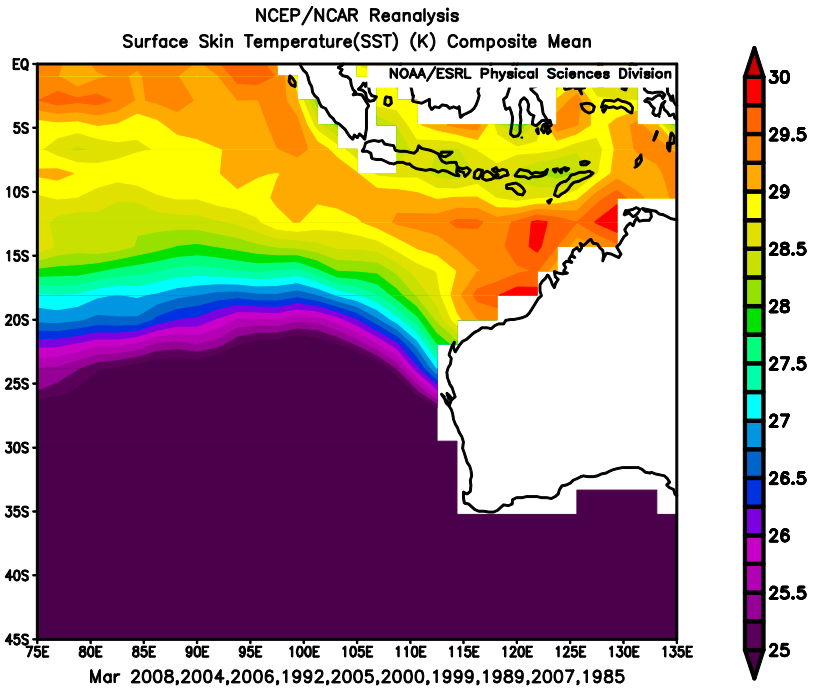
NCEP/NCAR Reanalysis
Surface Skin Temperature(SST) (K) Composite Mean
NOAA/ESRL Physical Sciences Division
EQ
5S
10S
15S
20S
25S
30S
35S
40S
45S
75E
80E
85E
90E
95E
100E
105E
110E
115E
120E
125E
130E
135E
30
29.5
29
28.5
28
27.5
27
26.5
26
25.5
25
Mar 2008,2004,2006,1992,2005,2000,1999,1989,2007,1985

C.

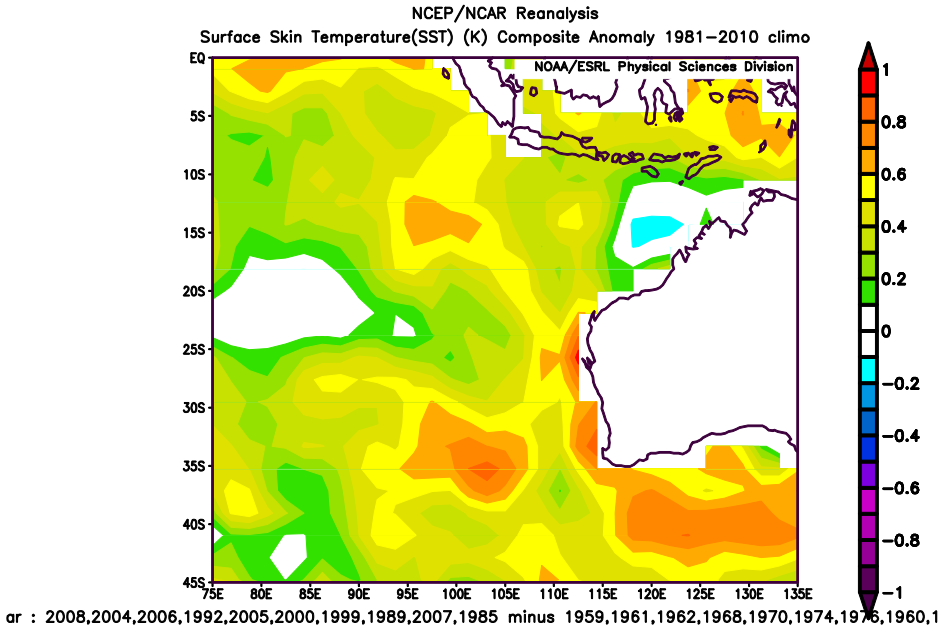

Figure 17A. The March SST values for the top 10 lowest ACE years for the southeastern portion of the Indian Ocean basin. The years included are 1959, 1961, 1962, 1968, 1970, 1974, 1976, 1960, 1958, 1965.

Figure 17B. The March SST values for the top 10 highest ACE years for the southeastern portion of the Indian Ocean Basin. The years included are 1985, 2007, 1989, 1999, 2000, 2005, 1992, 2006, 2004, 2008.

Figure 17C. The March SST anomaly values for the top 10 highest ACE vs top 10 lowest ACE years for the southeastern portion of the Indian Ocean Basin.

Figure 17 gives a clear comparison of the changes in March SSTs from the top 10 lowest ACE years to the top 10 highest ACE years. Higher ACE years have a tongue of extremely warm water near the west coast of Australia, extending out to the north and west parallel to the Maritime Continent and all the way to the equator. This warm water is near or above 30 degrees Celsius. In lower ACE years this tongue is weaker and doesn't extend as far - only to near 105 east. Years that have higher ACE tend to have slightly lower peak temperatures along the northwest coast of Australia maxing at 30 degrees.

A.

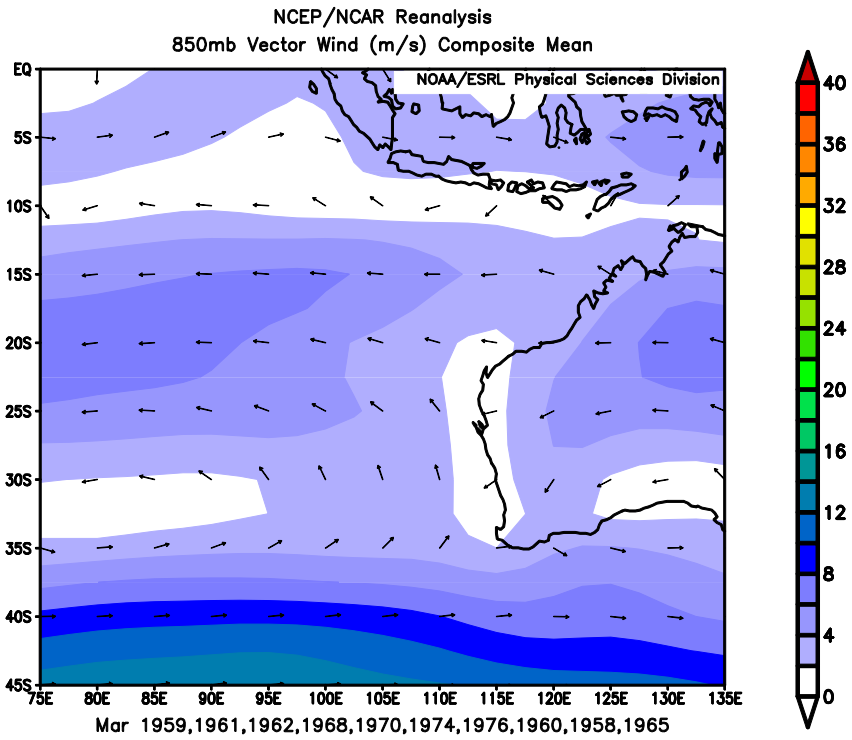
NCEP/NCAR Reanalysis
850mb Vector Wind (m/s) Composite Mean
NOAA/ESRL Physical Sciences Division
EQ
5S
10S
15S
20S
25S
30S
35S
40S
45S
75E
80E
85E
90E
95E
100E
105E
110E
115E
120E
125E
130E
135E
40
36
32
28
24
20
16
12
8
4
0
Mar 1959,1961,1962,1968,1970,1974,1976,1960,1958,1965

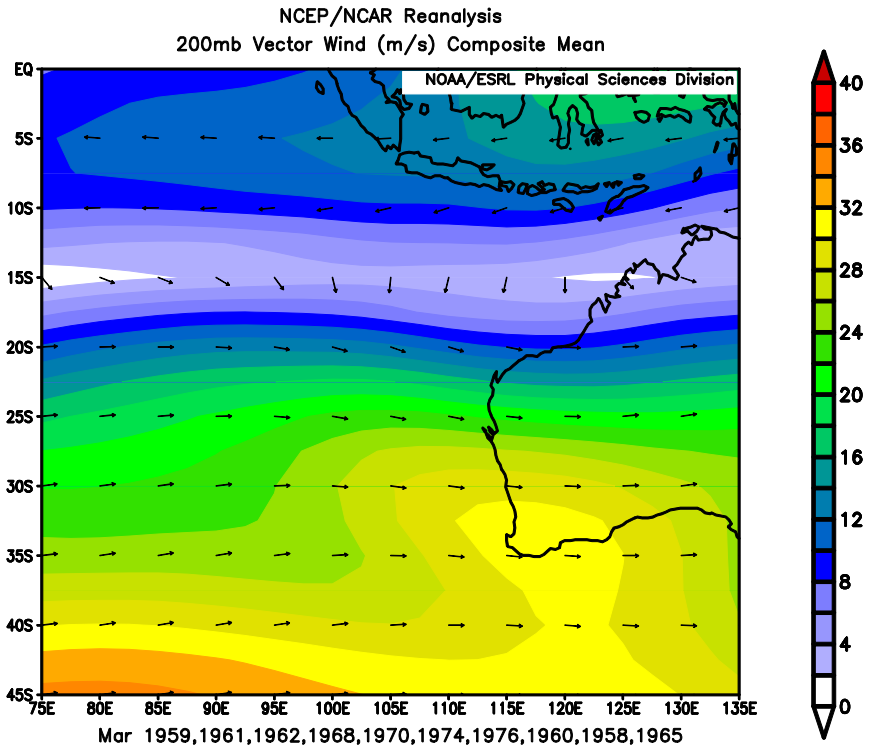
NCEP/NCAR Reanalysis
200mb Vector Wind (m/s) Composite Mean
NOAA/ESRL Physical Sciences Division
EQ
5S
10S
15S
20S
25S
30S
35S
40S
45S
75E
80E
85E
90E
95E
100E
105E
110E
115E
120E
125E
130E
135E
40
36
32
28
24
20
16
12
8
4
0
Mar 1959,1961,1962,1968,1970,1974,1976,1960,1958,1965

B.

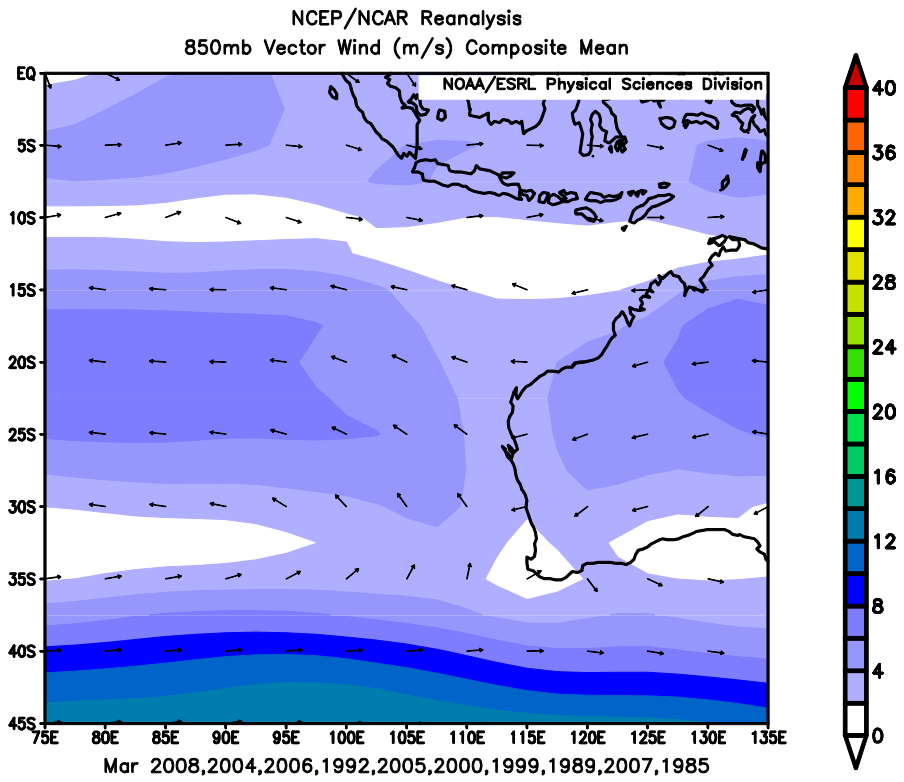
NCEP/NCAR Reanalysis
850mb Vector Wind (m/s) Composite Mean
NOAA/ESRL Physical Sciences Division
EQ
5S
10S
15S
20S
25S
30S
35S
40S
45S
75E
80E
85E
90E
95E
100E
105E
110E
115E
120E
125E
130E
135E
Mar 2008,2004,2006,1992,2005,2000,1999,1989,2007,1985
40
36
32
28
24
20
16
12
8
4
0

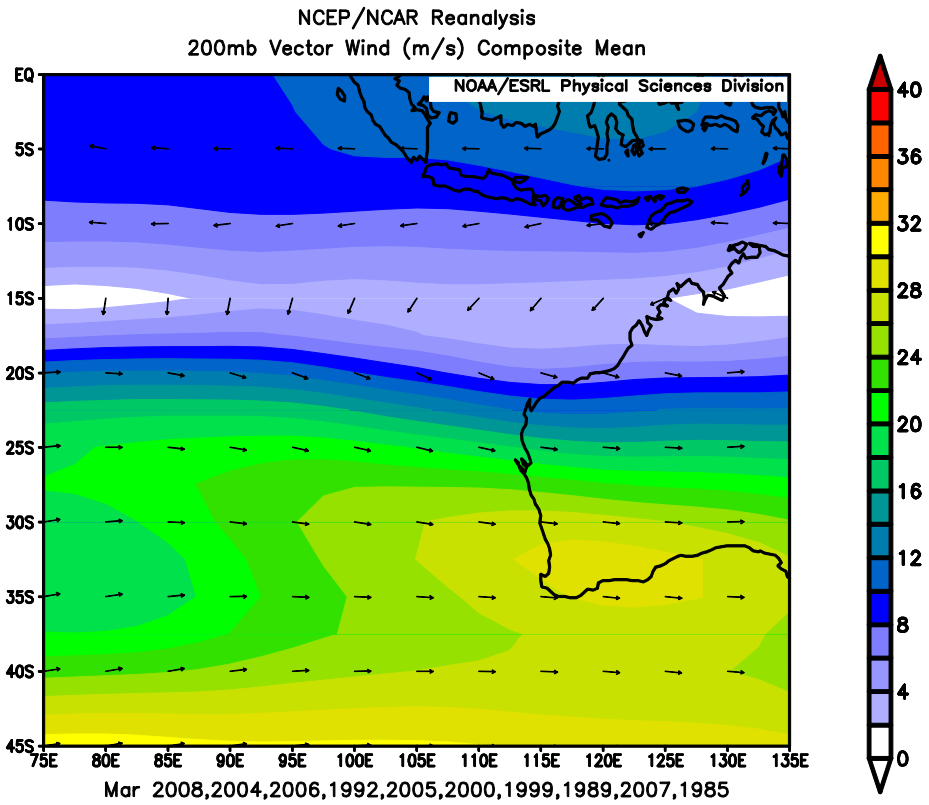
NCEP/NCAR Reanalysis
200mb Vector Wind (m/s) Composite Mean
NOAA/ESRL Physical Sciences Division
EQ
5S
10S
15S
20S
25S
30S
35S
40S
45S
75E
80E
85E
90E
95E
100E
105E
110E
115E
120E
125E
130E
135E
40
36
32
28
24
20
16
12
8
4
0
Mar 2008,2004,2006,1992,2005,2000,1999,1989,2007,1985

C.

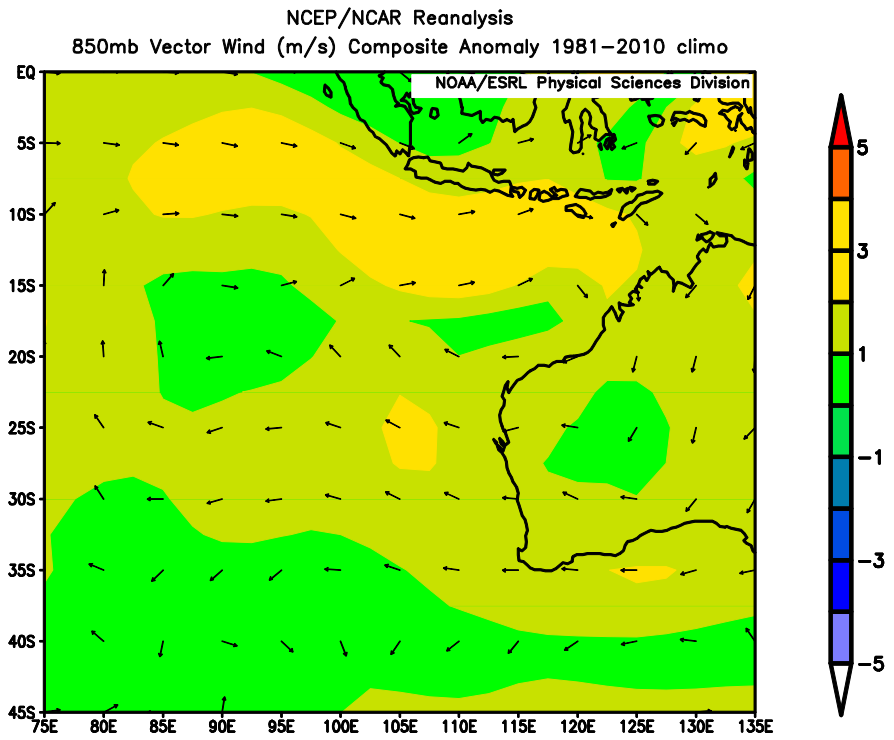

ar : 2008,2004,2006,1992,2005,2000,1999,1989,2007,1985 minus 1959,1961,1962,1968,1970,1974,1976,1960,1 \

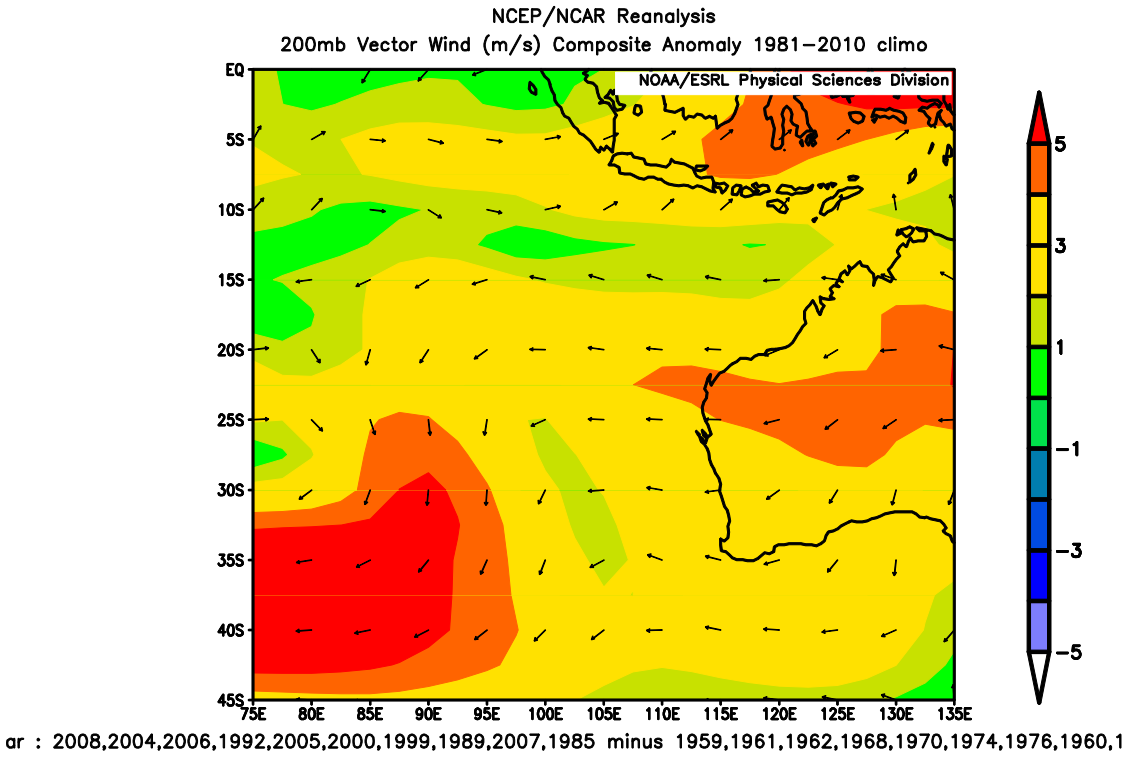

Figure 18A. March 850mb and 200mb winds for the years with low ACE in the southeastern portion of the basin. The years included are 1959, 1961, 1962, 1968, 1970, 1974, 1976, 1960, 1958, 1965.

Figure 18B. March 850mb and 200 mb winds for the years with high ACE in the southeastern portion of the basin. The years included are 1985, 2007, 1989, 1999, 2000, 2005, 1992, 2006, 2004, 2008.

Figure 18C. March 850mb and 200 mb wind anomalies for the years with high ACE vs low ACE in the southeastern portion of the basin.

Figure 18 shows the differences in the March winds (850mb and 200mb) between high ACE years and low ACE years. During high ACE years there is a band of slower 200mb wind speeds in a band between 10 and 15 degrees south as compared to low ACE years, thus wind shear is less. This band of slower winds can also be found closer to the midlatitudes reaching to about 20 to 25 degrees south.

A.

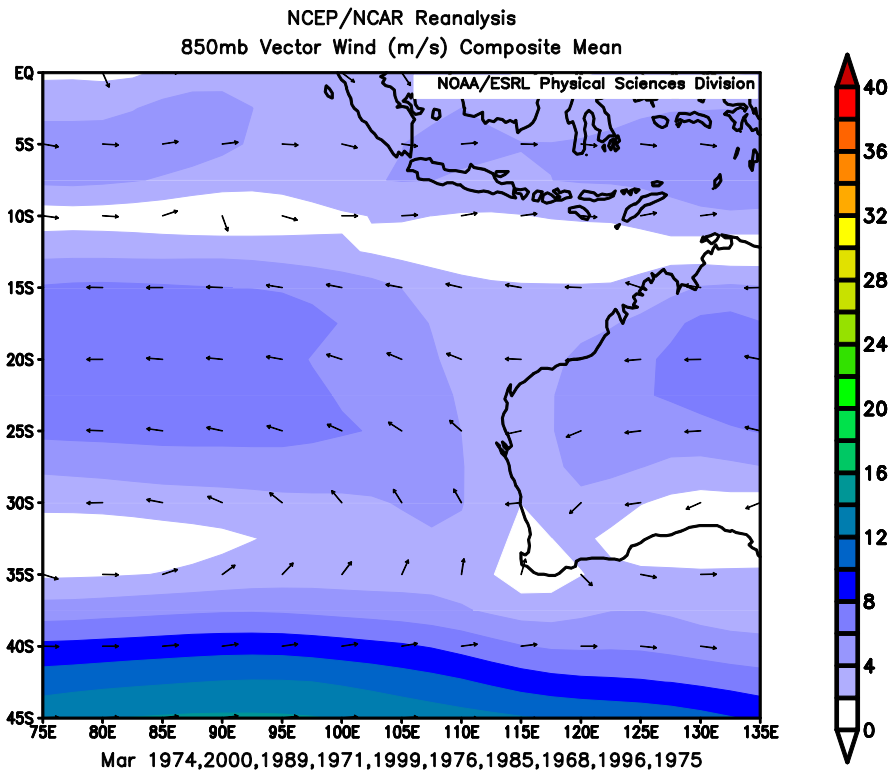
NCEP/NCAR Reanalysis
850mb Vector Wind (m/s) Composite Mean
NOAA/ESRL Physical Sciences Division
EQ
5S
10S
15S
20S
25S
30S
35S
40S
45S
75E
80E
85E
90E
95E
100E
105E
110E
115E
120E
125E
130E
135E
Mar 1974,2000,1989,1971,1999,1976,1985,1968,1996,1975
40
36
32
28
24
20
16
12
8
4
0

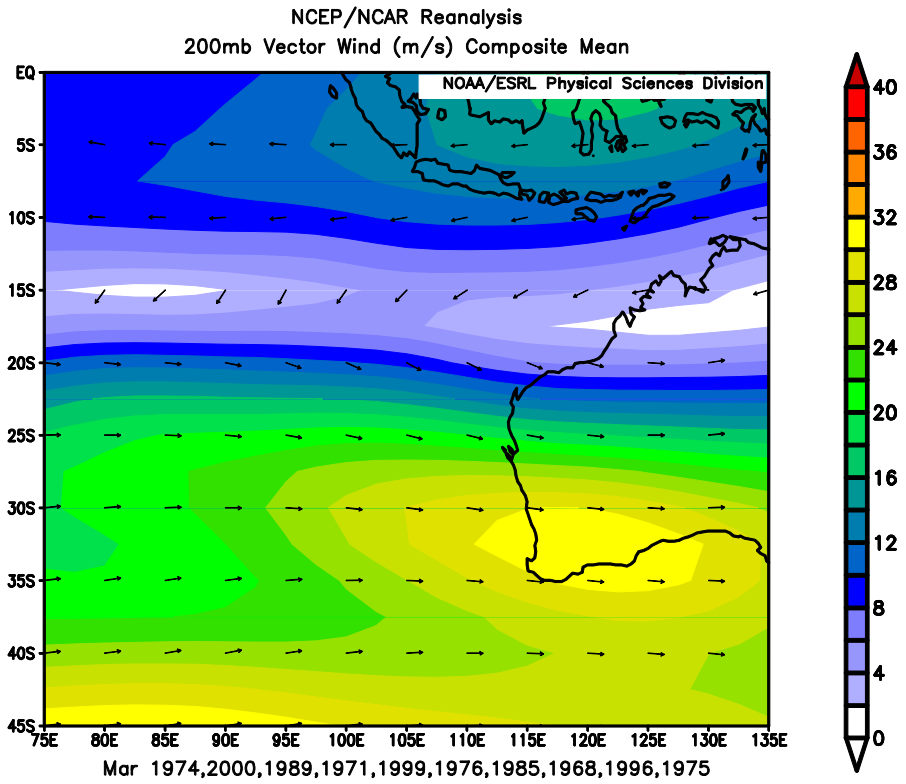
NCEP/NCAR Reanalysis
200mb Vector Wind (m/s) Composite Mean
NOAA/ESRL Physical Sciences Division
EQ
5S
10S
15S
20S
25S
30S
35S
40S
45S
75E
80E
85E
90E
95E
100E
105E
110E
115E
120E
125E
130E
135E
40
36
32
28
24
20
16
12
8
4
0
Mar 1974,2000,1989,1971,1999,1976,1985,1968,1996,1975

B.

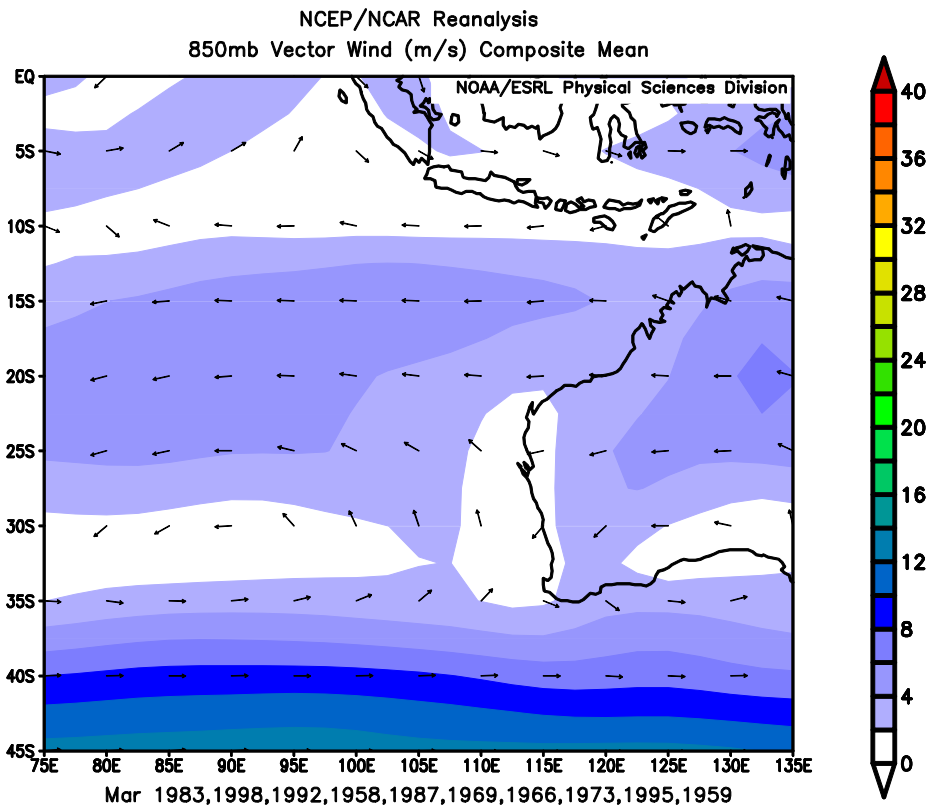
NCEP/NCAR Reanalysis
850mb Vector Wind (m/s) Composite Mean
NOAA/ESRL Physical Sciences Division
EQ
5S
10S
15S
20S
25S
30S
35S
40S
45S
75E
80E
85E
90E
95E
100E
105E
110E
115E
120E
125E
130E
135E
Mar 1983,1998,1992,1958,1987,1969,1966,1973,1995,1959
40
36
32
28
24
20
16
12
8
4
0

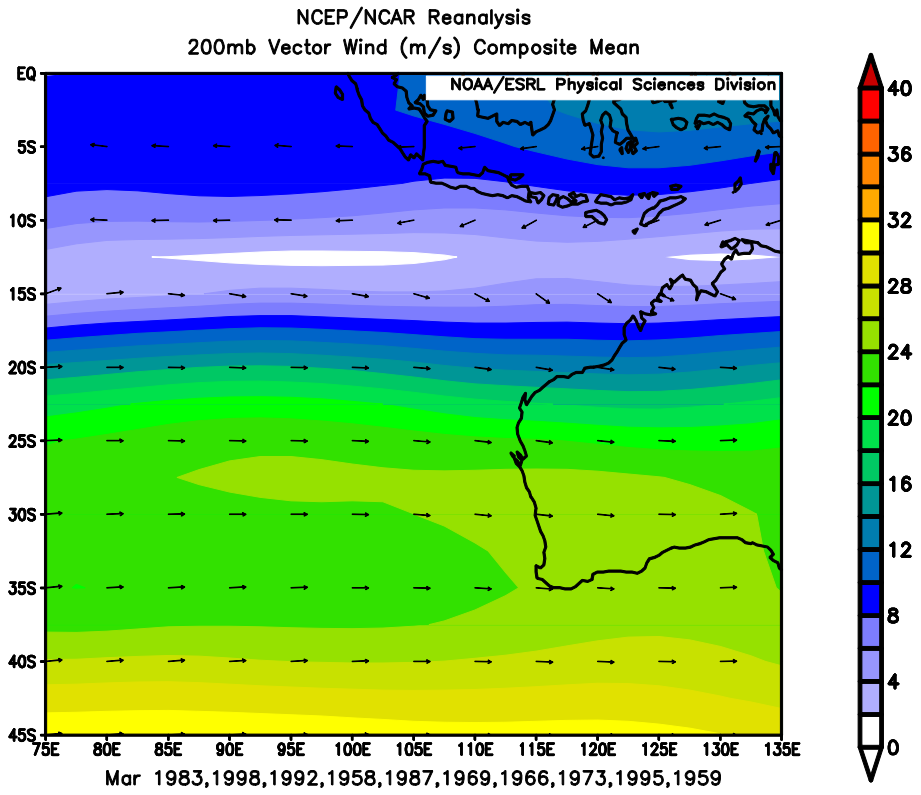
NCEP/NCAR Reanalysis
200mb Vector Wind (m/s) Composite Mean
NOAA/ESRL Physical Sciences Division
EQ
5S
10S
15S
20S
25S
30S
35S
40S
45S
75E
80E
85E
90E
95E
100E
105E
110E
115E
120E
125E
130E
135E
40
36
32
28
24
20
16
12
8
4
0
Mar 1983,1998,1992,1958,1987,1969,1966,1973,1995,1959

C.

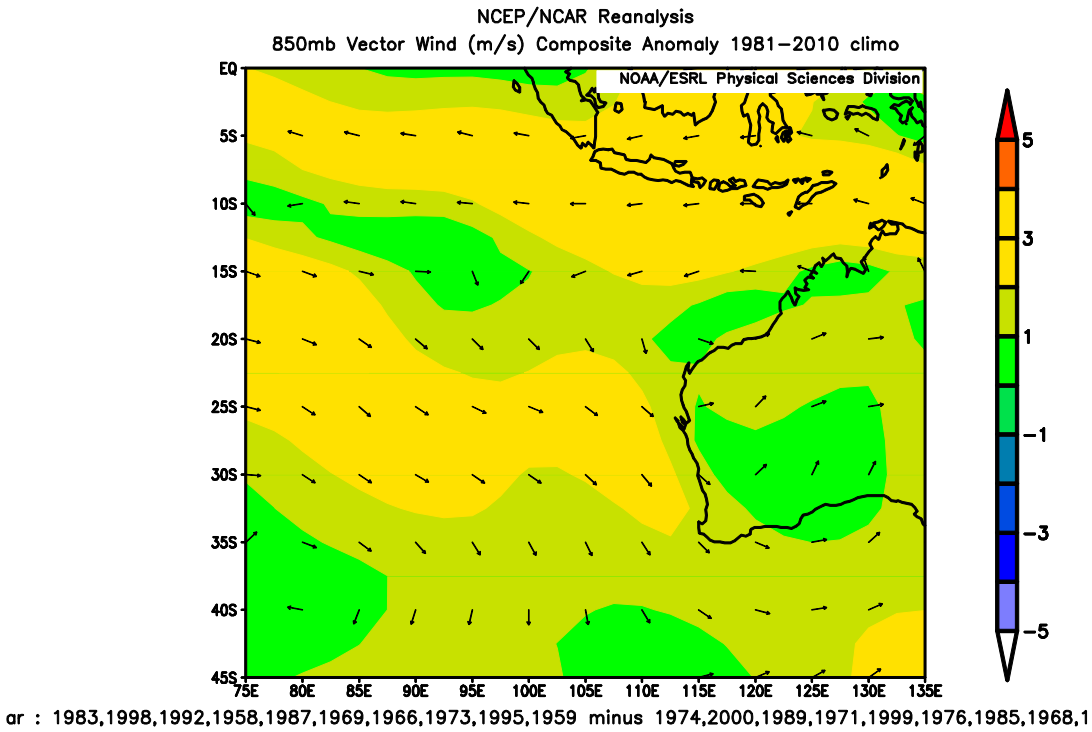
NCEP/NCAR Reanalysis
850mb Vector Wind (m/s) Composite Anomaly 1981–2010 climo
NOAA/ESRL Physical Sciences Division
EQ
5S
10S
15S
20S
25S
30S
35S
40S
45S
75E
80E
85E
90E
95E
100E
105E
110E
115E
120E
125E
130E
135E
5
3
1
−1
−3
−5
ar : 1983,1998,1992,1958,1987,1969,1966,1973,1995,1959 minus 1974,2000,1989,1971,1999,1976,1985,1968,1

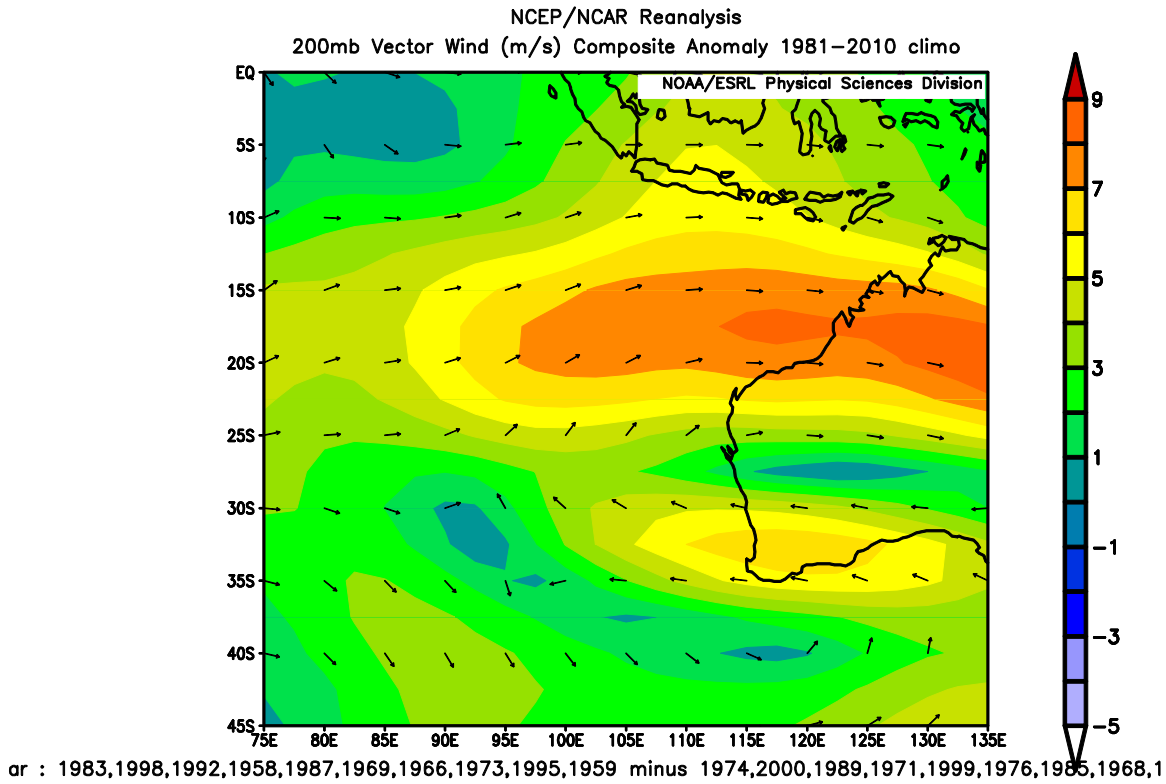

Figure 19A. March 850mb and 200mb winds for the top 10 strongest La Niña years in the southeastern portion of the Indian Ocean Basin. The years included are 1974, 2000, 1989, 1971, 1999, 1976, 1985, 1968, 1996, 1975.

Figure 19B. March 850mb and 200 mb winds for the top 10 strongest El Niño years in the southeastern portion of the Indian Ocean Basin. The years included are 1993, 1959, 1995, 1973, 1966, 1969, 1987, 1958, 1992, 1998, 1983.

Figure 19C. March 850mb and 200 mb wind anomalies for the top 10 strongest El Niño vs La Niña years years in the southeastern portion of the Indian Ocean Basin.

Since there was a positive correlation between ENSO and wind shear found for this region Figure 19 reveals the differences between El Niño and La Niña composites. During El Niño a band of higher wind shear is indicated by a large area of strong 200 mb winds that is displaced further north than during a La Niña event. During La Niña it appears that conditions would be more favorable for tropical cyclone development and higher ACE values based off the wind shear strength and location.

A.

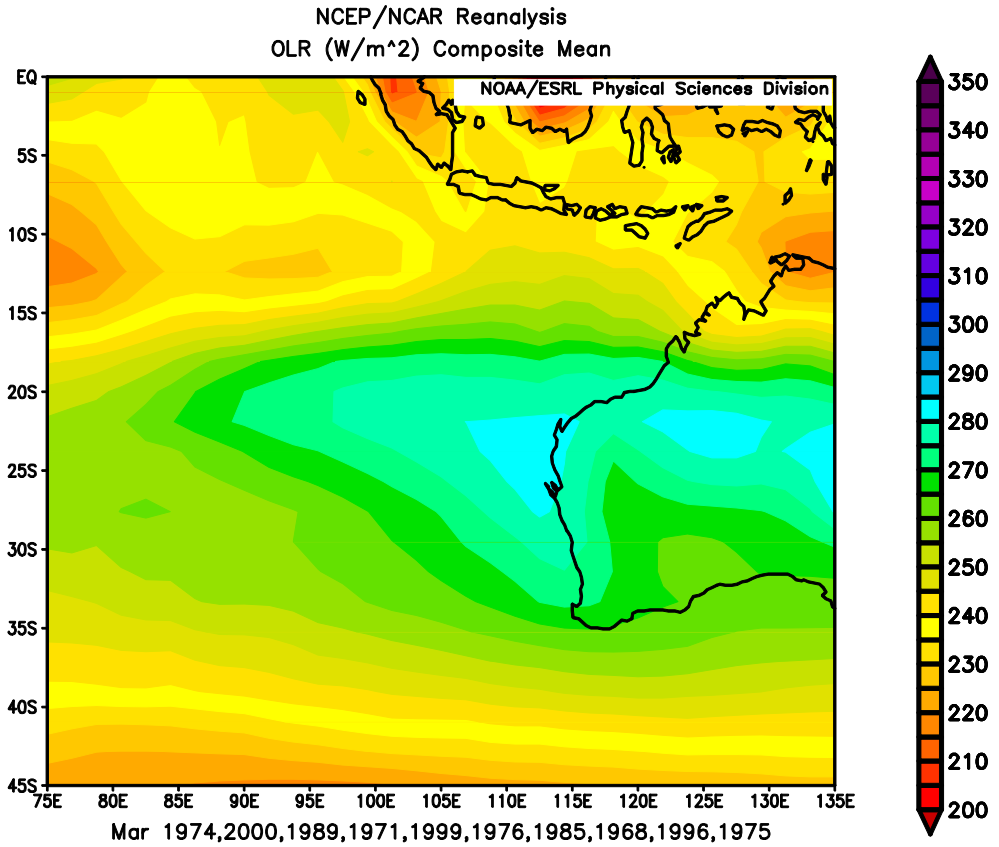
NCEP/NCAR Reanalysis
OLR (W/m^2) Composite Mean
NOAA/ESRL Physical Sciences Division
EQ
5S
10S
15S
20S
25S
30S
35S
40S
45S
75E
80E
85E
90E
95E
100E
105E
110E
115E
120E
125E
130E
135E
Mar 1974,2000,1989,1971,1999,1976,1985,1968,1996,1975
350
340
330
320
310
300
290
280
270
260
250
240
230
220
210
200

B.

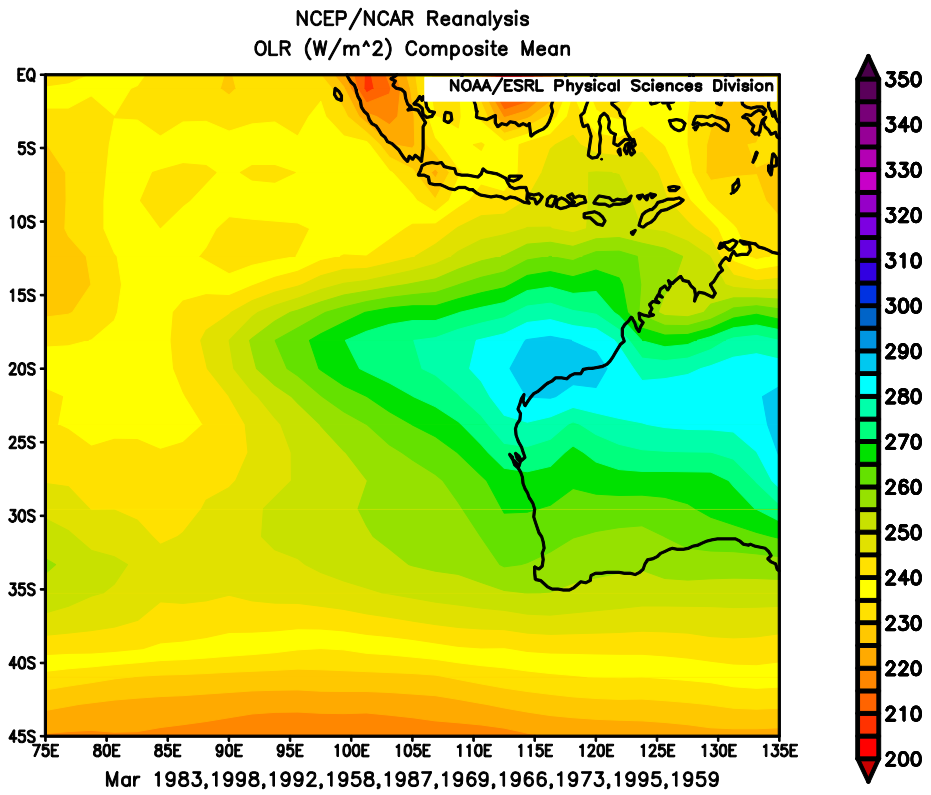
NCEP/NCAR Reanalysis
OLR (W/m^2) Composite Mean
NOAA/ESRL Physical Sciences Division
EQ
5S
10S
15S
20S
25S
30S
35S
40S
45S
75E
80E
85E
90E
95E
100E
105E
110E
115E
120E
125E
130E
135E
Mar 1983,1998,1992,1958,1987,1969,1966,1973,1995,1959
350
340
330
320
310
300
290
280
270
260
250
240
230
220
210
200

C.

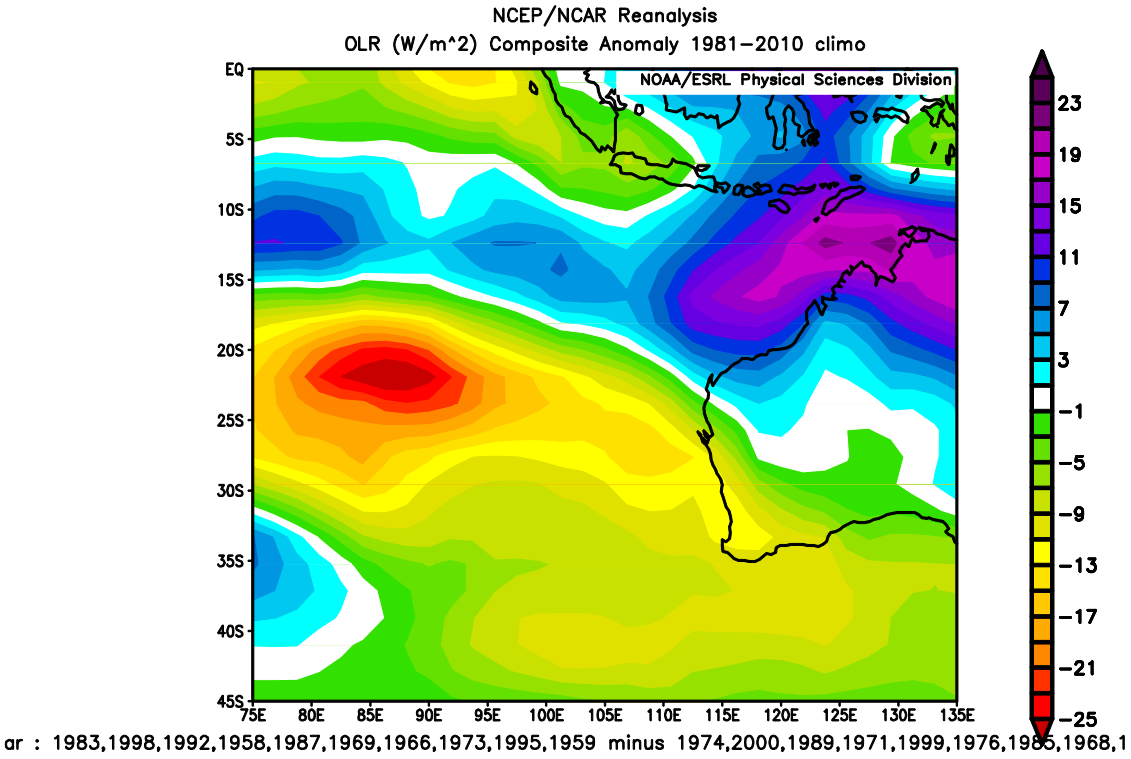

Figure 20A. March Outgoing Longwave Radiation for the top 10 strongest La Niña events for the southeastern portion of the basin. . The years included are 1974, 2000, 1989, 1971, 1999, 1976, 1985, 1968, 1996, 1975.

Figure 20B. March Outgoing Longwave Radiation for the top 10 strongest El Niño events for this southeastern portion of the basin. The years included are 1993, 1959, 1995, 1973, 1966, 1969, 1987, 1958, 1992, 1998, 1983.

Figure 20C. March Outgoing Longwave Radiation anomalies for the top 10 strongest El Niño vs La Niña events for this southeastern portion of the basin.

Figure 20 compares El Niño and La Niña events and their impacts on the OLR of this region. The biggest difference found in this region is that for El Niño events larger OLR values related to the subtropical high are restricted to closer to the Australian continent. Negative OLR anomalies in the El Niño minus La Niña field are evident within the main development region, which would be conducive for tropical cyclone development.

10. Discussion

In general the El Niño Southern Oscillation appears to have the most dominance over all the meteorological variables as well as the tropical cyclone ACE in the northern portion of the basin. This appears at least partially to be caused by its nature and size (i.e. a planetary scale oscillation versus a basin sized oscillation or sub basin sized oscillation). The only exception to this rule was the southeastern region where the Indian Ocean Dipole and Subtropical Indian Ocean Dipole were the variables with the largest correlation with the tropical cyclone ACE. However, this could in part be because ENSO was controlling the meteorological variables, which may have influenced the development of the smaller scale oscillations. This would make up for a lack of direct connection between ENSO and ACE in this region.

10.1 Northwest

In this region there is a connection between Outgoing Longwave Radiation, ENSO, and ACE. This connection is seen clearly in the Figures 10 and 11 above, as it appears that during strong El Niño events higher levels of OLR are in the region while during a La Niña event lower levels appear within the region. Lower levels of OLR means more disturbances in the area, which is one of the conditions needed for tropical development and higher ACE.

This connection has merit because it is well known that La Niña events lead to the ITCZ moving northward into this region and strengthening, while during El Niño the ITCZ stays south leading to drought in the Indian mainland (Kumar et al. 1999). However, when looking at Figure 10 it appears that high levels of ACE are related to convection and disturbances that traverse closer to the equator near 55 degrees east in the Arabian Sea.

Another point of interest for this region was that the peak in tropical cyclone ACE occurred during the northern hemisphere spring. This only occurred because of recent years, for example the month of June in 2010 having 55.83 units of ACE alone. This may be caused by the weakening of El Niño's impacts as discussed by Kumar et al. (1999) or because of a lack of strong recent El Niño events. The secondary peak during the late fall and early winter months had more years with storms but they were lower ACE producers. The cause of this is not readily clear from the results of this analysis and differs from the results of most past research into this area.

10.2 Northeast

As with the northwestern region this area is associated with ENSO. From previous research this can be expected because of ENSO's strong influence on the ITCZ (Felton et al. 2013). The most interesting result here was that even though both the northwest and northeast have double peaks associated with the migration of the ITCZ, the northeast region's strongest peak was in the northern hemisphere fall and winter months. There were many more storms and they had a larger amount of ACE with a sum of 108.5 units of ACE for the 3 month average of October-November-December.

Another interesting result was the fact that the SIOD had a marginally significant influence on this region, even though it is a southern hemisphere oscillation. This is possibly caused by subsidence (lift) created by the downward (upward) portion of the thermal circulations in cross-equatorial flow. This result shows the power of this dipole in the eastern portion of the basin.

When analyzing this region for tropical cyclone development potential it would appear that ENSO is most important, which is consistent with Camargo et al. (2007). La Niña is related to an increase in ACE and La Niñas are significantly related to anomalously low OLR values. Yet OLR is not directly related to ACE. Interestingly El Niño leads to a significant reduction in shear and increase in SST, which would seem to favor tropical cyclone development. In addition to ENSO being in the negative phase, SIOD would also need to be in a negative phase to induce larger values of ACE in the eastern portion of the basin.

10.3 Southwest

The fact that this region does not have any clear correlation between both the weather variables and large-scale oscillations with ACE is an interesting result. It appears that this portion of the Indian Ocean could possibly be insensitive to the climate of the rest of the basin and is possibly being influenced by the Madden Julian Oscillation (MJO). The MJO as stated earlier is an upward pulse of energy that develops along the edge of this region and travels around the world centered near the equator. This pulse aids in development of tropical cyclones along the ITCZ and may be one of the main influences of tropical cyclone development for this region. However, from the correlation between ENSO and SST and SIOD with OLR and the key items needed for tropical cyclone development at least some understanding of tropical cyclone activity can be gained. El Niño years appear to be more favorable for tropical cyclones because of an increase in SST across the basin as well as the ITCZ staying within this region for longer periods of time than average.

Also lower levels of OLR tend to remain in this basin during negative SIOD events rather than positive events. This seems counterintuitive because a negative phase tends to mean that

there are cooler sea surface temperatures within the western basin. However, the lower OLR and disturbed weather may limit radiative forcing. More disturbances would mean an increased chance of tropical cyclone development as long as other conditions are favorable at the time of formation.

Therefore this region appears to be more favorable for tropical cyclone development during an El Niño year in conjunction with a negative SIOD event. This configuration leads to more disturbances from the SIOD plus higher sea surface temperatures from the ENSO, which is acting to counteract the lower sea surface temperatures related to the negative SIOD phase. This pattern tends to lead to the climatological favored factors for enhanced tropical cyclone development in the region and therefore increases in the ACE over this portion of the basin.

10.4 Southeast

This is the portion of the basin where the IOD and SIOD reveal their strongest influence. This may occur because of the location of the sub-basin in relation to these climate oscillations. There is a large portion of this basin near the equator and between Australia and the Maritime Continent where cyclones can form. There is also a large area stretching into the subtropics along the coast of Australia out into the middle of the sea and eventually crossing over into the southwestern basin where tropical cyclones form. These development regions are impacted by the IOD and SIOD respectively. Although, it appears that the SIOD has a weaker impact on tropical cyclone ACE than the IOD.

However, ENSO may still be most important within the basin. ENSO has an apparent positive correlation with wind shear, while there is a negative correlation between wind shear and ACE. This link between ENSO-Shear and Shear-ACE (consistent with Camargo et al. 2007)

may relate to the IOD's and, to a lesser extent, the SIOD's correlation with ACE. It could be that ENSO influences the shear which then influences the ACE, which finally aids in changing the other oscillations. ACE is also related to a warmer than normal southeastern basin.

10.5 Conclusion

The Indian Ocean basin, which is for most climatological studies split into the northern and southern hemisphere by the equator appears to actually have a more complex tropical cyclone developmental configuration than Earth's other ocean basins. By subdividing this basin into 4 distinct regions it was shown that the Arabian Sea, Bay of Bengal, Southern African Hemisphere, and Australian Hemisphere all have their own very distinct patterns and correlations that become clear once analyzed using a multiple regression method. These patterns could apply directly to national forecasting centers, and may be missed by looking at the basin at larger spatial scales.

This study showed just how dependent the northern regions are on the El Niño Southern Oscillation for tropical cyclone energy. Changes in the regions' seasons are also beginning to become apparent with the Arabian Sea's peak changing from being in the Northern Hemisphere fall/winter to the spring/summer due to bursts of higher ACE development in recent years, especially towards the late 2000s. More work needs to be done on this finding to see if it is just because of better technology identifying more storms now than prior to the satellite era or if there is a climate shift such as a weakening of the impacts of ENSO upon the ITCZ. The possibility of a changing atmospheric pattern would explain why the storms that seem to be in this higher ACE period (from 1999 to 2010) appear to be stronger tropical cyclones versus many weak ones

(1970s and 1980s). It is unlikely that these strong tropical cyclones would have been missed in the past even with more limited technology.

Here I will repeat the hypotheses outlined above and determine the level of consistency with the results obtained in this study:

1. *As Camargo et al. (2007) suggest, the ENSO will have the largest influence on tropical cyclogenesis, and thus ACE, in the basin. During El Nino, the weakened Walker Circulation will cause less shear in the vicinity of the Maritime Continent causing greater ACE in the southeastern basin. The opposite will occur during La Nina.*

The influence of ENSO in all the sub-basins is clearly evident. ACE is related to lowered shear in the southeastern basin, however the region was complex. La Niña leads to lower shear and the low shear environment is favorable to high ACE. Surprisingly, La Niña was not directly related to ACE.

2. *The negative phase of the SIOD (when the waters are warm to the west of Australia, Fig. 4a) will likely lead to an increase in ACE in both of the southern sub-basins. The positive phase of the SIOD will have little affect on ACE as the warm waters are too far south for cyclogenesis.*

   A positive SIOD was related to greater tropical cyclone activity in the southeastern basin, which counters the stated hypothesis.

3. *The IOD will have remote effects due to changes in meridional circulations. During the positive phase the warm waters in the western equatorial Indian Ocean will lead to*

reduced ACE in the southwest and northwest and enhanced ACE in the northeast and southeast. The opposite will hold true for the negative phase of the IOD.

A negative IOD was related to greater ACE in the southeastern sub-basin. A negative IOD combined with a positive SIOD (see 2 above) would be consistent with cool temperature anomalies in the southeastern region and warm anomalies to the north on the equator, which may lead to a stronger meridional circulation and favor ACE closer to the equator. The La Niña also would be consistent with warmer than normal waters surrounding the Maritime Continent. High ACE in the southeastern basin was significantly positively related to SST.

Clearly seen here is the lack of direct influence by the Indian Ocean climate oscillations on the southwestern portion of the basin. It appears that the influences exerted by the oscillations on the weather variables may have an indirect effect on ACE. This may be because ENSO tends to have a greater influence in the northern hemisphere, or that ENSO and the SIOD and IOD are acting to cancel each other out in this portion of the basin. This appears to be happening with the phases of the SIOD and ENSO canceling out their effects on the sea surface temperatures in the region.

This is a large-scale climatological analysis of the Indian Ocean basin's oscillations, weather patterns, and tropical cyclones through a new kind of lens. More fine scale spatial relationships, possibly by utilizing GIS, could further the work. It is the intent of the present study to initiate a more specific development plan for tropical cyclone prediction and preparedness within the Indian Ocean.

11. Literature Reviewed

11.1 Scholarly Review

Ash, K.,Matyas, C., (2010) The influences of ENSO and the subtropical Indian Ocean Dipole on tropical cyclone trajectories in the southwestern Indian Ocean, International Journal of Climatology, January 2012, 32(1), 41-56

Ashok, Karumuri, Zhaoyong Guan, N. H. Saji, Toshio Yamagata, 2004: Individual and combined influences of enso and the indian ocean dipole on the indian summer monsoon. *J. Climate*, **17**, 3141–3155.

Behera S. Subtropical SST dipole events in the southern Indian ocean. Geophysical research letters. 2001-01-15;28:327-330.

Behera, S., Salvekar, P., Amagata, T., Simulation of Interannual SST Variability in the Tropical Indian Ocean. Journal Of Climate [serial online]. October 2000;13(19):3487. Available from: Academic Search Complete, Ipswich, MA.

Behera, Swadhin, K., Jing-Jia Luo, Masson, S., Delecluse, P., Gualdi, S., Navarra, A.,Yamagata, T., 2005: Paramount impact of the indian ocean dipole on the east african short rains: a cgcm study. *J. Climate*, **18**, 4514–4530.

Bessafi M, Wheeler M. Modulation of South Indian Ocean Tropical Cyclones by the Madden-Julian Oscillation and Convectively Coupled Equatorial Waves. Monthly Weather Review[serial online]. February 2006;134(2):638-656. Available from: Applied Science & Technology Full Text (H.W. Wilson), Ipswich, MA.

Bosart, L.F., Bartlo, J.A., 1991: Tropical storm formation in a baroclinic environment. Mon. Wea. Rev., **119**, 1979–2013.

doi: http://dx.doi.org/10.1175/1520-0493(1991)119<1979:TSFIAB>2.0.CO

Camargo, S.J., Emanuel, K.A., Sobel, A.H., 2007, Use of a genesis potential index to diagnose ENSO effects on tropical cyclone genesis, Journal of Climate, 20, 4819-4834

Cook, KH., 2000: The south indian convergence zone and interannual rainfall variability over southern africa. *J. Climate*, **13**, 3789–3804.

Dowdy,A., and Kuleshov, Y., 2011, An analysis of tropical cyclone occurrence in the Southern Hemisphere derived from a new satellite-era data set, Pan Ocean Remote Sensing: Connecting Regional Impacts to Global Environmental Change,2012, **33**(23), 7382-7397

England, M.H., Ummenhofer, C.C., and Santoso, A., 2006: Interannual Rainfall Extremes over Southwest Western Australia Linked to Indian Ocean Climate Variability. *J.* Climate, **19**, 1948–1969. doi: http://dx.doi.org/10.1175/JCLI3700.1

Felton, C. S., Subrahmanyam, B., and Murty, V. S. N. (2013). ENSO-modulated cyclogenesis over the bay of bengal*. *Journal of Climate*, ***26***(24), 9806-9818. Retrieved from http://search.proquest.com.jproxy.lib.ecu.edu/docview/1468910382?accountid=10639

Ferreira, R., Schubert, W.H., and Hack, J.J, 1996: Dynamical Aspects of Twin Tropical Cyclones Associated with the Madden–Julian Oscillation. *J.* Atmos. Sci., **53**, 929–945.

doi: http://dx.doi.org/10.1175/1520-0469(1996)053<0929:DAOTTC>2.0.CO;2

Gottschalck, J., Kousky, V., Higgins, W., and L' Heureux, M., 2005, Madden Julian Oscillation (MJO), CPC 1-20
http://www.cpc.ncep.noaa.gov/products/precip/CWlink/MJO/MJO_summary.pdf

GRAY, W.M., 1968: GLOBAL VIEW OF THE ORIGIN OF TROPICAL DISTURBANCES AND STORMS. Mon. Wea. Rev., **96**, 669–700.

doi: http://dx.doi.org/10.1175/1520-0493(1968)096<0669:GVOTOO>2.0.CO;2

Hall, M., Walker, SC., and Kendall, LP., Exploring Tropical Cyclones 2007.

Hastenrath S., Circulation mechanisms of climate anomalies in East Africa and the equatorial Indian Ocean, Dynamics of Atmospheres and Oceans April 2007, 43(1-2), 25-35

Kalnay, E.,Coauthors, 1996: The NCEP/NCAR Reanalysis 40-year Project. Bull. Amer. Meteor. Soc., 77, 437-471.

Krishnamohan, KS., Mohanakumar, K., and Joseph, PV., The influence of Madden-Julian Oscillation in the genesis of North Indian Ocean tropical cyclones THEORETICAL AND APPLIED CLIMATOLOGY ,July 2012, **109**(1-2), 271-282

Kumar, K. K., Rajagopalan, B., and Cane, M. A. (1999). On the weakening relationship between the indian monsoon and ENSO. *Science-AAAS, 284*(5423), 2156. Retrieved from http://search.proquest.com.jproxy.lib.ecu.edu/docview/14515279?accountid=10639

Landau, S., and Everitt, B.S., A Handbook of Statistical Analysis Using SPSS, Chapman and Hall/CRC, 2004

Li, Tim, Bin Wang, C-P. Chang, and Yongsheng Zhang, 2003: A Theory for the Indian Ocean Dipole–Zonal Mode*. *J. Atmos. Sci.*, **60**, 2119–2135.
doi: http://dx.doi.org/10.1175/1520-0469(2003)060<2119:ATFTIO>2.0.CO;2

Li, Z., Yu, W., Li, T., Murty, V. S. N., and Tangang, F. (2013). Bimodal character of cyclone climatology in the bay of bengal modulated by monsoon seasonal cycle*. Journal of Climate, ***26***(3), 1033-1046. Retrieved from http://search.proquest.com.jproxy.lib.ecu.edu/docview/1317399339?accountid=10639

Liebmann, B., Hendon, H.H., and Glick, J.D., The Relationship Between Tropical Cyclones of the Western Pacific and Indian Oceans and the Madden-Julian Oscillation, Journal of the Meteorological Scociety of Japan, June 1994, **72**(3), 401-403

Matyas, C., and Silva, J., 2011 Extreme weather and economic well-being in rural Mozambique, Springer, December 20 2011

Namias, J., 1973: Thermal Communication Between the Sea Surface and the Lower Troposphere. *J. Phys.* Oceanogr., **3**, 373–378.

doi: http://dx.doi.org/10.1175/1520-0485(1973)003<0373:TCBTSS>2.0.CO;2

Pierce, D., 1997. El Niño. . http://meteora.ucsd.edu/~pierce/elnino/whatis.html

Pui, A. (2012-05-01). Impact of the El Niño-Southern Oscillation, Indian Ocean Dipole, and Southern Annular Mode on Daily to Subdaily Rainfall Characteristics in East Australia. Monthly weather review, **140**(5), 1665.

Saji, N. H., and Yamagata, T., 2003: Structure of SST and Surface Wind Variability during Indian Ocean Dipole Mode Events: COADS Observations*. *J. Climate*, **16**, 2735–2751. doi: http://dx.doi.org/10.1175/1520-0442(2003)016<2735:SOSASW>2.0.CO;2

Schiele, E., Ocean Conveyor Belt Impact NASA Ocean Motion and Surface Currents Dataset.

Schott, F., and McCreary, J., The monsoon circulation of the Indian Ocean, Progress in Oceanography, 2001, **51**(1), 1-123

Shi L. How Predictable is the Indian Ocean Dipole?. Monthly weather review. 2012-12-**01**;140:3867-3884

Sikka, D. R., and Gadgil, S., (1980) On the maximum cloud zone and the ITCZ over Indian, longitudes during the southwest monsoon Monthly Weather Review, **108** (11). pp. 1840-1853. ISSN 0027-0644

Singh, O.P., Indian Ocean dipole mode and tropical cyclone frequency, Current Science, January 10 2008**, 94**(1), 29-31

Skowronska, K., 212 Variability in the ENSO-Monsoon relationship: Integration of high resolution proxy data, Quaternary Science degree programme at Royal Holloway, University of London, http://www.skowronska.com/

Waliser, D.E., Intertropical Convergence Zone, Tropical Meteorology, April 10 2002, 1-10

Wang, G., and Hendon, H. H., (2007). Sensitivity of australian rainfall to inter-el niño variations. Journal of Climate, ***20***(16), 4211-4217,4219-4222,4224-4226. Retrieved from http://search.proquest.com.jproxy.lib.ecu.edu/docview/222878070?accountid=10639

Webster, P. J., and Yang, S., (1992), Monsoon and Enso: Selectively Interactive Systems. Q.J.R. Meteorol. Soc., 118: 877–926. doi: 10.1002/qj.49711850705

Wu, R., and Kirtman, B. P., (2003), On the impacts of the Indian summer monsoon on ENSO in a coupled GCM. Q.J.R. Meteorol. Soc., **129:** 3439–3468. doi: 10.1256/qj.02.214

Yagamata, T., Behera, S.K., and Rao, S.A., Guan, Z., Ashok, K., Saji, H.N., The Indian Ocean Dipole: a Physical Entity, 2006

Zinke J. ENSO and Indian Ocean subtropical dipole variability is recorded in a coral record off southwest Madagascar for the period 1659 to 1995. Earth and planetary science letters. 2004; **228**:177-194.

11.2 Links to Data Sets and Figures

Table 1. The COMET Module on Tropical Cyclones and Tropical Cyclone requirements for development. http://www.goes-r.gov/users/comet/tropical/textbook_2nd_edition/navmenu.php_tab_9_page_3.1.0.htm

Figure 1. Warning Coverage Map: http://www.bom.gov.au/catalogue/warnings/AoResp_W.shtml

Figure 2. Image showing an Example of a Strong El Niño and a Strong La Niña http://sealevel.jpl.nasa.gov/files/archive/science-elnino/el-nino-la-nina.jpg

Figure 3. Maps showing what occur during a Positive and Negative Indian Ocean Dipole Event. http://www.jamstec.go.jp/frsgc/research/d1/iod/IOD1.html

Figure 4. Map showing the differences between the Indian Ocean Dipole and the Subtropical Indian Ocean Dipole http://www.jamstec.go.jp/frsgc/research/d1/iod/IOD1.html

Figure 5. Indian Ocean Basin Map from Google Maps https://maps.google.com/

Figure 8. MJO http://www.cpc.ncep.noaa.gov/products/precip/CWlink/ir_anim_monthly.shtml

Table 2. Data set beginning and endings years.

Tropical Cyclone Data North http://jtwccdn.appspot.com/NOOC/nmfc-ph/RSS/jtwc/best_tracks/ioindex.html

Tropical Cyclone Data South http://jtwccdn.appspot.com/NOOC/nmfc-ph/RSS/jtwc/best_tracks/shindex.html

Table 3. A sample of the tropical Cyclone ACE

Table 4. A sample of the ENSO data found at the Climate Prediction Center. http://www.cpc.ncep.noaa.gov/products/analysis_monitoring/ensostuff/ensoyears.shtml

IOD Data
http://www.jamstec.go.jp/frcgc/research/d1/iod/HTML/Dipole%20Mode%20Index.html

SIOD Data http://www.jamstec.go.jp/res/ress/behera/iosdindex.html

11.3 Miscellaneous Links

Australia's BOM IOD Page. http://www.bom.gov.au/climate/enso/history/ln-2010-12/IOD-what.shtml

NOAA's El Niño Page http://www.pmel.noaa.gov/tao/elnino/impacts.html

NOAA's Buoy Data

http://www.noaanews.noaa.gov/stories2009/20090504_indianoceanbuoys.html

World Bank GDP http://data.worldbank.org/indicator/NY.GDP.MKTP.CD